UDC 621
CODEN: MINSC5
In print: ISSN 1857 – 5293
On line: ISSN 1857 – 9191

MECHANICAL ENGINEERING SCIENTIFIC JOURNAL

МАШИНСКО ИНЖЕНЕРСТВО НАУЧНО СПИСАНИЕ

Volume 41
Number 2

Skopje, 2023

Mech. Eng. Sci. J.	Vol. **41**	No. 2	pp. 75–144	Skopje 2023
Маш. инж. науч. спис.	Год.	Број	стр.	Скопје

MECHANICAL ENGINEERING – SCIENTIFIC JOURNAL
МАШИНСКО ИНЖЕНЕРСТВО – НАУЧНО СПИСАНИЕ

Published by
Faculty of Mechanical Engineering, Ss. Cyril and Methodius University in Skopje, North Macedonia
Издава
Машински факултет, Универзитет „Св. Кирил и Методиј" во Скопје, Северна Македонија

Published twice yearly – Излегува два пати годишно

Proof-reader	Коректор
Alena Georgievska	**Алена Георгиевска**
Technical editor	Технички уредник
Blagoja Bogatinoski	**Благоја Богатиноски**
UDC: "St. Kliment Ohridski" Library – Skopje	УДК: НУБ „Св.. Климент Охридски" – Скопје
Copies: 300	Тираж: 300
Price: 520 denars	Цена: 520 денари
Address	Адреса
Faculty of Mechanical Engineering	**Машински факултет**
(Mechanical Engineering – Scientific Journal)	(Машинско инженерство – научно списание)
Editor in Chief	Одговорен уредник
P.O.Box 464	пошт. фах 464
MK-1001 Skopje, Republic of North Macedonia	MK-1001 Скопје, Република Северна Македонија

Mech. Eng. Sci. J. is indexed/abstracted in INIS (International Nuclear Information System)
www.mf.ukim.edu.mk

MECHANICAL ENGINEERING – SCIENTIFIC JOURNAL
FACULTY OF MECHANICAL ENGINEERING, SKOPJE, REPUBLIC OF NORTH MACEDONIA

МАШИНСКО ИНЖЕНЕРСТВО – НАУЧНО СПИСАНИЕ
МАШИНСКИ ФАКУЛТЕТ, СКОПЈЕ, РЕПУБЛИКА СЕВЕРНА МАКЕДОНИЈА

Mech. Eng. Sci. J.	Vol.	No.	pp.	Skopje
	41	2	75–144	2023
Маш. инж. науч. сūис.	Год.	Број	стр.	Скопје

TABLE OF CONTENTS
(С О Д Р Ж И Н А)

MOTOR VEHICLES
(Моторни возила)

THERMAL ENGINEERING
(Термичко инженерство)

MECHATRONICS
(Мехатроника)

Mechanical Engineering – Scientific Journal, Vol. **41,** No. 2, pp. 75–81 (2023)
Number of article: 666
In print: ISSN 1857–5293
Received: May 17, 2023
On line: ISSN 1857–9191
Accepted: December 1, 2023
UDC: 629.33.027:[519.876.5:534.13/.14
https://doi.org/10.55302/MESJ23412666075d

Original scientific paper

CONTRIBUTION ON INVESTIGATING THE POSSIBILITY OF USING TWO-PARAMETER FREQUENCY ANALYSIS IN EXPERIMENTAL PARAMETER IDENTIFICATION OF TORQUE VIBRATIONS OF VEHICLE CARDAN SHAFTS

Miroslav Demić

Academy of Engineering Sciences, Belgrade
demic@kg.ac.rs

A b s t r a c t. During exploitation, motor vehicles are subjected to vibration loads that lead to fatigue of their users and materials of their aggregates. Therefore, vibrations must be studied from the earliest stage of development, using mathematical models, experiments, or their combinations. In theoretical studies, vibrations of concentrated masses are usually observed, although, with the development of numerical methods (especially finite element method), attention is paid to vibrations of elastic vehicle systems. Then, idealizations are usually made, especially regarding operational conditions and relationships between motor vehicle aggregates. In this paper, an attempt was made to develop a method for identifying real vibration loads of elastic vehicle cardan shafts under operational conditions. Namely, 2D Fourier transformation was used for two-parameter frequency analysis. The possibility of the procedure's application was demonstrated on an idealized elastic cardan shaft. The research showed that two-parameter frequency analysis can be used to generate torsional vibrations of elastic vehicle cardan shafts in laboratory conditions.

Key words: vehicle; elastic cardan shaft; torsional vibrations; two-parameter frequency analysis

ПРИЛОГ КОН ИСТРАЖУВАЊЕ НА МОЖНОСТА ЗА КОРИСТЕЊЕ АНАЛИЗА НА ФРЕКВЕНЦИЈАТА СО ДВА ПАРАМЕТРА ЗА ЕКСПЕРИМЕНТАЛНА ИДЕНТИФИКАЦИЈА НА ПАРАМЕТРИТЕ НА ВРТЕЖНИОТ МОМЕНТ НА КАРДАНСКИТЕ ОСКИ НА ВОЗИЛОТО

А п с т р а к т. За време на експлоатацијата, моторните возила се подложени на вибрациони оптоварувања што доведуваат до замор на материјалите на нивните агрегати. Затоа вибрациите мора да се проучуваат уште од најраната фаза на развој, користејќи математички модели, експерименти или нивни комбинации. Во теоретските студии обично се разгледуваат вибрации на концентрирани маси, иако, со развојот на нумеричките методи (особено методот на конечни елементи), им се посветува внимание и на вибрациите на еластичните системи на возилата. Потоа обично се прават идеализации, особено во однос на условите за работа и односите меѓу агрегатите на моторните возила. Во овој труд беше направен обид да се развие метод за идентификување на реалните вибрациони оптоварувања на еластичните карданскi вратила на возилото при работни услови. Имено, за анализа на фреквенцијата со два параметра се користеше 2D Фуриеова трансформација. Можноста за примена на постапката беше демонстрирана на идеализирана еластична осовина. Истражувањето покажа дека анализата на фреквенцијата со два параметра може да се користи за да се генерираат торзиони вибрации на еластичните вратила на возилото во лабораториски услови.

Клучни зборови: возило; еластично вратило; торзиони вибрации; анализа на фреквенција со два параметра

1. INTRODUCTION

During exploitation, motor vehicles are subjected to vibration loads that lead to fatigue of their users and materials of their aggregates. Therefore, vibrations must be studied from the earliest stage of development, using mathematical models, experiments, or their combinations.

In theoretical studies, vibrations of concentrated masses are usually observed, although, with the development of numerical methods (especially finite element method), attention is paid to vibrations of elastic vehicle systems. Then, idealizations are usually made, especially regarding operational conditions and relationships between vehicle aggregates [1].

The specificity of vehicle operational conditions is their random character [1], which significantly complicates theoretical considerations using models, so experiments are practical and irreplaceable. Namely, despite significant progress in developing software for automatic vehicle design and calculation [4], the final judgment on their characteristics is based on experimental research. Therefore, experimental methods are still significant today.

When it comes to elastic vehicle cardan shafts subjected to torsional vibrations, a problem often arises in identifying the parameters of these vibrations. Methods for identifying them are developed, as is the case with modal analysis [5–10]. In practical terms, vibration modes are determined in laboratory conditions. However, a problem arises in the case when actual exploitation conditions are necessary to generate the torsional loads of the cardan shaft on test benches, as the modal analysis does not provide sufficient opportunities for generating these signals in the time domain.

Therefore, it was deemed useful to develop a procedure for identifying the parameters of torsional vibrations of elastic vehicle cardan shafts, which would enable their generation in laboratory conditions.

One possibility is frequency analysis using the Fourier transform, which enables the determination of the frequency content of signals by calculating the spectra magnitudes and phase angles [11, 12], that allow the generation of an original, time-dependent signal using the inverse Fourier transform, which is routinely performed in cases where the signal depends only on time [11].

However, vibrations of elastic systems depend on multiple parameters (dimensions and time), suggesting that a multi-parameter Fourier transform must be used. In the case of an idealized cardan shaft (with other types of vibration ignored), torsional vibrations change along the length of the shaft and depend on time, so the so-called two-parameter Fourier transformation (2D) must be applied [13, 14].

This paper will analyze the possibility of using a two-parameter Fourier transform to create conditions for studying vibrations of elastic vehicle cardan shafts in laboratory conditions.

Therefore, a general expression for the Fourier transform in case of multiple variables will be given [15]:

$$F(\xi_1, \xi_2 \dots . \xi_n) = \int_{R^n} e - 2\pi i (x_1\zeta_1 + x_2\zeta_2 + \\ + \cdots x_n\zeta_n) * f(x_1, x_2 \dots . x_n) dx_1 dx_2 **** dx_n \quad (1)$$

where:

$f(x_1, x_2 \dots . x_n)$ – a function of n variables,

$x_1, x_2, \dots . x_n$ – variables,

$\xi_1, \xi_2 \dots \dots \xi_n$ – circular frequency, and

$\int_{R^n}$ – multiple integrals (double for 2D, triple for 3D, etc.).

2. METHOD

As previously mentioned, this paper aims to investigate the possibility of using two-parameter frequency analysis (2D Fourier transformation) in identifying parameters of torsional vibrations of elastic vehicle cardan shafts. In the absence of experimental data on registered torsional vibrations of the shaft, the method is illustrated with data obtained from a dynamic simulation using its mathematical model. As is known, vibrations of elastic elements are described by partial differential equations [13,14]. For further consideration, Figure 1 will be observed.

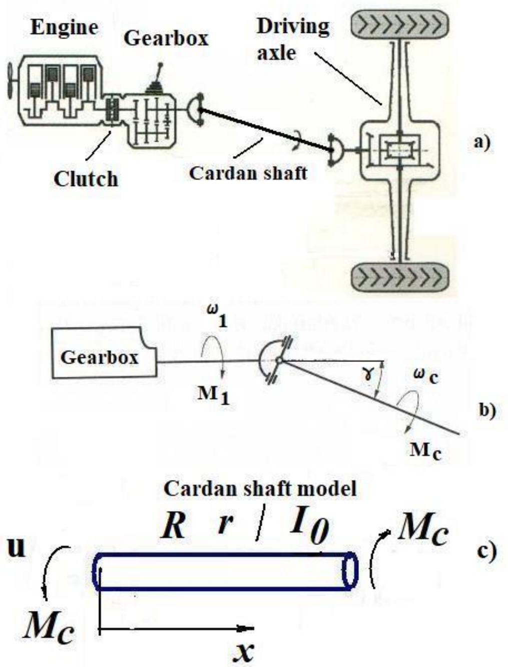

Fig. 1. The concept of transmission (1 a), partial scheme of cardan shaft (1 b), and cardan shaft model (1c)

Figure 1 shows the concept of transmission of the observed commercial motor vehicle (1a). Given that this transmission concept is widely applied in practice, it has been deemed appropriate not to give any further explanations. The cardan shaft is intended to transmit the torque from the gearbox to the drive axle in cases where their axes do not overlap, as illustrated in Figure (1b). A simplified model of an elastic cardan shaft is shown in Figure (1c).

When defining the model to describe the torsional vibrations of the elastic cardan shaft, the following assumptions were made:

– the influence of its mass on the occurrence of transverse vibrations was neglected,

– the shaft was cylindrical (tube) with a constant outer and inner diameter along its length,

– the shaft was completely dynamically balanced and the influence of clearance in the joints was neglected, but friction losses in the joints of the shaft were included.

Given that the partial differential equations that describe torsion vibrations of elastic bodies, which also applies to the cardan shaft, is described in detail in [13, 14], it will not be done here, but its final form will be given. Given the assumptions made, forced torsional vibrations of the elastic cardan shaft [13,14] are described by the partial differential equation:

$$\frac{\partial^2 u}{\partial t^2} = c^2 \frac{\partial^2 u}{\partial x^2} + f(x,t), \quad (2)$$

where:

$u(x, t)$ – torsional vibrations of the cardan shaft,

x – coordinate along the length of the shaft,

$f(x, t)$ – forced torque originating from unbalanced motor forces and the random character of micro-roughness,

t – time, and

$$c^2 = \frac{G}{\rho},$$

where:

G – shear modulus, and

ρ – density of the shaft material.

As is known [13,14,16], to find the general integral of the partial differential equation (2), it is necessary to know the boundary and initial conditions. As is known, the torsional torque caused by vibrations of the cardan shaft can be expressed [13, 14, 16]:

$$M = GI_0 \frac{\partial u(x,t)}{\partial x}. \quad (3)$$

where:

I_0 – a polar moment of inertia given by the expression for a circular ring cross-section:

$$I_0 = \frac{\pi(R^4 - r^4)}{2}$$

where:

R – outer, and

r – inner radius of the cardan shaft tube.

The left boundary condition of the cardan shaft is defined by the equality of the output torque from the gearbox and the torsional torque transferred to it. The right boundary condition of the cardan shaft is defined by the equality of the torque that needs to be brought to the drive axle and the torsional torque of the shaft.

For further consideration, Figure 1b will be observed.

Without delving into the theory of spherical motion of the universal joint, which is extensively explained in [17, 18], the vector of the angular velocity of the output shaft of the gearbox is projected onto the axis of the cardan shaft, and the following relationship applies:

$$\omega_c = \omega_1 \cos(\gamma)$$

where γ is the angle of the universal joint.

The opposite situation occurs at the right end, where the following relationship can be written for the angular velocity of the input shaft of the drive shaft:

$$\omega_c = \omega_2 \cos(\gamma),$$

where ω_2 the angular velocity of the drive shaft.

To define the boundary conditions, it is necessary to calculate the output torque from the gearbox and the input torque to the drive axle. Based on the power equality that is transmitted from the gearbox to the left cross joint of the cardan shaft, we have:

$$M_1\omega_1 = M_c\omega_c = M_c\omega_1 \cos(\gamma). \quad (4)$$

The same can be written for the right cross joint of the cardan shaft (where the influence of friction is included in the joints of the cardan shaft via the efficiency factor η_c):

$$M_c\omega_c\eta_c = M_2\omega_2 = M_2 \frac{\omega_c}{\cos(\gamma)}. \quad (5)$$

where M_2 is the input torque to the drive axle.

The torque M_2 will be calculated from the traction balance during slow uniform motion of the observed commercial motor vehicle on a road with a longitudinal slope defined by the longitudinal angle α. Given the conditions of the observed vehicle motion, the required moment on the input shaft of the drive axle M_2 is defined by the expression [19]:

$$M_2 = \frac{mg(f\cos\alpha + \sin\alpha)r_d}{i_0\eta_0}. \quad (6)$$

where:

m – the mass of the vehicle,

g – the acceleration due to gravity,

α – the longitudinal slope angle,

f – the coefficient of rolling resistance,

i_0 – the gear reduction in the drive shaft,

η_0 – the efficiency of the drive axle.

Based on expressions (3), (4), and (6), the boundary condition for the left end of the cardan shaft is obtained:

$$\frac{\partial u(x,t)}{\partial x} = \frac{1}{GI_0}\frac{M_1}{\cos(\gamma)}, \quad (7)$$

while based on expressions (3), (5), and (6), the boundary condition for the right end of the cardan shaft can be written:

$$\frac{\partial u(x,t)}{\partial x} = \frac{1}{GI_0}\frac{M_2}{\eta_c\cos(\gamma)}. \quad (8)$$

For the left end of the shaft, $x = 0$ should be placed, and for the right end, $x = L$ (where L is the length of the cardan shaft).

The following initial conditions were assumed for the dynamic simulation:

$$u(x,t) = 0; \quad \frac{\partial u(x,t)}{\partial t} = 0 \quad (9)$$

for $t = 0$.

It was deemed appropriate to use a forced torque (excitation function) in partial differential equation (2) that takes into account the imbalance of the engine's torque or the random nature of the longitudinal micro-roughness of the road.

More precisely, in the absence of real data, it was assumed that the engine torque changes with twice the frequency of the number of revolutions (the so-called second harmonic), and that the effect of longitudinal road roughness can be represented by a random function [19], i.e.:

$$f(x,t) = a_m\sin(4\pi nt)$$

$$f(x,t) = a_m[(rnd - 0.5) + \sin(4\pi nt)]$$

where:

a_m – amplitude,

rnd – random numbers uniformly distributed in the interval 0,1,

n – number of engine revolutions, and

t – time.

The partial differential equation (2), with boundary and initial conditions (7), (8), and (9), can be solved only in the case of harmonic excitation [13, 14], so an attempt was made to solve it using the Wolfram Mathematica 13.2 program [15]. However, difficulties arose with listing numerical data, so it was decided to solve the problem numerically [20], using the finite difference method. As this procedure is known from [20], it will not be discussed here, and the problem was solved using a developed program in Pascal.

The dynamic simulation was performed for a steel elastic cardan shaft, using the following data: m = 22000 kg; i_0 = 7.85; i_I = 6.87; r_d = 520 mm; η_0 = 0.90; η_c = 1; G = 8·104 N/mm^2; ρ = 8·10–6 kg/mm^3; R = 125 mm, r = 100 mm; n_x = 256; h_x = 5 mm; n_t = 256; h_t = 0.01 s; a_m = 20 Nm; ρ = 6 °.

As torsional vibrations of the elastic cardan shaft depend on two parameters, 3D graphics are required to represent them graphically. For illustration, the results of the numerical integration of the partial differential equation (2) are shown for the used boundary and initial conditions in Figures 2 and 3.

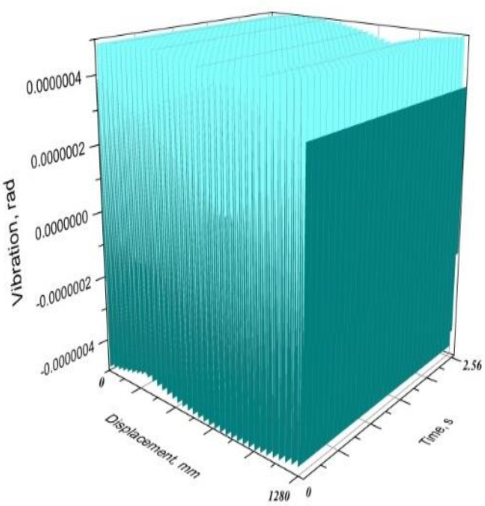

Fig. 2. Torsional vibrations of the cardan shaft for the forced torque $f(x, t) = a_m \cdot \sin(2nt)$

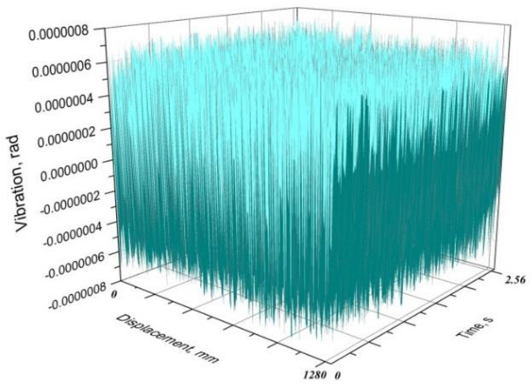

Fig. 3. Torsional vibrations of the cardan shaft for the forced torque $f(x,t) = a_m[\sin(2nt) + (rnd–0.5)]$

In Figure 2, harmonic waves along the length of the shaft can be observed due to the unbalanced second harmonic of the motor, which is following the theoretical solutions from [13, 14].

Figure 3 shows the simultaneous effect of the unbalanced engine torque and road microroughness on the torsional vibrations of the elastic cardan shaft, but in this case, randomly-shaped waves appear.

Since the torsional vibrations of the elastic cardan shaft depend on two parameters (displacement x and time t), it is necessary to apply 2D Fourier transformation. To implement it, the author developed software in Pascal. However, considering the available commercial software on the market, it was deemed appropriate to use Origin 8.5 [21] in further analyses, as potential users will have easier access to that software.

Using the mentioned software, the spectra magnitudes and phases of the two-parameter Fourier transformation were calculated, and, for illustration purposes, the results are shown in Figures 4–7.

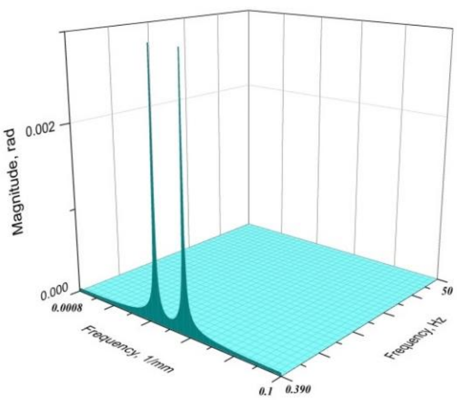

Fig. 4. The module spectrum of torsional vibrations of the cardan shaft for the forced torque $f(x,t) = a_m*\sin(2nt)$

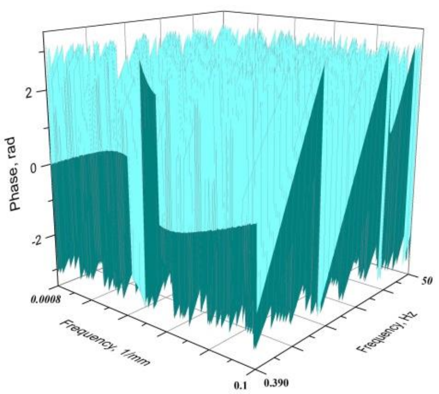

Fig. 5. The phase angle of torsional vibrations of the cardan shaft for the forced torque $f(x,t) = am*\sin(2nt)$

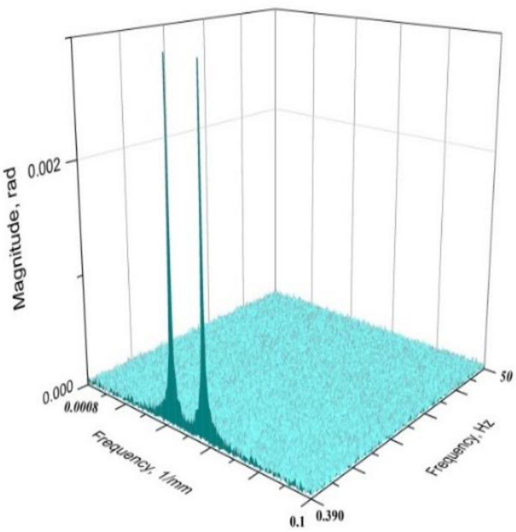

Fig. 6. The module spectrum of torsional vibrations of the cardan shaft for the forced torque $f(x,t) = a_m[\sin(2nt) + (rnd–0.5)]$

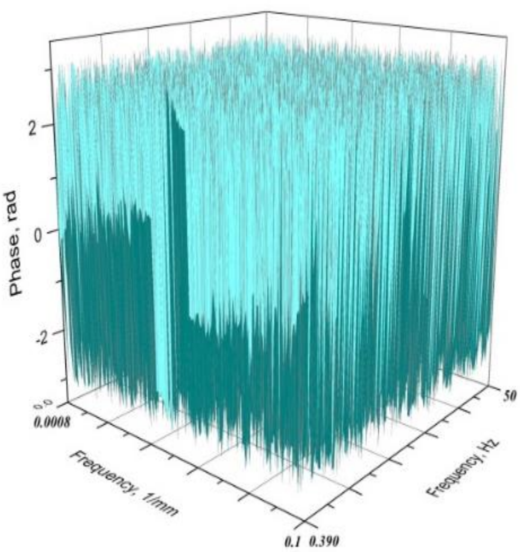

Fig. 7. The phase angle of torsional vibrations of the cardan shaft for the forced torque $f(x,t) = a_m[\sin(2nt) + (rnd–0.5)]$

3. DATA ANALYSIS

Based on the data analysis shown in images 4-7, it can be concluded that the spectra magnitude modules and phase angles describe the wave character of torsional vibrations of the elastic propeller shaft, which is consistent with the theoretical solutions from [13, 14].

The waves are more clearly visible in cases of harmonic disturbance of the form $a_m \cdot \sin(2nt)$, while in the case of using a disturbance function $a_m[\sin(2nt) + (rnd - 0.5)]$, the waves are random, as expected.

Based on previous analyses, it can be claimed that 2D Fourier transformation reliably enables data analysis of torsional vibrations of the elastic cardan shaft, which can have practical applications, as the inverse Fourier transformation enables laboratory generation of identical vibrations in operational conditions [22]. The inverse Fourier transformation can be realized using the aforementioned software Origin 8.5 [21].

During operational testing, it is necessary to register torsional vibration parameters of the elastic cardan shaft (stress, angular displacement, speed, or acceleration) along its length, over longer periods. Minimum and maximum frequency values depend on the length of the shaft, i.e. length of the time signal and discretization step.

First, it is necessary to adopt the maximum interesting frequencies fx_{max} and ftmax, then the setting step of the transducer and sampling of the time signal is defined based on the equation (Nyquist frequency) [11]:

$$h_x = \frac{1}{2fx_{max}} \qquad h_t = \frac{1}{2ft_{max}}.$$

The minimum interesting frequency is determined based on the length of the shaft ($L = nx \cdot hx$) or the length of the time signal ($T = nt \cdot ht$), according to the expressions:

$$f_{x_{min}} = \frac{1}{L} \qquad f_{t_{min}}$$

It should be noted that there are no explicit procedures for calculating spectral analysis errors for two-parameter Fourier transforms, unlike in the case of one-dimensional Fourier transforms [11]. Taking this into account, as well as the fact that this paper aims to illustrate the possibilities of applying two-parameter frequency analysis in the study of torsional vibrations of elastic cardan shafts in vehicles, analysis of statistical errors was not performed in detail.

The developed procedure has created conditions for analysis of the influence of the integration step on the accuracy and stability of partial differential equation (2) solutions, the influence of design parameters on torsional vibrations of elastic cardan shafts, the influence of forced torques, and so on. However, considering that the results of dynamic simulation in this paper served as a replacement for missing experimental results, it was evaluated that a more detailed analysis is not necessary.

4. CONCLUSION

Based on the conducted research, it can be stated that the two-parameter Fourier transform reliably enables the analysis of experimental data on torsional vibrations of elastic cardan shafts.

The calculated spectra magnitudes and phase angles, with the application of inverse 2D Fourier, transform, enable the generation of identical vibrations in the laboratory as well as in exploitation conditions.

REFERENCES

[1] Genta, G. (2003): *Motor Vehicle Dynamics: Modeling and Simulation*, Series on Advances in Mathematics for Applied Sciences, Vol. 43, World Scientific, ISBN-10 9810229119.

[2] Bathe, K. J. (1982): *Finite Element Procedures in Engineering Analyses*, Prentice Hall, Englewood Clifs, N.J.

[3] Ukraincuk, N. (2003): *Finite Element and Finite Difference Methods*, University of Zagreb, Department of Mathematics (in Croatian).

[4] Softwares: NASTRAN, ADAMS, CATIA, COSMOS, NASE, SAP, ALGOR, ANSYS, NISA, PAK…

[5] Lorenzo, E. Di. et al. (2019). Characterization of torsional vibrations: Torsional-Order Based Modal Analysis, Rotating Machinery, *Vibro-Acoustics & Laser Vibrometry*, Vol. **7** (pp.77–89), DOI:10.1007/978-3-319-74693-7_8

[6] Venekar, K. et al. (2014): Gear fault detection using vibrations analysis and continuous Wavelet transform, *Procedia Materials Science*, **5,** pp. 1846–1852.

[7] Sriramireddy. K. et al. (2018): Mechanical modal vibration analysis of crankshaft of IC engine, *IJESC*, Vol. **8**, Iss. No. 6, pp. 19391–18396.

[8] Vex, I. et al. (2006): *Noise and Vibration Control Engineering – Principles and Applications*, Wiley, John Willey &. Sons Inc.

[9] Ewins, D. (1984): *Modal Testing: Theory and Practice*, John Wiley and Sons Inc. New Jersey.

[10] Zavery, K., et al. (1985): *Modal Analysis of Large Structures – Multiple Exciter Systems*, Bruel&Kjajer.

[11] Bendat, J. S., Piersol, A. G. (2000): *Random Data-Analysis and Measurement Procedures*, John Wiley and Sons.

[12] Brandt, A. (2011): *Noise and Vibration Analysis and Experimental Procedures*, John Willey & Sons Inc.

[13] Singeresy, S. R. (2007): *Vibration of Continuous System*, John Wiley and Sons Inc. New Jersey.

[14] Sobolev, S. L. (2016): *Partial Differential Equations of Mathematical Physics*, Pergamon Student Edition, Elsevier.

[15] Wolfram Mathematica: https://Reference.Wolfram.com/language/tutorial/NDSolverPDE.html.

[16] Piersol, A. et al. (2010): *Shock and Vibration Handbook*, McGraw-Hill Handbooks.

[17] Durković, R. (2015): *Power Transmission*, Faculty of Mechanical Engineering, University of Montenegro (in Serbian).

[18] Simić, D., Janković, A. (1993): *Cardan Shaft, Mobility and Vehicle Mechanics* (special issue), Faculty of Mechanical Engineering, University of Kragujevac (in Serbian).

[19] Demić, M., Lukić, J. (2010): *Theory of Motion of Motor Vehicles*, Faculty of Mechanical Engineering, University of Kragujevac (in Serbian).

[20] Stanton, R. G. (1961): *Numerical Methods for Science and Engineering*, Prentice Hall, Englewood Clifs, N.J.

[21] Software: OriginPro 8.5.0 SR1 b161 (1991–2010): Origin Lab Corporation, Northampton, MA. 01060 USA

[22] Dean, A., Voss D. (1999): *Design and Analysis of Experiments*, Springer. https://doi.org/10.1007/b97673.

Mechanical Engineering – Scientific Journal, Vol. **41,** No. 2, pp. 83–88 (2023)
Number of article: 667
In print: ISSN 1857–5293
Received: October 16, 2023
On line: ISSN 1857–9191
Accepted: November 11, 2023
UDC: 621.431.7.038:661.343.082.2
https://doi.org/10.55302/MESJ23412667083j
Original scientific paper

ENERGY EFFICIENCY OF INDUSTRIAL CONCENTRATORS WITH EJECTOR THERMOCOMPRESSION

Aleksandar Gjerasimovski[1], Nataša Gjerasimovska[2], Vasko Šarevski[1]

[1]*Faculty of Mechanical Engineering, "Ss. Cyril and Methodius" University in Skopje, P.O.Box 464, MK-1001 Skopje, Republic of North Macedonia*
[2]*Department of Renewable Energy – Energy Sector, Macedonian Ministry of Economy, Skopje, Republic of North Macedonia*
aleksandar.gerasimovski@mf.edu.mk

A b s t r a c t: Research on the energy characteristics of systems with ejector thermocompression applied in industrial concentrators is presented in this paper. Ejector thermocompression achieves a significant increase in energy efficiency. The heat pump cycle in ejectors is realized through the compression of a portion of the waste steam from the solution being concentrated, which, together with motive steam from a boiler or another heat generator, is used as the driving steam for the concentration process. Thermocompression realized with thermal energy can represent a significant advantage over mechanical thermocompression. A setup for the production of concentrated sodium hydroxide (NaOH) solution with two ejector thermocompressors is presented, as well as a polygeneration system with a gas engine – electricity generator, and an ejector thermocompression system. The proposed solutions have high energy efficiency. By implementing thermocompression systems in the production of concentrates, the energy production costs are significantly reduced, which positively affects the cost of the produced concentrate. The surplus of electrical energy, as well as steam not used in the thermocompression processes, is used to supply energy for the needs of consumers in the production facilities.

Key words: industrial concentrators; NaOH solution; polygeneration thermal systems; energy efficiency; gas engine – electricity generator; thermocompression

ЕНЕРГЕТСКА ЕФИКАСНОСТ НА ИНДУСТРИСКИ КОНЦЕНТРАТОРИ СО ЕЈЕКТОРСКА ТЕРМОКОМПРЕСИЈА

А п с т р а к т: Во трудот се презентирани истражувања на енергетските карактеристики на системи со ејекторска термокомпресија применети во индустриски концентратори. Со ејекторска термокомпресија се постигнува значително зголемување на енергетската ефикасност. Топлинскиот пумпен циклус кај ејекторите се реализира со термокомпресија на еден дел од отпадната водна пареа од растворот кој се концентрира, која заедно со примарна пареа од котел или друг генератор на топлина се користи како погонска пареа за процесот на концентрирање. Термокомпресијата реализирана со топлинска енергија може да претставува значајна предност во однос на механичката термокомпресија. Презентирана е постројка за производство концентриран раствор на натриумов хидроксид (NaOH) со два ејекторски термокомпресора, како и полигенеративен систем со гасен мотор – електрогенератор, и систем со ејекторска термокомпресија. Предложените решенија овозможуваат постигнување висока енергетска ефикасност. Со имплементација на термокомпресорски системи во производството на концентратот значително се намалуваат производните трошоци за енергија, што позитивно влијае врз цената на произведениот концентрат. Вишокот на електричната енергија, како и на пареата која не се користи во процесите на термокомпресија, се користи за снабдување со енергија за потребите на потрошувачите во производните погони.

Клучни зборови: индустриски концентратори; раствор на NaOH; полигенеративни термички системи; енергетска ефикасност; гасен мотор – генератор; термокомпресија

1. INTRODUCTION

The decrease in traditional energy resources, their increasing prices, as well as the current issues related to global warming and ozone layer depletion, have necessitated the development of technical solutions for rational energy use and increased utilization of alternative energy sources. Increasing energy efficiency is a vital component of sustainable development, and it is a particularly relevant topic that has sparked numerous research and development activities in the field of thermotechnics and thermoenergetics.

Thermocompression systems, presented in this paper, are considered as high-energy efficiency thermal systems. Ejector thermocompression systems utilize thermal energy, and their implementation in modern technologies represents a significant component in the energy sector research [1, 2, 3].

Energy consumption during the production of a specific product significantly contributes to the product's cost. Therefore, achieving a high-quality product while minimizing energy costs per unit of product is a top priority in the industrial processes. This work presents research focused on increasing the energy efficiency of industrial concentrators through the use of ejector thermocompression systems. Industrial concentrators find applications in various technological processes across the process industry (food, pharmaceutical, chemical, inorganic, and other industrial sectors). They are characterized by high energy consumption. Hence, it is essential to find solutions aimed at reducing energy consumption.

In ejector thermocompression systems, primary steam from a boiler or another heat generator (waste heat from industrial processes, solar, geothermal energy, etc.) is utilized. Using thermal energy to realize the thermocompression process can be highly advantageous compared to mechanical thermocompression, especially when waste heat is employed in the production of primary steam [4]. The use of high-temperature heat pumps with ejector thermocompression, where waste heat (water vapor from the solution) from the concentrator plant is elevated to higher pressure and temperature using primary steam from the boiler (or other heat generator) and is used as a driving steam for realization of the concentration process is a promising technical solution [5]. Utilization of waste heat in high temperature heat pumps with mechanical and ejector thermocompression in the process industry and also for HVAC&R of buildings is subject of many research and development activities in recently published papers [6, 7, 8, 9].

The evaporation temperature is a crucial parameter for the production of concentrates of certain products since maintaining the material's essential properties during concentration requires treatment at proper temperatures. In concentrators using ejector thermocompression, this requirement represents an alternative advantage over classical systems. The implementation of ejector thermocompression systems results in significant energy savings, contributing to the reduction of the production cost of concentrates.

Depending on the required temperature lift to be achieved by the thermocompression process and the ratio between the amount of heat (waste steam from the solution being concentrated) and the primary steam from the boiler, relatively high coefficients of thermotransformation (COP_e) can be obtained. COP_e is the most relevant parameter for the plant's efficiency.

The concept of dispersed electricity generation using a natural gas engine – electricity generator, and the implementation of an ejector thermocompression system for the production of technological steam and hot water, using the energy from the combustion products and engine cooling, represents a highly energy-efficient solution.

2. EJECTOR THERMOCOMPRESSION HEAT PUMP PROCESS IN INDUSTRIAL CONCENTRATORS

Thermocompression in ejector systems is achieved using steam from a steam boiler. Steam production from a boiler relies on thermal energy, which can provide a significant advantage over mechanical thermocompression, especially when waste heat is used for steam production.

A scheme of a concentrator with ejector thermocompression is presented in Figure 1. The figure also includes a pressure-enthalpy ($p – h$) chart showing the thermocompression processes, as well as the supersonic steam/steam ejector.

In the main heat exchanger (evaporator/condenser) of the concentrator, the water content in the concentrator solution evaporates, utilizing the energy from the driving steam from the ejector. Preheating of the solution to the evaporation temperature occurs in the subcooler using the heat from the cooling condensate. The heat pump cycle is implemented by thermocompressing a portion of the waste steam contained in the solution, from the evaporation pressure p_e and temperature $T_{er} = T_e + \Delta T_r$, to a higher pressure p_c (corresponding to the condensation temperature T_c), to achieve an effective temperature difference ΔT_e between the temperature of the driving steam T_c, that condenses inside the pipes, and the solution's evaporation temperature T_{er} ($\Delta T_e = T_c – T_{er}$). The increase in the boiling (evaporation) temperature of the solution (T_{er}) above the boiling (evaporation) temperature of water (T_e), for a given pressure (p_e), ($\Delta T_r = T_{er} – T_e$) depends on the thermodynamic and thermos-physical properties of the solution. For higher concentrations of dry matter x in the solution, ΔT_r is larger.

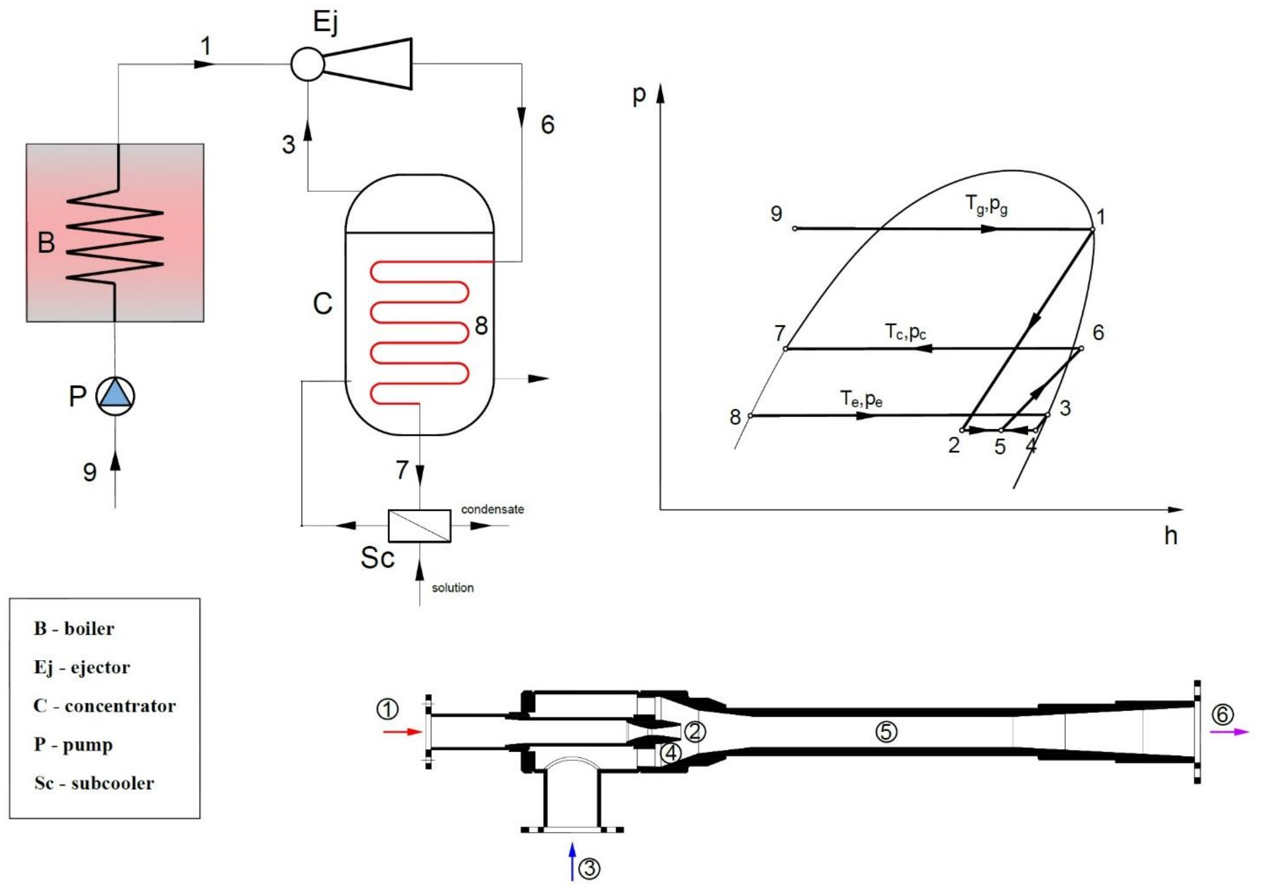

Fig. 1. Ejector thermocompression concentrator, *p* – *h* chart and ejector

The increase in the boiling temperature of the solution ΔT_r from sodium hydroxide (NaOH) depending on the concentration of dry matter x is given in Table 1.

Table 1

Dependence of the increase in boiling temperature of the solution ΔT_r from the concentration of dry matter x [11]

x (kg/kg)	10	15	20	25	50
ΔT_r (K)	3.5	7.5	11.5	15	40

The temperature difference ΔT_e has a significant impact on the consumption of boiler motive steam in the ejector thermocompression and on the optimization of the main heat exchanger (evaporator/condenser). Additional optimization criteria can be defined based on the properties of the concentrate. For certain concentrates, low-temperature treatment in the concentration process is crucial for obtaining a high-quality product. Moreover, high temperatures can cause issues on the heat exchange processes related to fouling of the heat exchanger surfaces, increased aggressive and corrosive properties of the solution, and more.

In some concentration processes, it's necessary to install a vacuum pump to achieve and maintain a vacuum in the concentrator.

The energy efficiency of ejector thermocompression heat pumps is estimated using the coefficient of thermotransformation Ψ_e, or COP_e.

$$\Psi_e = COP_e = \frac{Q_c}{Q_p} = \frac{M_c}{M_p}$$

The coefficient of thermotransformation Ψ_e represents the ratio between the obtained thermostransformed heat Q_c and the consumed heat Q_p for the production of primary boiler steam M_p, by which a portion of the waste steam (waste steam M_e') in the ejector is transformed from pressure pe and temperature t_e to higher pressure pc and temperature t_c. The obtained driving steam M_c, which condenses while performing the thermal concentration process, is calculated as:

$$M_c = M_e' + M_p.$$

The performance of the ejector highly depends on the operating conditions of the thermocompressor system in the concentrator. The compression ratio Π and the temperature lift $\Delta T = T_c - T_e$, achieved by the ejector thermocompressor, primarily depend on the entrainment ratio ω.

$$\omega = \frac{M_s}{M_{pr}} = \frac{M_e'}{M_p}.$$

The coefficient of thermotransformation Ψ_e (COP_e) of the ejector's heat pump cycle is approximately:

$$\Psi_e = COP_e = 1 + \omega.$$

For various operating conditions, i.e., different values of the temperature lift ΔT_e, different ω values are obtained, resulting in varying Ψ_e or COP_e. With optimal design of the flow field of the ejector components (primary nozzle, secondary nozzle, mixing chamber, diffuser, etc.), high Ψ_e or COP_e can be achieved under given design operating conditions.

3. INDUSTRIAL SODIUM HYDROXIDE (NAOH) CONCENTRATOR

Scheme of a two-stage industrial concentrator for sodium hydroxide (NaOH) with an ejector thermocompression system is provided in Figure 2. An original technical solution is implemented by the authors [3]. This system is installed at Zeolite Inc. – Probishtip, a company primarily involved in the production of various zeolites and water glasses. In one phase of the technological process, a 5% NaOH solution is obtained as a by-product, while a 25% NaOH solution is used in another phase, necessitating concentration of the solution.

The concentration of the 5% solution takes place in two stages, within two plate heat exchangers located in a cylindrical vessel. Thermocompression is achieved with ejector thermocompressors TC1 and TC2 for the first and second stages of the concentrator, respectively.

Based on defined parameters of the concentration process, calculations, dimensioning, and manufacturing of the two ejector thermocompressors have been carried out. The facility is equipped with industrial measurement instruments. The data provided in Figure 2, as well as the calculated coefficients of thermotransformation Ψ_e, correspond to a steady-state operation of the concentrator. The significant impact of raising the boiling point temperature (evaporation) of sodium hydroxide (above the corresponding boiling point temperature of water) on the performance of the thermocompression system and the concentrator has been highlighted.

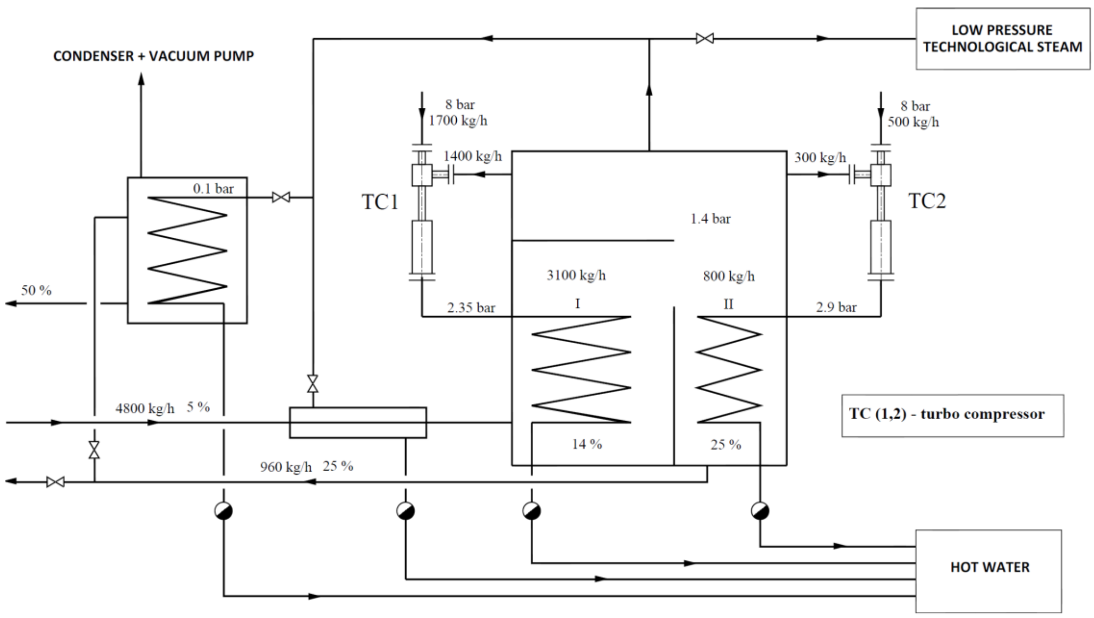

Fig. 2. Scheme of industrial NaOH concentrator

The total temperature lift achieved with TC1 is ΔT = 16 K, but only ΔT_e = 9 K is an effective temperature difference, while $\Delta T_{er} \approx 7$ K (for a concentration of x = 14%) is lost due to the elevated boiling point temperature. The total temperature lift achieved with TC2 is ΔT = 23 K, but ΔT_{er} = 15 K (for a concentration of x = 25%) is lost, and only ΔT_e = 8 K is an effective temperature difference. The thermotransformation coefficients are Ψ_{e1} = 1.8 and Ψ_{e2} = 1.6. The evaporated water in the concentrator (reboiler) that is not thermocompressed is used as process steam. A proposed additional third stage, a vacuum concentrator, is suggested where the NaOH solution is concentrated to 50%. During the concentration process, fouling of the heat exchange surfaces occurs, negatively affecting the heat transfer process and the concentrator's lifespan. Cleaning procedures according to appropriate methods are planned to address this issue.

4. SYSTEM FOR PRODUCTION OF ELECTRICITY AND TECHNOLOGICAL WATER VAPOR WITH EJECTOR

In the industrial systems in the process industry, steam is typically produced in steam boiler facilities. With the development of clean production concepts and strategies to increase energy efficiency in thermal processes and technologies, alternative methods for steam production are proposed, utilizing waste heat from industrial thermal systems, and applying new technologies like high-temperature heat pumps and thermal steam compression / recompression. This topic has sparked special scientific interest and research activities [10]. Using thermal energy to realize the thermocompression process can offer a significant advantage over mechanical thermocompression, especially when waste heat is employed for primary steam production. Compared to classic systems that use motive energy from a steam boiler for the realization of ejector thermocompression, this solution uses waste energy from a motor-generator.

Below is the presentation of an original technical solution of a polygeneration system for production of electrical energy, technological water vapor with defined parameters (pressure and temperature) and technological and sanitary hot water, that uses a gas engine – electricity generator, for electrical energy production and ejector thermocompression (Figure 3).

The input energy from the natural gas (NG) (100% HHV – Higher Heating Value of natural gas) in the gas engine is transformed into mechanical energy (GEN) at 34% and thermal energy at 66%. In the electric generator (ELG), 32% of the input energy from natural gas is converted into electrical energy (power).

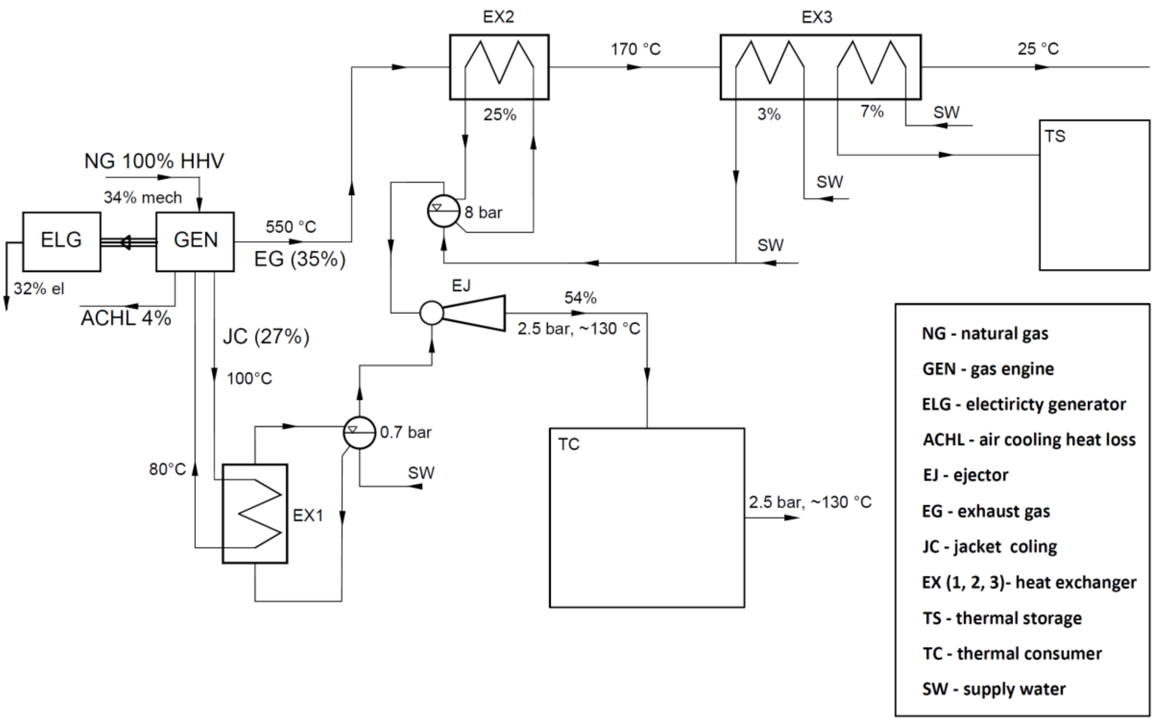

Fig. 3. Gas engine – electricity generator, and ejector thermocompression system

Approximately 4% represents heat losses to the environment, including heat losses in the turbocharger-intercooler (ACHL).

In heat exchanger EX1 (27% HHV), waste heat from engine cooling jacket (JC) is used to produce low-pressure, saturated water vapor with a pressure of 0.7 bar and a temperature of approximately 90°C, which is then thermally compressed to the required pressure using ejector thermocompression.

In heat exchanger EX2 (25% HHV), waste heat from engine exhaust gases (EG) is used to generate saturated water vapor with a pressure of 8 bar and a temperature of approximately 170°C, which is used as primary steam in ejector thermocompressor EJ. With the implemented ejector thermocompression, 52% HHV saturated water vapor at a required pressure of 2.5 bar and a temperature of approximately 130°C is produced.

In heat exchanger EX3 (10% HHV), waste heat from engine exhaust gases is used to produce sanitary and technological hot water STTW (7% HHV) and to prepare supply water SW (3% HHV).

CONCLUSIONS

The significance of the new concept in sustainable development in the energy sector lies in thermocompression systems and their optimal implementation in high-energy efficiency thermal technologies, such as industrial concentrators. Solutions for energy-efficient concentrators are presented, utilizing ejector thermocompression systems. Ejector thermocompression is achieved using primary steam from a boiler or another heat generator, which, along with waste steam from the solution, serves as the driving steam. The use of ejector thermocompression systems results in high values of the coefficient of thermotransformation, which positively impacts energy consumption and the production of high-quality products at lower costs. Thermal characteristics of a sodium hydroxide (NaOH) concentrator, consisting of two ejector thermocompressors, are presented. A concept of an energy-efficient system with a gas engine-electric generator and ejector thermocompression is introduced, which ensures independent power supply for manufacturing facilities' electricity needs and provides thermal energy for the concentrator and other thermal energy consumers.

REFERENCES

[1] Gjerasimovski, A., Sharevska, Maja, Gjerasimovska, N., Sharevska, Monika, Šarevski, V. (2020): A new concept for sustainable energetic development in process industry, *Proceedings Procesing* 2020, SMEITS, Belgrade, Serbia.

[2] Gjerasimovski A., Sharevska Maja, Gjerasimovska N., Sharevska Monika., Šarevski, V. (2020): Characteristics of thermal systems for simultaneous production of electricity, heat and refrigeration, *Procesing* 2020, SMEITS, Belgrade, Serbia.

[3] Šarevski, M. N., Šarevski, V. N. (2016): Water (R718) Tturbo Compressor and Ejector Refrigeration / Heat Pump Technology, ISBN: 978-0-08-100733-4, Elsevier Ltd.

[4] Gjerasimovski, A., Sharevska, Maja, Gjerasimovska, N., Sharevska, Monika, Filkoski, R. (2023): Thermal characteristics of combined compressor – ejector refrigeration / heat pump systems for HVAC&R, *Thermal Science*.

[5] Xing-Qi Cao, et al. (2014): Performance analysis of different high-temperature heat pump systems for low-grade waste heat recovery, *Applied Thermal Engineering*, Vol. **71**, 1, pp. 291–300.

[6] Brückner, S., Liu, S., Miro, L., Radspieler, M., Cabeza, L. F., Lavemann, E. (2015): Industrial waste heat recovery technologies: An economic analysis of heat transformation technologies, *Applied Energy*, **151**, 157–167. https://doi.org/10.1016/j.apenergy.2015.01.147

[7] Mateu-Royo, C. et al. (2018): Theoretical evaluation of different high-temperature heat pump configurations for low-grade waste heat recovery, *International Journal of Refrigeration*, Vol. **90**, pp. 229–237. https://doi.org/10.1016/j.ijrefrig.2018.04.017

[8] Gjerasimovski, A., Šarevska, Maja, Gjerasimovska, N., Šarevska, Monika, Šarevski, V. (2022): 656. HVAC&R polygeneration system with a gas engine and conventional cooling machines/heat pumps, *Mechanical Engineering – Scientific Journal*, **40** (2), 105–110.

[9] Šarevski, M. N., Šarevski, V. N. (2017): Thermal characteristics of high-temperature R718 heat pumps with thermal vapor recompression, *Applied Thermal Engineering*, 117, 355–365.

[10] Šarevski, V. N., Šarevski, M. N. (2012): Energy efficiency of the thermocompression refrigeration and heat pump systems, *Int. J. Refrigeration*, **35** (4), 1067–1079.

[11] Šušić, S., Petrov, S. (1994): *Fundamentals of sugar technology* (in Serbian), University of Belgrade.

Mechanical Engineering – Scientific Journal, Vol. **41,** No. 2, pp. 89–98 (2023)
Number of article: 668
In print: ISSN 1857–5293
Received: September 12, 2023
On line: ISSN 1857–9191
Accepted: November 20, 2023
UDC: 636.4.083:662.767.2.032(497.7)
https://doi.org/10.55302/MESJ23412668089a

Original scientific paper

ENERGETIC AND ECONOMIC ANALYSIS FOR UTILIZATION OF BIOGAS FROM PIG FARMS IN NORTH MACEDONIA

Kliment Angelov, Igor Šešo

Faculty of Mechanical Engineering, "Ss. Cyril and Methodius" University in Skopje, P.O.Box 464, MK-1001 Skopje, North Macedonia
klimentangelov@yahoo.com

A b s t r a c t: Today, when the world is facing an increasing need for energy, and therefore, the exploitation of natural resources is increasing, the problem of environmental pollution and global warming grows. The question of finding and using alternative and clean energy sources, imposes itself. The problem of environmental pollution and the need for renewable energy sources have increased the interest in allocating more funds for scientific research work for the use of biodegradable waste, so that in many countries more and more plants are being built that use biomass for biogas production. Biogas is a very interesting and important source of energy. All organic matter originating from mowing the lawn, cutting branches, farm waste, plant biomass from agricultural production, can be used as raw material for biogas production. Macedonia has large quantities of this type of waste, so there is a good precondition for economical use of them and to get electricity and heat from them. The paper focus is on assessment of the economic viability for utilization of biogas in pigs farms in Macedonia through integration of cogeneration power plant. The economic analysis is performed with method of benefit to cost ratio. Also sensitivity analysis is performed as a function of levelized cost of energy in regard of 7 critical factors: capital cost (amount of capital investment cost), interest rates (*D* is equal to 0%, 5%, 10 % and 15%), capacity factor (plant size), fuel cost (cost of procurement, preparation and transport of the substrate), cost of capital, debt ratio and net plant efficiency. The results indicate that the payback period could be in less than 9 years.

Key words: biogas; renewable energy sources; biogas plants; combined heat power plants

ЕНЕРГЕТСКА И ЕКОНОМСКА АНАЛИЗА ЗА ИСКОРИСТУВАЊЕ БИОГАС ОД ФАРМИ ЗА СВИЊИ ВО СЕВЕРНА МАКЕДОНИЈА

А п с т р а к т: Денес, кога светот се соочува со зголемена потреба од енергија, со што се зголемува и експлоатацијата на природните ресурси, расте проблемот со загадувањето на животната средина и глобалното затоплување. Се наметнува потребата од изнаоѓање и користење на алтернативни и чисти извори на енергија. Проблемот со загадувањето на животната средина и потребата од обновливи извори на енергија го зголемија интересот за издвојување повеќе средства за научноистражувачка работа за искористување на биоразградливиот отпад, така што во многу земји се градат сѐ повеќе постројки кои користат биомаса за производство на биогас. Биогасот е многу интересен и важен извор на енергија. Целата органска материја која потекнува од косење трева, сечење гранки, отпад од фарми, растителна биомаса од земјоделско производство, може да се користи како суровина за производство на биогас. Македонија располага со големи количества на овој вид отпад, така што има добар предуслов за негово економично искористување во производството на струја и топлинска енергија. Фокусот на трудот е процена на економската исплатливост на производство и искористување на биогасот од свињарските фарми во Македонија преку интегрирање на когенеративна постројка. Економската анализа се врши со методот на соодност корист/трошок. Исто така, анализата на сензитивноста се врши како функција на нивелираните трошоци на енергија во однос на 7 критични фактори: капитални трошоци (износ на трошоците за капитални инвестиции), каматни стапки (*D* е еднаква на 0%, 5%, 10% и 15%), фактор на капацитет (големина на постројката), трошок за гориво (трошок за набавка, подготовка и транспорт на подлогата), трошок на капитал, коефициент на долг и нето ефикасност на постројката. Резултатите покажуваат дека периодот на враќање може да биде покус од 9 години.

Клучни зборови: биогас; обновливи извори на енергија; постројки за биогас; комбинирани постројки за топлинска и електрична енергија

1. INTRODUCTION

The rapid development of society that emerges as a consequence of the technical and technological revolution that is always ongoing, is based on the ability to meet the growing needs for energy. Due to the mismatch of energy needs and opportunities for its provision, energy crises occur, and as a consequence is the increased interest in better and more rational use of existing and new renewable energy sources. Encouraging the use of renewable energy sources is a strategic goal of the EU, as it is in line with the Sustainable Development Strategy and enables the achievement of the goals of the Kyoto Protocol in terms of reducing greenhouse gas emissions and protecting the environment [1]. Renewable or alternative energy sources are already in use, but some are in development and their application is yet to be developed. Along with the energy crises, there is another crisis in the world, the global environmental crisis, which is created as a result of waste disposal problems, because uncontrolled and irresponsible waste disposal endangers human health and the environment. Through the processes of anaerobic fermentation of biodegradable waste, biogas is obtained which mostly contains methane as an energy resource, then carbon dioxide, and less hydrogen, oxygen, ammonia and others. Various technologies for the use of biomass as a renewable energy source for obtaining electricity and heat, as well as fuels for vehicles have already been widely established in the world. Hundreds of larger and smaller installations for production of biogas have been made in the European Union which are suppling biogas for power plants, steam boilers, vehicles and more. The process of decomposition is called anaerobic digestion and occurs naturally in many environments with limited oxygen presence: for example, in ponds and swamps, in rice fields, but also in the stomachs of ruminants. This natural process can be used in biogas plants where organic material is placed. The basic part of the plant is a closed chamber or hermetically sealed container (or often called a reactor – digester) in which the reaction of digestion takes place. The end product of decomposition is a combustible gas called biogas and organic residue in a mineral-containing digester that is suitable for use as a liquid or solid biofertilizer. Biogas is mostly composed of methane which contains the energy of combustion. Biogas, depending on the conditions at the time of creation, contains from 45% to 85% methane and 15% to 45% carbon dioxide. Biogas also contains small amounts of hydrogen sulphite, ammonia, and nitrogen. Biogas often also contains water vapor [2].

Biomass means biodegradable materials obtained from agriculture, animal husbandry and related industries and activities, as well as biodegradable part of industrial and municipal waste. Biomass is an organic material derived from living organisms; plants, animals, humans and microorganisms, which contain stored energy from the Sun, where they bind solar energy through the process of photosynthesis. Biomass by its characteristics is a very quality fuel with the fact that for its use activities should be undertaken for: collection, transport, storage, treatment and the like. Anaerobic decomposition processes can vary according to the content of the substrate and the number of reactors or stages of the process in which the process is performed. In a single-stage process, different phases of anaerobic decomposition are performed in one digester, while in a multi-stage process, two or more digesters are performed in which the phases of anaerobic decomposition are separated from each other. Due to the flow of the substrate through the reaction system, there are a number of different designs of anaerobic decomposition digesters, and a choice can be made between three basic types of digesters: boiler, flow boiler and tubular digester. Complete mixing processes in the field of agricultural biogas production, mainly reactors with complete mixing of cylindrical, vertical shape are used. Fermenters consist of a tank with a concrete bottom and walls made of steel or reinforced concrete. The reservoir may be completely or partially buried in the ground or may be built entirely above ground. A gas-tight cover is upgraded on the tank, which can be performed in different ways depending on the requirements and the construction. Membrane roofs and concrete roofs are most commonly used. The complete mixing is realized with the help of mixers placed in the reactor, i.e. on the reactor.

In the implementation of the anaerobic decomposition process, the basic criteria related to the selection of the digester are the composition of the reaction medium (substrate), the kinetics of decomposition of the substrate and the growth of biomass, as well as the shape of the biocatalyst. The time required to digest the material in the reactor before being removed from it is called the storage time. Storage time varies, depending on the properties of the substrate and how much methane can be extracted from it. Storage time is sometimes expressed as hydraulic retention time (HRT), which usually varies between 10 and 80 days [3]. If a temperature of 10 to 20 °C is maintained in the digester, the reactions are called psychrophilic, and the material should be processed for 90 days. If a temperature of 37 °C is maintained in the digester, the reactions are called mesophilic and the material should be processed for 30 days, and if a temperature of about 55 ºC is maintained, the reactions are called thermophilic, and the reaction ends in 10 days [4]. The largest producers of raw material for biogas plants are: animal farms, slaughterhouses, restaurants, hospitals and all other entities that produce organic waste. These types of waste represent huge amounts of raw material for anaerobic fermentation installations and production of biogas as energy and compost as quality fertilizer. Biomass of animal origin – animal manure, is a useful energy source only for livestock breeding. Among the most compatible substrates for biogas production is fertilizer, solid or liquid, because it is most often used by a farm and is free. Energy plants are also often used as the basis for the operation of a biogas plant for higher biogas yields. The rest of the fermentation is a by-product of biogas production and is commonly used as fertilizer. Energy plants mean purposefully cultivated agricultural biomass, which usually reinforces the substrate.

As can be concluded from examples in previous plants and from the waste yields themselves, waste characteristics and waste quantities, the composition of the substrate is generally defined from the available resources, i.e. each substrate composition is defined as a single plant. There is no exact rule as to what the substrate must be, but the composition of the substrate depends on the yield of biogas from a certain amount of substrate, and thus the profit.

2. EXAMPLE OF BIOGAS PLANT WITH CHP

Slurry coming from a pig farm may have a rough screening before entering the anaerobic digester with 30 days of hydraulic retention time (20–50 days recommended). The proposed anaerobic digests would have a depth of 3.0 meters. The anaerobic digester has a mixing system to improve the efficiency of the digester, to optimize the production of biogas and to avoid (as much as possible) sedimentation and accumulation of solids in the digester. The efficiency of biochemical removal of oxygen demand in anaerobic lagoons is 50–85% [5]. Schematic plan of the whole plant should be defined before the calculations, as shown in Figure 1.

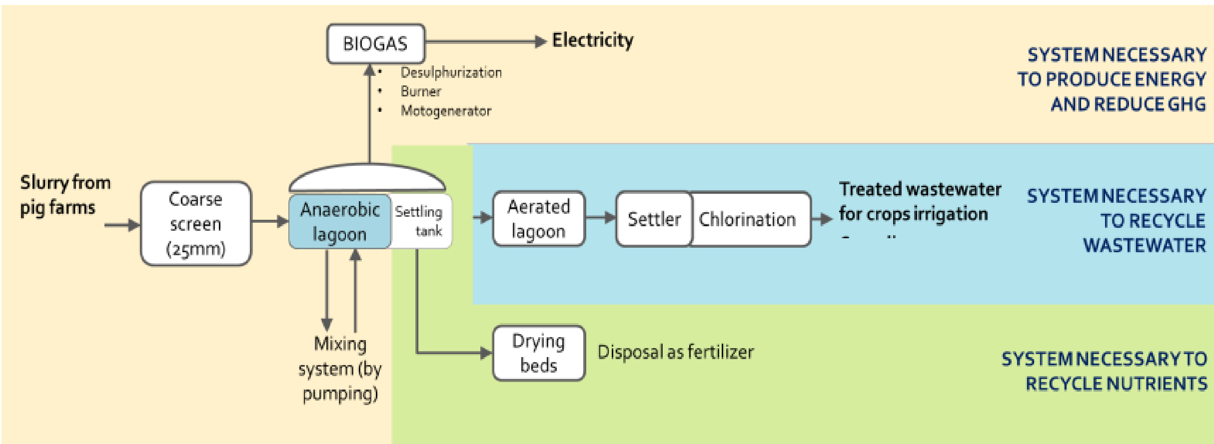

Fig. 1. Plant schematic plan [5]

The composition of the substrate would look like this:

– 27.5 tons of liquid pig waste (46%),

– 16.5 tons of solid pig waste (28%),

– 15 tons of corn silage (26%).

In the considered case it can be concluded that the most compatible mode of operation in mesophilic mode. From the above data it can be seen that the psychrophilic regime does not give a sufficient yield of biogas over time and it takes a very long time to retain the substrate which is not compatible for us given the large amount we have to process. The thermophilic operating mode of the digester is not recommended for animal waste. Therefore, as in most examples so far, it has been decided to use the mesophilic operating mode, because it offers consumption of a medium (reasonable) amount of heat energy and a reasonable retention time. on the substrate. Cogeneration using internal combustion engines is commonly used in biogas plants. Electricity efficiency is high, and investments are lower. A gas turbine and an internal combustion engine can also be used as a cogeneration device in a combined heat and power plant. To determine which unit to choose, the characteristic dimensions of a combined plant such as heat generated, and electricity must be considered also and daily biogas production. So, biogas produced in the anaerobic digestor and the one released in the solid deposition digestor department can be collected and transported by pipes to a treatment system. The corresponding amount of biogas from pig farm waste would be 1646 m^3/d approximately, with 58% methane shown in the following calculations:

$$\text{Methane produc.} = 3180\,\frac{\text{kg}}{\text{d}}\cdot 300\frac{\text{Nm}^3\text{CH}_4}{\text{kg}} = 954\,\frac{\text{Nm}^3\text{CH}_4}{\text{d}} \quad (2.1)$$

$$\text{Biogas production} = 954\,\frac{\text{Nm}^3\text{CH}_4}{\text{d}}\cdot\frac{1}{0.58}\,\frac{\text{Nm}^3\text{biogas}}{\text{d}} \quad (2.2)$$

Biogas should be burned (released) when the biogas pressure exceeds a certain level, and the combustion engine does not work due to maintenance or if there is an additional tank to be stored. The production of electricity from biogas exceeds the consumed electricity on the farm, the remaining electricity will be sold in the national grid, to the national electricity company. The purchase price for electricity produced from biogas in Macedonia now is 180 euros/MWh [6]. Pig production does not have constant heat requirements, so biogas is not recommended to be used exclusively for combustion in a boiler for heat production. The production of fuel for vehicles is not evaluated in this study and is relevant only if the entire fleet of vehicles is supplied with gas. The only reasonable use of biogas is the production of electricity, and as a by-product is the thermal energy. Thus, the biogas produced in the anaerobic digester and the one released in the digester storage compartment of the solids can be collected and transported by pipes to a treatment system. In this example it is defined to be used as a cogeneration device by an internal combustion engine, due to the smaller initial investment and due to the larger selection of powers available for sale. The sizing of the plant will be based on the production of electricity, it will be based on the maximum utilization of biogas and main production of electricity, and as a by-product will appear thermal energy. A small part of the electricity (12%) will be used for the needs of the farm while the remaining part will be sold to the electricity distribution company and will be given to the electricity network. Part of the thermal energy (47%) will be used for heating the substrate and the fermenter and technical water, and in the winter for heating the premises of the farm itself. Before economical calculations we must define schematic representation of a CHP cogeneration plant, as shown in Figure 2.

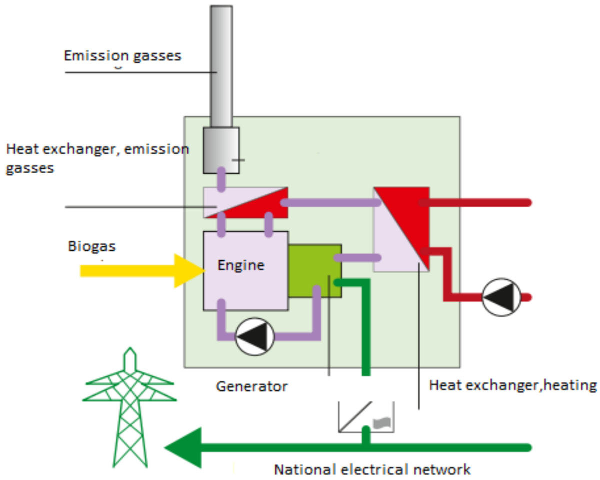

Fig. 2. CHP schematic plan [10]

Modern internal combustion engines have a degree of utilization of over 40%, but even then, a large amount of heat is available. Cogeneration is achieved by using the heat energy of the coolant and combustion products. The heat energy obtained from the coolant is at a low temperature, so it can only be used to heat water up to about 90 °C. Hot water can be used to heat fermenters or nearby work or residential premises. Suitable heat exchangers are required to achieve cogeneration, utilization of coolant heat energy and combustion products. The electrical efficiency of a cogeneration plant is calculated as the product of the efficiency of the engine and the efficiency of the generator. To dimension a plant, it is necessary to make an energy balance that graphically shows the distribution of energy.

The generator – engine technical data in the analysis is for the MTU 6R500 GS [7]. This genset has consumption at full power of 70 m^3/h and the available biogas in the plant is 68 m^3/h. The idea is to have genset that can consume the whole amount of produced biogas. A cogeneration plant is installed with an assumed electrical efficiency of 42%. In terms of annual load hours, the starting point is 8000 hours. The capacity of the gas tank is sufficient so that the produced gas can be used in its entirety and does not have to be burned through a torch. The lower thermal power of methane is 9.97 kWh/m^3 [8]. Every producer of CHP plants must supply energy balance of theirs generator – engine set, as shown in Figure 3.

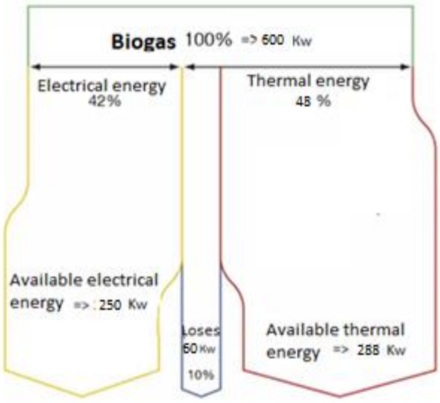

Fig. 3. Example – energy balance and efficiency of a CHP [7]

For the considered digestor it is assumed mesophilic temperature mode of working, with 37 °C degrees in the digester. From the existing biogas plants it can be derived value of about 50 kWh of thermal energy, required per ton of substrate to heat the substrate and maintain the temperature in the digester or a maximum level of up to 20 percent of the produced heat energy [9]. Additional 5.4 kwh/ton substrate, electrical energy for mixers, pumps and equipment in the biogas plant [10]. The daily net amounts of produced energy are:

Electricity = 6000 kwh – 319 kwh – 356 kwh = 5325 kwh

(= daily electricity production – daily consumer for the operation of the equipment of the plant – daily average consumer for the needs of the farm itself = residual electricity)

Thermal energy = 6912 kwh – 2950 kwh – 667 kwh = 3295 kwh

(= daily heat production – daily consumption of heat for digester and substrate – average daily consumption of heat for space heating and technical water = residual heat)

The average consumption of electricity for the needs of the farm can be taken as a constant value, while the average consumption of heat varies depending on outside temperatures, in winter we have increased consumption while in summer we have reduced consumption. The remaining electricity will be sold to the electricity distribution company. From the genset we have three options for heat recovery with temperatures of 180, 90 and 40 °C. All heat requirements are satisfied like heating digester and administration offices and farm. From this we have left 3295 kwh daily of heat energy. Lot of this energy can be sold to outside company or we can heat one small neighbourhood. There it is a lot of option to do with the extra heat energy.

3. ECONOMIC ASSESMENT – CASE STUDY

The purpose of this analysis is to determine whether the combined plant is technically properly selected and whether it will offer significant potential economic benefit to the company in order for the company to decide whether to fund a more comprehensive study. It is analyzed the existing electrical and thermal needs of the company, collected data related to the operation of the company and the permanent equipment and data on the produced waste. To perform an economic analysis of a system with this level of data, the use of assumptions and averages is required. Therefore, this preliminary analysis should be considered as an indicator only for technical and economic potential. This analysis primarily refers to the marginal production costs, plant maintenance costs and credit costs for CHP plant or the various options considered. The specific investments, both in relation to the whole plant and in relation to the cogeneration unit, are in principle higher compared to the larger plants. It is also relatively noticeable that the workload of a smaller plant is generally higher, especially if larger amounts of solids are to be used as a liquid fertilizer additive. All costs are calculated by already existing examples, as kw/$. Investment prices are defeined by existing plant examples, usually they are called as CAPEX. Investment prices for our project are defined and shown in Table 1.

Table 1

Prices by sector (CAPEX)

Investition	Anaerobic	Sludge	Aerobic	Sumary
Description	USD	USD	USD	USD
Electromechanical gear	154 225	69 614	88 476	312 306
Constructions work	192 300	73 500	94 455	360 255
Electrical installations	125 952	43 256	47 288	216 496
Pipelines and mechanical installations		140 000	100 125	240 225
Engineering project	56 411	84 616	28 205	169 235
Start up	39 215		78 430	117 645
Summary	794 279	92 386	161848	1 416 162

For complete economic analysis we must show and operational costs or OPEX costs. OPEX cost are defined by producers of the equipment used and by already existing examples of plants. In the OPEX cost are included all operational costs which can be fixed and variable costs per year, as shown in Table 2.

Table 2

OPEX costs, fixed and variable costs by sectors

Operational costs	Anaerobic	Sludge	Aerobic	Summary
Fixed costs	USD/year	USD/year	USD/year	USD/year
Working costs	14 331	7 850	11 230	33 411
Depreciation	29 352	5 033	10 000	44 385
Interest rate and insurance	12 121	12 121	12 121	36 363
Summary fixed costs	55 804	25 004	33 351	116 159
Variable costs	USD/year	USD/year	USD/year	USD/year
Sludge	0	83 240	0	83 240
Maintenance	15 000	9 252	7 925	32 177
Chemical reagents/ Biogas treatment	7 406	0	1 763	9 169
Summary variable costs	22 406	92 492	9 688	134 586
Summary OPEX	78 210	117 496	43 039	238 745

The project would have some cost savings due to energy production and the use of part of that energy for own needs. Calulation of the saving are one of the key faktor to calculate the payback period, savings for our project are shown in Table 3.

Table 3

Savings

Moto-generator	kW	221
Working hours	h/yr.	8 000
Production electricity	kWh/yr.	1 775 000
Price for electricity	$/kWh	0.21
Savings electricity for pig's farm	USD/yr.	372 750
Consumption diesel fuel for heating	Lit./yr.	20 000
Price diesel fuel	USD/lit.	2
Savings for diesel fuel	USD/yr.	40 000
Summary savings	USD/yr.	392 750

Finally, the surplus electricity from the anaerobic system with a motor generator in a farm of 10,000 pigs is approximately 221 kW. Another cost savings included in the savings is diesel fuel used for combustion in the boiler and to obtain heat energy and for combustion in a generator in cases where there is no electricity. To estimate this cost savings, it is necessary to know the historical consumption of diesel, the number of hours per year that farms need to operate a diesel generator due to lack of electricity.

Payback period

Payback period is one of the key factors to decide if we want to invest or not. In payback period we do not consider the inflation rates or interest rates associated with bank loans.

In Table 4 is shown summary of the payback period for our project.

In Figure 4 it is shown graph of the payback period, with years horizontally and USD vertically.

T a b l e 4

Summary – payback period

CAPEX	USD	1 416 162
OPEX	USD/yr.	238 745
Savings	USD/yr.	392 750
Payback period	Year	9.19

Net present value

The NPV (net present value) of the project is calculated by subtracting the present value of the savings from the present value of the investment and the cost. With this calculation we can define the value of the plant in future, as shown in Figure 5. NPV values are calculated by next formula:

$$\mathrm{NPV} = \sum_{n=0}^{N} \frac{Fn}{(1+d)^n} + \frac{F_1}{(1+d)^1} + \frac{F_2}{(1+d)^2} + \cdots + \frac{F_N}{(1+d)^n} \tag{3.1}$$

where is:

NPV – Net present value

Fn – Net cash flows in year *n*

d – Intrest rate

n – Year

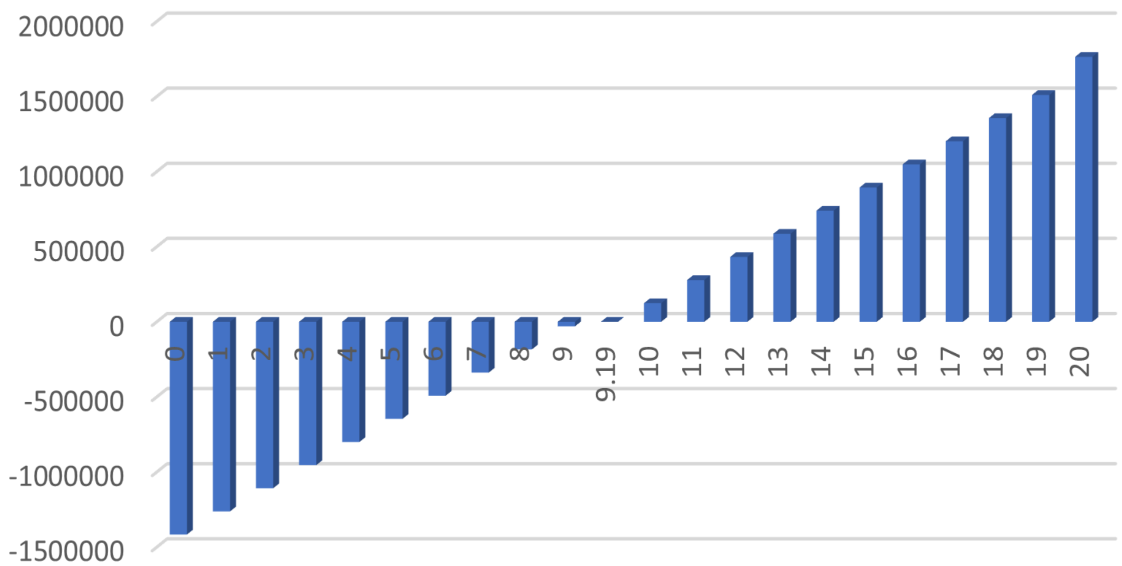

Fig. 4. Payback period graph

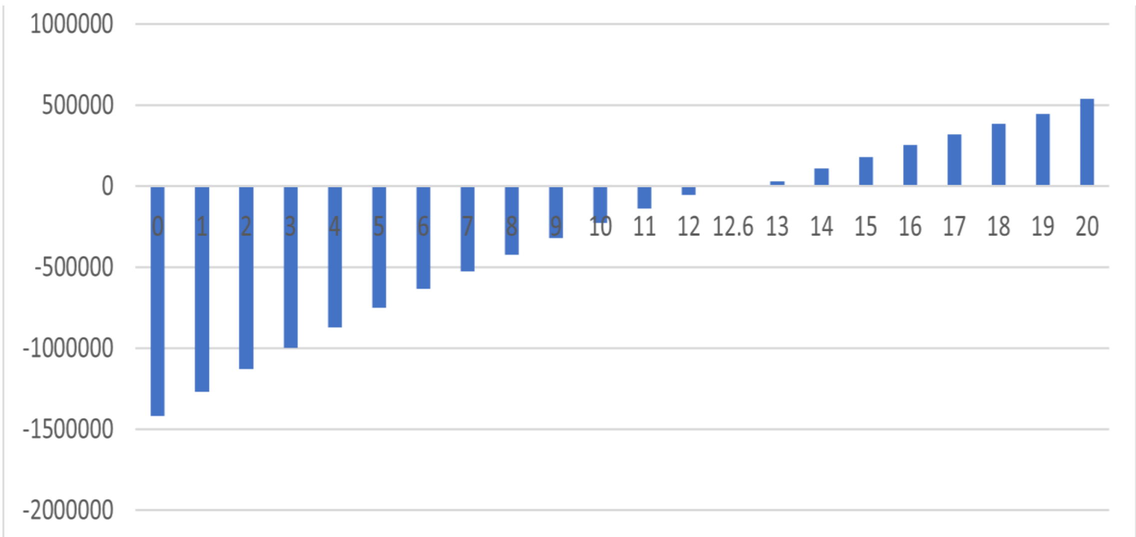

Fig. 5. Cash flow – net present value (NPV)

The net present value (NPV) of the project is the net savings from its life cycle. It is the absolute monetary value of the project. A positive NPV (net present value) indicates how much money a project will earn over its lifetime. NPV shows the total potential earnings of the project. The NPV considers the effect of interest rates on future net savings. NPV is a major decision-making tool for project owners. If NPV > 0, the project is profitable (economically feasible).

Benefit/cost ratio

The relative value, BCR (ratio of savings and investments) of the project is calculated by dividing the present value of the savings / the present value of the investments. If benefit / cost ratio is bigger than 1.0, then the project is profitable.

$$BCR = PV_{\mathrm{AS}} / PV_{\mathrm{I}}, \qquad (3.2)$$

where is:

PV_{AS} – benefits present value

PV_{I} – costs present value

Example:

BCR = 2 443 030 / 2 112 511 = 1.13

Internal rate of return

Internal rate of return (IRR) is a hypothetical discount rate at which BCR = 1.0 or NPV = 0. IRR requires a recurring, computer-friendly calculation. If the IRR ≥ discount rate used in the analysis, the investment is worthwhile (economically feasible). High IRR earns more profit per dollar invested. IRR is a major decision-making tool for lenders, usually the first question they ask. Each investor can arbitrarily set their own acceptable IRR.

In our example IRR = 11%, this value is calculated using the equation in excel.

Levelized cost of electricity

Levelized cost of electricity (LCOE) is the value that must be obtained for each unit of energy produced to ensure that all costs and reasonable profits are incurred. The profit is provided by discounted (decreasing) future income at a reduced rate equal to the rate of return that can be obtained for other investments with comparable risk, i.e. the possible cost of capital. The specific production price of energy is calculated with an excel calculation, and it is 0.076 $/kWh.

Levelized cost of heat energy (LCOE)

The LCOE method is also applied to thermal energy which can also be called LCOH. The calculation is performed according to the next formula (3.3). The specific production price of energy is calculated with an excel calculation, which is 0.058 $/kWh (Table 5).

$$\sum_{t=1}^{t=N} \frac{\mathrm{LCOE} * Q_t}{(1+d\prime)^t} = \sum_{t=0}^{t=N} \frac{C_t}{(1+d)^t} \qquad (3.3)$$

Table 5

Current $ level annual cost (LAC)

Cost of money	0.0500
Net current value (year)	224464
Net current value	1 555 485
Capital recovery factor (current)	0.0802
Current $ level annual revenue requirements ($/y)	103016
Current $ LAC of Heat Energy ($/kWh)	**0.058**

Sensitivity analysis

Sensitivity analysis is a method for considering uncertainty that does not require probability estimates. Sensitivity of economic tests the performance to alternative numbers of key uncertainty factors. The sensitivity analysis always provides multiple answers in economic terms, and it shows decision points such as the economic viability of a renewable energy project, downside rates, time horizons and other critical factors.

In Figure 6 it is illustrated the sensitivity of fuel savings, i.e. the specific energy price achieved by the combined plant with 7 critical factors: capital cost (amount of capital investment cost), interest rates (D is equal to 0%, 5%, 10 % and 15%), capacity factor (plant size), fuel cost (cost of procurement, preparation and transport of the substrate), cost of capital, debt ratio and net plant efficiency.

In the considered case, the main impact of the escalation of the energy price is with a relative change in the net efficiency of the plant. A big change can also be seen in the relative change in the loan-to-equity ratio. In these two factors sharper changes can be noticed, compared with the other factors, which have milder reflections on the specific price of energy with their change.

This example graphically illustrates the situation often encounter in the economic viability of energy efficiency and renewable energy projects.

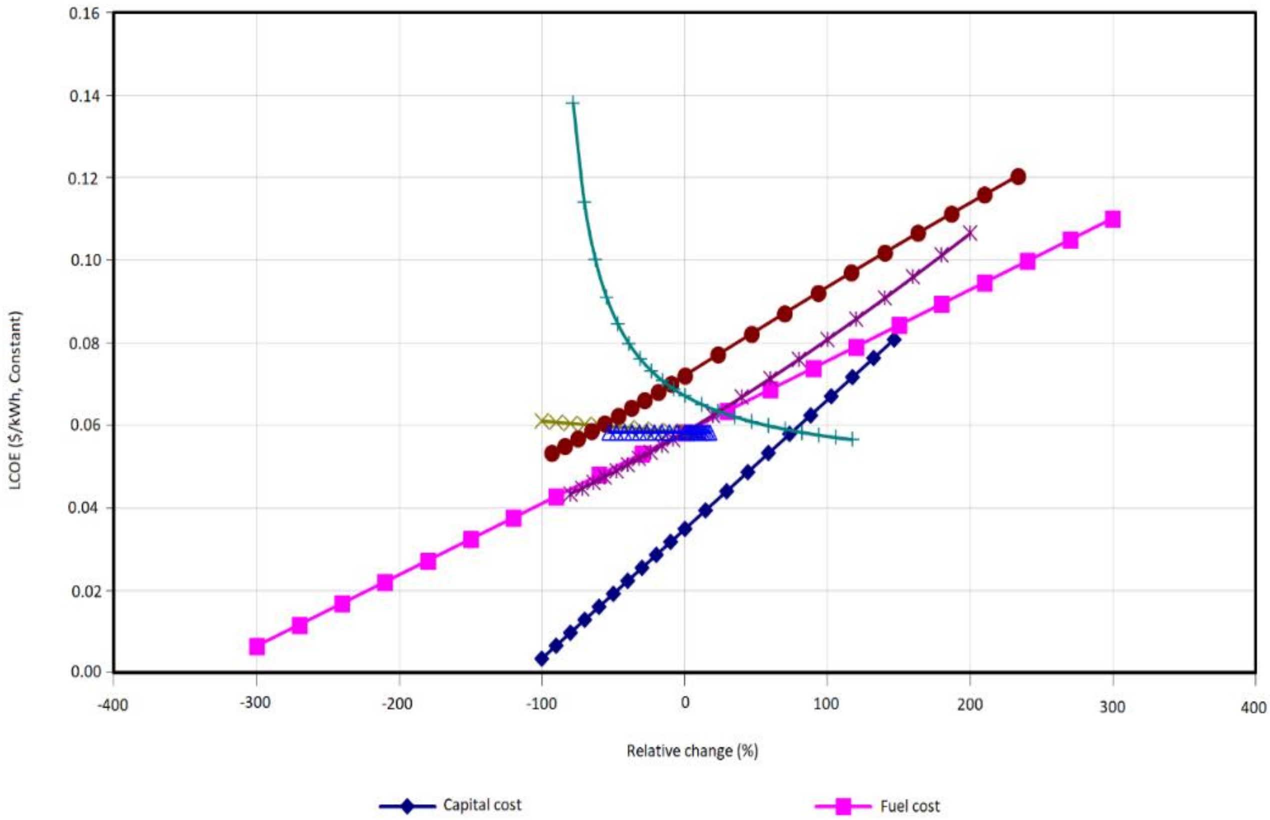

Fig. 6. Sensitivty analysis project

4. CONCLUSION

In the paper is analyzed techno-economic possibility for integration of anaerobic system and the biogas system in pig farms in Macedonia. The investment costs are assumed as 1.416.162 USD and the simple payback period for the considered financial conditions is less than 9 years.

According to the economic assessment results, it can be concluded that investment in cogeneration power plants in pig farms can be sustainable solution. With investing in biogas plant there are in general two main benefits: financial and ecological. Beside the financial and ecological benefits, the pig farms with CHP units has independent electricity and heat supply and as a byproduct-benefit are the fertilizers.

Summary variable and fixed costs are around 238.745 USD per year.

On annual basis compared with the existing system there are several main benefits: saved 20.000 liters light oil and production of 3295 MWh electricity.

The results from the NPV calculations, indicate that the whole project after the technical lifetime period of 20 years will be in economical positive with 540 770 USD with payback period of less than 9 years for the whole plant.

The LCOE method is applied in order to define the energy price for electricity and heat energy and compare with the market prices.

With the sensitivity analysis we could see all important factors or decision makers. One relative change to one factor can affect in direction of big cost of one amount energy. It should be noted, that each of the considered factors in the sensitivity analysis is important and need to be taken into account in the decision process. In the sensitivity analysis for the considered conditions, the electricity market price, the loan to equity ratio and cogeneration power plant efficiency have the main impact on the plant economic feasibility. The world trends which are indicating potential price escalations in electricity and fossil fuels, will positively reflect on the economic viability of biogas power plants.

REFERENCES

[1] Short, W., Packey, D. J., Holt, T. (March 1995): *Manual for the Economic Evaluation of Energy Efficiency and Renewable Energy Technologies*, Golden.

[2] Armenski, S. (2004): *Renewable Energy Sources*, NIP Studentski zbor, Skopje.

[3] Renewable Resources Agency, *Biogas Principal*, 2016.

[4] Tashevski, D., Seso I. (2012): *Integrated CHP of Biogas – Digester / Gas Turbine Combined*, "Ss. Cyril and Methodius" University in Skopje, Faculty of Mechanical Engineering, Macedonia.

[5] Dimitrovski, M., Dimitrovski, D, Spaskov, D. (2012): *Handbook for Intrested Users of Technology for Biogas on a Livestock Farm*, Faculty of Mechanical Engineering, Skopje.

[6] https://www.erc.org.mk/page.aspx?id=291, accessed: 1.08. 2023.

[7] Gas-Powered Series 500 (mtu-solutions.com), accessed: 1.08.2023.

[8] Wellinger, A., Baxter, D., Patrick Murphy, J. P. (2013): The Biogas Handbook: Science, Production and Applications,

[9] Tabatabaei, M., Ghanavati, H. (2018): *Biogas: Fundamentals, Process, and Operation*. Energy. ISBN: 978-3-319-77334-6, DOI:10.1007/978-3-319-77335-3

[10] Editor(s): Dieter Deublein, Angelika Steinhauser (2008): *Biogas from Waste and Renewable Resources: an Introduction*, Wiley, Library, Online ISBN:9783527621705 DOI:10.1002/9783527621705

Mechanical Engineering – Scientific Journal, Vol. **41,** No. 2, pp. 99–107 (2023)
Number of article: 669
In print: ISSN 1857–5293
Received: October 30, 2023
On line: ISSN 1857–9191
Accepted: November 22, 2023
UDC: 534.62-042.52:006.831
https://doi.org/10.55302/MESJ23412669099n

Short communocation

METHODOLOGY DEVELOPMENT AND PERFORMANCE TESTING OF AN ACOUSTICALLY ISOLATED BOOTH USING THE ISO 23351-1:2020 STANDARD

Elena Nakova, Ivica Stojanovski, Haritina Sakova, Simona Domazetovska Markovska, Maja Anačkova

Faculty of Mechanical Engineering, "Ss. Cyril and Methodius" University in Skopje, Skopje, Republic of North Macedonia
maja.anachkova@mf.edu.mk

A b s t r a c t: An acoustically isolated meeting booth is a specially designed structure used to isolate and reduce the level of speech. This pod is made in order to create a sound-isolated space, where you can work, record or perform sound in conditions of minimal noise and interference. Acoustically isolated pods are used for various applications such as music recording studios, movie theaters, conference rooms, and wherever it is important to limit sound transmission and ensure a quality acoustic environment. In this type of acoustically isolated rooms, acoustic characterization of all types of sound sources, as well as sound receivers, usually sound sensors, is carried out. The main objective of this research is to develop a methodology using the ISO 23351-1:2020 standard and test the performance of an acoustically isolated cabin. In addition to the primary goal of research, an additional goal is the analysis of the accuracy of the results obtained from a low-cost noise sensor through its comparison with a class 1 sound meter. The obtained results provide an opportunity for research and application of standardization that enables the development of a methodology for measurement and assessment of the characteristics of an acoustically isolated booth. In particular, the focus is on applying the methodology, measuring and comparing the results of noise measurements between a class 1 sound meter and a low-cost sensor unit.

Key words: acoustically isolated environment; sound sensors; measurement methodology; ISO 23351-1:2020 standard; acoustic measurements

РАЗВОЈ НА МЕТОДОЛОГИЈА И ТЕСТИРАЊЕ НА ПЕРФОРМАНСИ НА АКУСТИЧНО ИЗОЛИРАНА КАБИНА КОРИСТЕЈЌИ ГО СТАНДАРДОТ ISO 23351-1:2020

А п с т р а к т: Акустично изолираната кабина е специјално дизајнирана структура или простор што се користи за изолација и редуцирање на нивото на говор. Оваа кабина се изработува со цел да се креира звучно-изолиран простор, каде може да се работи, снима или изведува звук во услови на минимален шум, бучава и интерференции. Акустично изолираните кабини се користат за разни примени како што се студијата за снимање музика, кино-салите, просториите за конференции, и секаде каде што е важно да се ограничи преносот на звук и да се овозможи квалитетна акустична околина. Основна цел на ова истражување е развој на методологија користејќи го стандардот ISO 23351-1:2020 и тестирање на перформансите на развиена акустично изолирана кабина. Покрај примарната цел на истражување, како дополнителна цел е анализа на точноста на резултатите добиени од нискобуџетен сензор за бучава преку негова споредба со звукомер од класа 1. Добиените резултати даваат можност за истражување и примена на стандард кој овозможува развој на методологијата за мерење и процена на карактеристиките на акустично изолирана кабина. Фокусот е насочен кон примена на методологијата, мерење и споредба на резултатите од мерењата на бучава помеѓу звукомерот од класа 1 и нискобуџетната сензорска единица.

Клучни зборови: акустично изолирана средина; сензори за звук; методологија за мерење; стандард ISO 23351-1:2020; акустични мерења

1. INTRODUCTION

An increasing number of individuals now work in open-plan and activity-based offices [1], while schools, hospital wards, and public spaces like libraries and lounges are increasingly adopting open architecture [2]. In such open environments, studies have shown that those trying to focus on individual tasks fail due to the disturbing noise caused by nearby intelligible conversations and frequent phone ringing [3, 4, 5]. Additionally, effective communication often requires a certain level of speech privacy, which can be challenging to maintain in a bustling open space [6]. This has led to the need for a silent space, where individuals can finish important tasks when needed, as well as make phone calls, without disturbing the rest of the group.

Fully isolated rooms with enhanced sound isolation can be a big investment for large institutions [7], so this study has a primary focus on developing a methodology for testing compliance of a modular furniture setup with a chosen standardization. The setup is consisted of a portable enclosure that users can easily assemble and position within open spaces, offering both accessibility and a means to monitor occupancy. A secondary focus is using the booth to later compare low-cost and high-grade standardized Class 1 sound sensors, as well as hypothesize that a low-cost sensor can be used in standardized experiments to define a space's acoustic classification. For this, the ISO 23351-1:2020 standardization guidelines [8] were defined as the most suitable standard for developing the measurement methodlogy.

In the field of acoustics, research in cutting-edge materials [9] and understanding the importance of investing in sound-isolating environments has been growing [10]. Using the right materials and dimensions for the cabin results in better isolation quality and a better sound environment in the cabin [11]. To define the effectiveness of these environments, proper standardization is necessary [12], as well as developing cost-effective methodologies for its testing [13, 14]. Similar studies on such environments have been created in the past for industry-based working areas [15], as well as offices, where the focus was the speech privacy when making phone calls [16]. These enclosures are entirely enclosed and typically come equipped with essentials such as doors, electrical outlets, lighting, windows, and ventilation fans [17, 18].

The primary performance indicator for this type of acoustically isolated booths in terms of sound reduction, according to existing standardization, is the class division indicator. The class division of acoustically isolated cabins depends on the level of noise prediction and sound pressure and is usually expressed by classes A+, A, B, C, and D [19], as shown in Table 1.

The Class 1 sound level meter has high accuracy and allows several analyses in time and frequency domain, while the low-budget sensor unit can only show the sound level and will be used in this paper to explore its performance, but testing this sensor is crucial in making acoustic testing available for lower budgets. The results of this paper are part of a student project financed by the University of Ss. Cyril and Methodius in Skopje, North Macedonia.

Table 1

Class division of acoustically isolated cabins according to speech level reduction, thus speech privacy guarantee, following the ISO 23351-1:2020 standard guidelines

Class	Speech level reduction (dB)	Speech privacy guaranteed?
A⁺	> 33	Yes
A	30 – 33	Yes
B	25 – 30	Yes
C	20 – 25	Depends on background noise level
D	15 – 20	Depends on background noise level
Unclassified	< 15	No

2. METHODOLOGY

Proper definition of standardized measurements is of vital importance for this study. Initially, using the ISO 23351-1:2020 standard allows us to develop a methodology and select an appropriate experimental measurement protocol, including the choice of suitable sound sensors. With its assistance, it is defined and precisely determined which sound characteristics will be measured, which aids in a comprehensive segmentation and analysis of the sounds received in the isolated environment.

First, defining an environment where the isolation cabin will be placed is essential. The established standard acoustic conditions that largely prevent the penetration of external sources of noise must also be defined. If the room in which this cabin is located has windows, it needs to be positioned at least one meter away from the wall with the window and minimizing the number of objects in the room is necessary to reduce sound reflection [20].

The room in which the measurement is conducted should be a reverberation room that complies with the ISO 3741:2010 standard. One of the main criteria for accommodating an acoustically isolated environment is the size of the chosen room, which should have a minimum volume of 150 m^3 to be able to register a frequency of 125 Hz, while the volume of the cabin should be up to 5% of the volume of the room where the measurement will be performed [21].

According to the standard ISO 23351-1:2020 for analyzing the performance of acoustically isolated spaces, the measurement methodology is divided into four phases shown on Figure 1:

• **Phase 1:** Selection of hardware equipment.

• **Phase 2:** Defining 3 case studies.

• **Phase 3:** Defining measurement points and duration.

• **Phase 4:** Analysis, comparison, and validation of results.

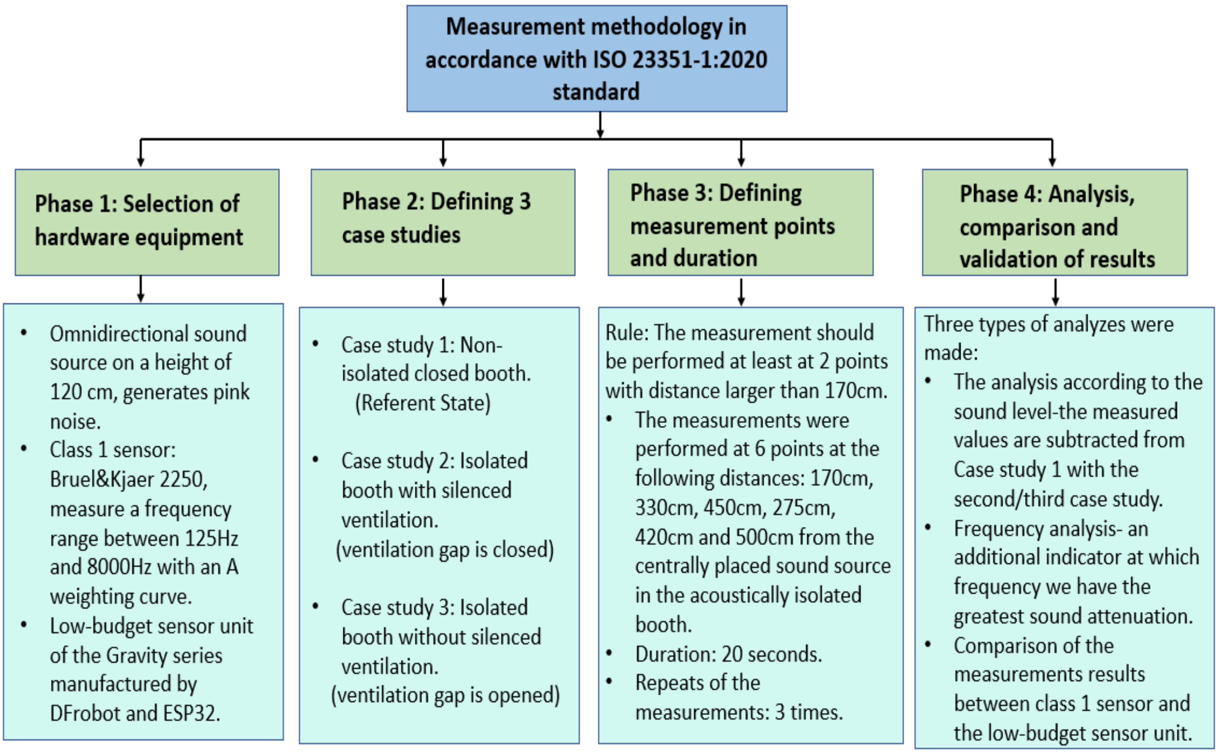

Fig. 1. Different phases of the measurement methodology following the ISO 23351-1:2020 standard

According to Figure 1, phase 1 is related to the hardware equipment, where Class 1 hand-held analyser is used for measuring the sound level, while the omnidirectional sound source is used for generating pink noise. To be able to do additional analysis, a low-cost budget sensor is used for seeing its performance.

The 2nd phase defines three case studies while performing the measurements, in order to be able to classify the booth. The initial referent measurement is performed in an open space, and in order to calculate the classes according to the speech level reduction, additional measurements in three case studies are performed. In the 1st case study, the measurement is performed while the sound source is in the booth without acoustically isolated materials, while in the 2nd and 3rd study cases, the booth is isolated. The difference between the 2nd and 3rd case study is the open and closed ventilation gap that is located on the top of the cabin.

The 3rd phase defines 6 measurement points, while at each measurement point the measurement is performed with time duration of 20 seconds and it is repeated 3 times. The 4th phase is related to analysis, comparison and validation of the gained results. According to the above defined phases, the experimental testing is done in the following section.

3. EXPERIMENTAL WORK

For better performance testing of the acoustically isolated booth, the sound level in the working environment was first measured without any isolating material and then various acoustic absorbers to improve sound absorption were added. This allowes obtaining multiple case studies with more results for analytical comparisons. The designed acoustically isolated environment shown in Figure 2 is designed to be used as a booth for a single occupant, while remaining more cost-effective than the currently available commercial cabins.

Fig. 2. Proposed prototype design of acoustically isolated booth for testing with dimensions of 2.2 × 1.5 × 1.5 m

Effective acoustic isolation is required to achieve good performance of the acoustically isolated booth. To implement this, several factors are taken into account, such as materials, construction, and sound transmission reduction [22]. When designing an effective acoustically isolated cabin, the following characteristics need to be considered: the chosen suitable acoustic materials should have good sound absorption and sound blocking properties, the room or object design with double or triple walls, floors, or roofs with air gaps between them should increase the space for sound isolation, and the use of acoustic materials that absorb sound would help reduce sound reflection in the space [23]. To achieve improved sound absorption, acoustic absorbers are of great importance. An absorptive material called "z-line" was used, made of high-quality polyester with a high coefficient of sound absorption for middle and high frequencies. Due to its open-cell structure and specific geometry, this corrugated absorber possesses exceptional sound isolation properties [24].

The designed booth was tested according to the developed methodology based on the standard ISO 23351-1:2020, while the measurement was carried out with 6 steps as shown on Figure 3.

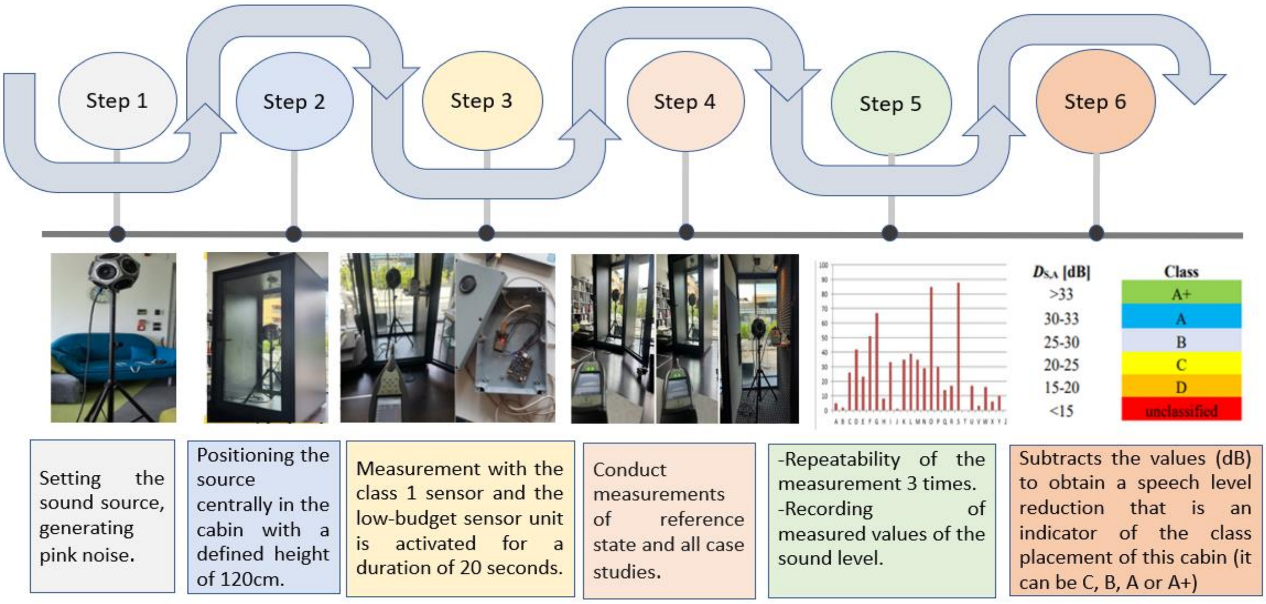

Fig. 3. Six steps of conducting the sound isolation measurements

Omnidirectional sound source with an amplifier according to ISO 3382-1, is a sound source that generates pink noise with a defined height of 1.2 m (from the floor) adapted for acoustic measurement tests made in cabins for a sitting position [25]. Sound level meters from Class 1 are the main indicator when doing measurements and obtaining valid results for the goals of this paper. On the other hand, the low-budget sensor can obtain results, but they cannot be verified according to the standard. The data collected from the low-cost sensor unit is compared with the results of a B&K Class 1 sound meter which is taken as a reference device with greater accuracy and precision in obtained values. Their working principle for the sound level meter Class 1 and the low-budget sensor is shown on Figures 4 and 5, respectively.

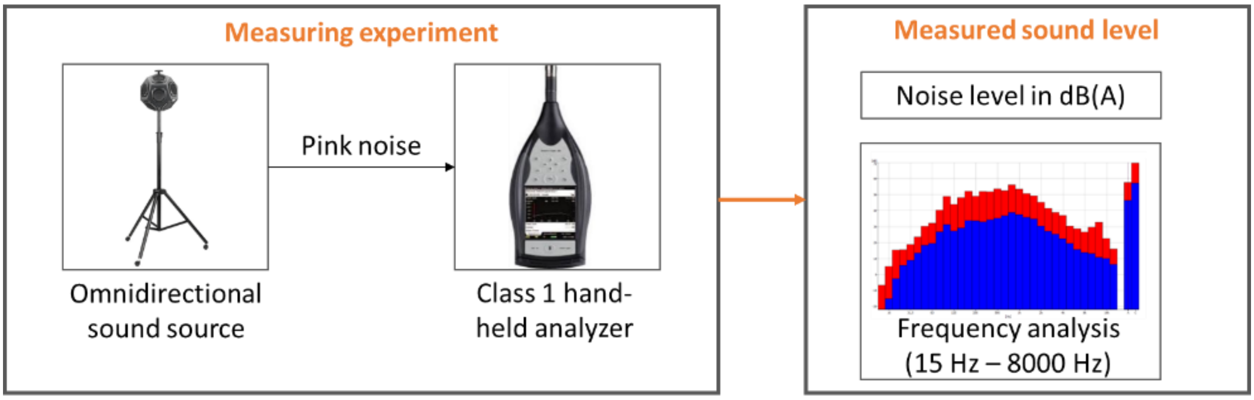

Fig. 4. Measuring experiments using the 1st class hand-held analyzer

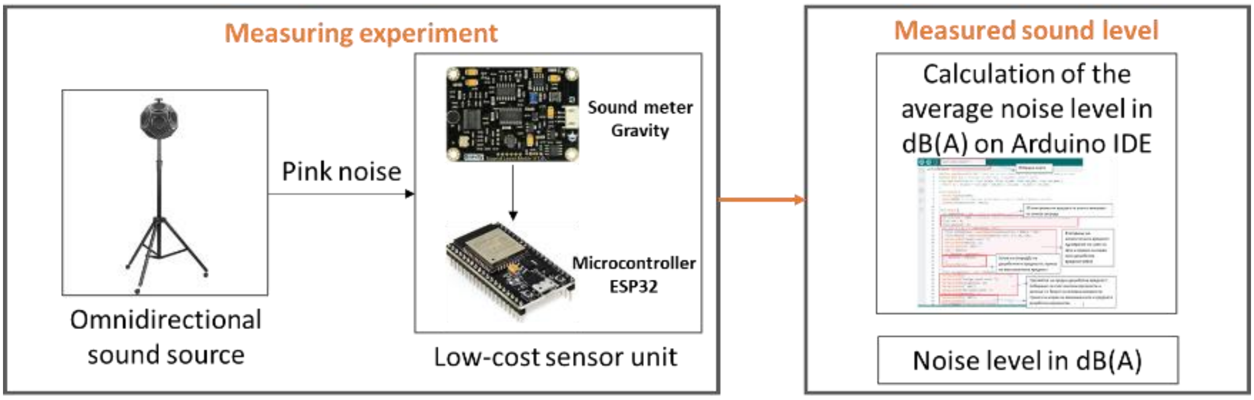

Fig. 5. Measuring experiments using the low-cost sensor unit

The B&K 2250 audiometer detects pink noise generated by the omnidirectional sound source and performs octave spectrum measurements, which means that it divides the entire audio spectrum into octave frequency bands. Specifically for this case, the frequency ranges are determined in accordance with the standard and are between 125 Hz and 8000 Hz with an A weighting curve. This analysis aims to determine how the intensities of different frequencies in the sound signal are distributed. The results are mean values from the 3 measurements. The low-cost sensor unit is consisted of Gravity Sound Sensor and sends the values to the ESP32 microcontroller, while the results that are sent to the Arduino IDE are average values of the sound level in dB(A) for 20 second interval, which means that 20 measured values (samples) enter this interval. The average equivalent sound value is calculated according to the formula:

$$L_{ekv} = 10 \times \log \frac{\sum_{i=0}^{n} 10^{\frac{ki}{10}}}{n}, \quad (1)$$

where *ki* is the *i*th measured value in dBA, while *n* is the number of measurements.

4. RESULTS AND DISCUSSION

4.1. *Analysis of the performance of the acoustically isolated booth*

In order to perform an analysis of the performance of the acoustically isolated booth in the three case studies, it is necessary to calculate the difference between these sound levels or subtract their values to determine the reduction in speech levels. The measurement was done using the Class 1 hand-held analyzer for the three case studies as shown in the methodology, while the results are shown on Table 2.

The sound power level (SWL) emitted by a loudspeaker is measured according to ISO 3741 in two phases: (1) without the product for a bare omnidirectional sound source, and (2) with the product including the omnidirectional sound source at the centrally defined position.

The mathematical principle of determining speech level reduction is presented below. First, the level reduction is determined in octave bands 125–8000 Hz. Level reduction, D_i (dB), is the difference between the sound power level measured in the two phases mentioned before.

$$D_i = L_{w,P,1,i} - L_{w,P,2,i}, \quad (2)$$

where $L_{w,P,1,i}$ (dB) is the sound power level radiated by the sound source without furniture ensemble, and $L_{w,P,2,i}$ (dB) is the sound power level radiated by the specimen when the sound source is inside the booth. The octave band is denoted with i and P indicates pink noise.

Second, the speech level reduction, $D_{s,A}$ [dB], is calculated. $D_{s,A}$ is a single-number quantity that expresses the corresponding reduction in Aweighted sound power level of standard effort speech within 125–8000 Hz. The value of $D_{s,A}$ is calculated by

$$D_{s,A} = L_{w,s,A,1} - L_{w,s,A,2} \quad (3)$$

$$D_{s,A} = L_{w,s,A,1} - L_{w,s,A,3} \quad (4)$$

where $L_{w,s,A,1}$ is the sound power level from case study 1 which is the referent state (Non-isolated closed booth) from who we are subtracting $L_{w,s,A,2}$ (sound power level of study case 2- Isolated booth with silenced ventilation) and $L_{w,s,A,3}$ (sound power level of study case 3 – Isolated booth without silenced ventilation.

From the results it can be seen that the difference between the first case study with an open cabin and the second case study is approximately 9 dB. Furthermore, when comparing the difference between the first and third case study, there is a 3 dB difference measured.

The most significant comparison observed is between case study 2 and case study 3, which shows a 7dB difference. This difference effectively highlights the effects of ensuring a quality soundproof ceiling and silenced ventilation, resulting in the maximum difference that grants the cabin a higher classification (in this case Class A with a potential for A+). Cabins in this class have the highest efficiency in noise isolation. They are able to isolate even the most audible noises and sound pressures, which makes them ideal for applications where the highest quality of isolation is most important.

Although the second case study provides the best results, it is not a realistic solution due to the need for proper air exchange in the cabin. Therefore, the most optimal solution is to upgrade the cabin with a ventilation system that facilitates air circulation and exchange between the cabin and the external environment while providing maximum sound attenuation.

Table 2

Results from the measurements for defining the speech level reduction of the booth in the three case studies

Measurement point	Case study 1 Speech level reduction of the non-isolated booth dB(A)	Case study 2 Speech level reduction of the isolated booth with silenced ventilation dB(A)	Case study 3 Speech level reduction of the isolated booth without silenced ventilation dB(A)
1	25.1	31.7	26.7
2	24.0	30.9	26.9
3	24.1	33.8	26.4
4	23.8	33.7	26.9
5	22.6	31.6	25.5
6	22.9	32.2	26.4

4.2. *Frequency analysis*

The frequency analysis serves for further analysing and observing at which frequency range there is the most significant noise mitigation. From the analysis of the results in Figure 6, at the representative point with distance of 4.5 m, the highest sound levels measured in the open state without soundproofing material are observed at frequencies of 1000, 2000 and 4000 Hz. The most significant reduction (difference) of 46.3 dB is observed at a frequency of 8000 Hz. The highest sound level occurs at a frequency of 2000 Hz, with a value of 70.76 dB.

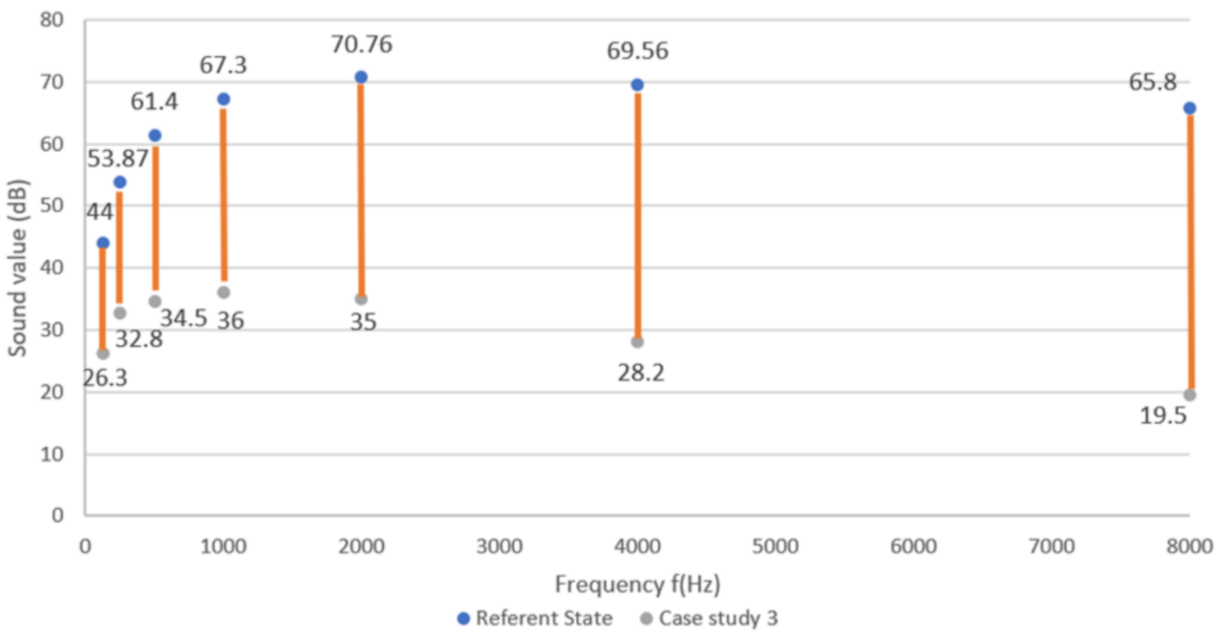

Fig. 6. Frequency data collected from representative measurement point 3

It can be noted that after isolating the cabin, the highest sound levels are found in the frequency range of 500 to 2000 Hz. Based on this, if further sound reduction is desired when selecting sound-proofing materials, it is necessary to choose a material that provides attenuation in these frequencies between 500 Hz and 2000 Hz.

4.3. *Comparison between the results of the low-cost sensor unit and Class 1 hand-held analyzer*

The results of the low-cost sensor unit compared with the sound level meter are analyzed. Table 3 shows the results where the smallest difference in measurements is between the Class 1 sound level meter and the low-budget sensor unit. This value is between 0,4 and 1 dB, meanwhile the highest difference is 3.3 dB. The results from the low-budget sensor unit can serve as a good indicator for representing the noise level but cannot be used when measuring according to a standard.

It can be noticed that the low-cost sensor unit gives higher values of the measured sound level than the 1st class hand-held analyzer. The results from the low-budget sensor unit can serve as a good indicator for representing the noise level but cannot be used when measuring according to a standard.

Table 3

Results from differences between noise level of the low-cost sensor and the Class 1 hand-held analyser

	Measurement point 1	Measurement point 2	Measurement point 3
	Difference in dB(A)	Difference in dB(A)	Difference in dB(A)
Case study 1	1	2.2	0.4
Case study 2	4.4	2.7	0.9
Case study 3	1.2	2.8	0.4
	Measurement point 4	**Measurement point 5**	**Measurement point 6**
	Difference in dB(A)	Difference in dB(A)	Difference in dB(A)
Case study 1	1	0.3	2.1
Case study 2	1.4	2.8	1.3
Case study 3	1	1.2	0.4

5. CONCLUSIONS

The developed methodology enabled an acoustic study of the acoustically isolated booth. From the obtained results and their analysis, it can be estimated that the booth exhibits adequate performance in terms of acoustic isolation, potentially allowing it to be Class B or Class A. Additional measurements and research are needed to accurately determine the class to which the acoustically isolated booth belongs. Using the equipment, a measurement of sound levels was performed, as well as a frequency analysis that could provide guidance for selection of materials for additional sound isolation for the cabin.

As part of the conducted measurements, an additional analysis included the evaluation of the accuracy of the low-budget sensor unit, which was enhanced with software that directly records results according to the requirements for this testing. The results from the low-budget sensor unit were compared with results obtained from a Class 1 instrument, indicating that the low-budget sensor unit can be a good indicator for assessing sound levels. However, for these types of analyses, a Class 1 sound level meter is still required for precise measurements.

Through this paper, a methodology has been developed in accordance with the ISO 23351-1:2020 standard, which can serve as a basis for testing various acoustically isolated cabins in the future. In addition, there is an opportunity to improve the standard's acoustic conditions in order to improve the class placement itself, as well as the opportunity to enrich the hardware equipment, application of new sensor technology, automation of measurements and generation of results, testing of other measuring instruments and thus to obtain better results.

REFERENCES

[1] Miller, G. N. (2014): Workplace trends in office space: implications for future office demand, *Journal of Corporate Real Estate*, Vol. **16**, No. 3, pp. 159–181. https://doi.org/10.1108/JCRE-07-2013-0016

[2] Fomina E. V., Barsukova N. I. (2022): Multilevel open urban spaces: current trends. *Urban Studies*. № 4. pp. 20–33. DOI: 10.7256/2310-8673.2022.4.38355 EDN: PFDIDI URL: https://en.nbpublish.com/library_read_article.php?id=38355

[3] Hongisto, V. (2005): A model predicting the effect of speech of varying intelligibility on work performance. *Indoor Air*, **15** (6), pp.458–468.

[4] Oldham, G. R., Daniel, B. J. (1979): Employee reactions to an open-plan office: A naturally occurring quasi-experiment, *Administrative Science Quarterly*, Vol. **24**, No. 2, pp. 267–84. JSTOR, https://doi.org/10.2307/2392497. Accessed 24 Nov. 2023.

[5] Toftum, J., Lund, S., Kristiansen, J., Clausen, G. (2012): Effect of open-plan office noise on occupant comfort and performance, Paper presented at the *10th International Conference on Healthy Buildings*, Brisbane, Australia.

[6] Sundstrom, E., Herbert, R. K., Brown, D. W. (1982): Privacy and communication in an open-plan office: A case Study. *Environment and Behavior*, **14** (3), 379–392. https://doi.org/10.1177/0013916582143007

[7] FIXR, Graham A. (2022): How much does it cost to soundproof a room?, 16.09.2022, URL:https://www.fixr.com/costs/soundproof-room#:~:text=The%20average%20cost%20of%20soundproofing,walls%20and%20redo%20the%20plaster.

[8] Standard ISO 23351-1-2020.

[9] Song, H., Ding, X., Cui, Z., Hu, H. (2021): Research progress and development trends of acoustic metamaterials, *Molecules*, **26**, 4018. https://doi.org/10.3390/molecules26134018

[10] Verified Market Research, "Global Acoustics Market Size by Material (Glass Wool, Acoustic Fabrics & Insulator, Fabric Absorbers Fabric Noise Barriers), by End-Use (Building & Construction, Industrial/HVAC & OEM, Transport), by Geographic Scope and Forecast", https://www.verifiedmarketresearch.com/product/acoustics-market/, 20.10.2023.

[11] Henke, M. (2022): *An Exploration of Architectural Acoustics and Design in Commercial Recording Studios*.

[12] Goydke H. (1997): New international standards for building and room acoustics, *Applied Acoustics*, Vol. **52**, Iss. 3–4, pp. 185–196, ISSN 0003-682X https://doi.org/10.1016/S0003-682X(97)00045-5.

[13] González, A. O. et al. (2019): Low-cost and easily implemented anechoic acoustic chambers https://doi.org/10.22517/23447214.18421

[14] Hongisto, V., Keränen, J., Virjonen, P., Hakala, J., *Test Method for Determining Sound Reduction of Furniture Ensembles*, Finnish Institute of Occupational Health, Lemminkäisenkatu 14–18 B, 20520 Turku, Finland., pp. 1–13.

[15] Nikulin A., Ikonnikov D., Afanasev P. (2020): Application of individual mobile soundproof cabin at process operator working area, *Journal of Applied Science and Engineering*, Tamkang University Press, https://doi.org/10.6180/jase.202006_23(2).0016

[16] Tschakert R. (2016): Telephone booths for confidential calls in office spaces, Institute of Noise Control Engineering, Proceedings of the *INTER-NOISE 2016*, 45th International Congress and Exposition on *Noise Control Engineering – Towards a Quieter Future* August 21–24, 2016, Hamburg, Germany, pages 6841–7829, pp. 7774–7778 (5), 21.08.2016.

[17] Tsunetoshi N, Tsuyoshi N. (2014): Investigation of the inlet and outlet location on the soundproofing ventilation unit. *The Open Acoustics Journal*, **7**, 1–7, Sojo University, Japan. Electronic publication date 31/12/2014. DOI: 10.2174/1874837601407010001

[18] Takashi Y., Sohei N., Yuya N., Huy Quang N., Tsuyoshi N. (2010): The Acoustic design of soundproofing doors and windows, *The Open Acoustics Journal*, **3**. 30–37, Kumamoto National College of Technology, 2659-2 Suya

Koshi shi Kumamoto, Japan, Electronic publication date 6/9/2010. DOI: 10.2174/1874837601003010030

[19] Hushoffice Team (2022): Figuring out the office acoustics. Class A or Class B office pods per ISO 23351-1:2020 – which is better, 21.03.2022
URL: https://hushoffice.com/en-us/figuring-out-the-office-acoustics-class-a-or-class-b-office-pods-per-iso-23351-12020-which-is-better/

[20] Keränen, J., Hakala, J., Laukka, H. (2020): Keränen et al. FA2023_ ISO 23351-2_392, Turku University of Applied Science, Turku, Finland, pp. 1–4.

[21] Jeong, J. H. (2023): Comparison of acoustics performance measurement and evaluation standard of office space and office acoustics criteria of European countries. *The Journal of the Acoustical Society of Korea*, **42** (2), pp. 133–142.

[22] Studiobricks, EDUCATION,
https://www.acousticabins.com/education/, 30.08.2023

[23] Buluklu, H. M., Koçyiğit, F. B. and Ercan, K. Ö. S. E. (2023): Low-cost alpha cabin like test box proposal for the development of new acoustic sound insulation materials. *Gazi University Journal of Science*, **63** (1), pp. 1–18.

[24] Zhang, X., Cheng, L. (2020): Acoustic silencing in a flow duct with micro-perforated panel liners. *Applied Acoustics*, **167**, https://doi.org/10.1016/j.apacoust.2020.107382.

[25] Christensen, C. L., Koutsouris, G., Rindel, J. H. (2013 June): The ISO 3382 parameters: Can we simulate them? Can we measure them? In: *Proceedings of the International Symposium on Room Acoustics*, Toronto, ON, Canada, Vol. **910**.

Mechanical Engineering – Scientific Journal, Vol. **41,** No. 2, pp. 109–113 (2023)
Number of article: 670
In print: ISSN 1857–5293
Received: November 18, 2023
On line: ISSN 1857–9191
Accepted: October 15, 2023
UDC: 629.326.017.2-551.454
https://doi.org/10.55302/MESJ23412670109v

Original scientific paper

DESIGN AND IMPLEMENTATION OF SELF-BALANCING MOTORCYCLE

Damjan Vasilevski, Damjan Pecioski, Simona Domazetovska Markovska

Faculty of Mechanical Engineering, "Ss. Cyril and Methodius" University in Skopje,
Skopje, Republic of North Macedonia
damjan.pecioski@mf.edu.mk

A b s t r a c t: In this research paper, an investigation was conducted into the development of mechatronic systems for two-wheeled vehicles, with a primary focus on a self-balancing motorcycle. The self-balancing motorcycle, which is currently in the developmental phase, has a primary objective of enhancing traffic safety by eliminating the requirement for external assistance. The study delves into its design, programming, and potential for further enhancement and eventual commercial utilization. Fundamental equations of bicycle dynamics were derived, and a PID controller, guided by MEMS sensor data, was employed for steering control. The paper encompasses the presentation of experimental tests and refinements to the feedback system, providing valuable insights into the system's overall performance. The research embarks on the intersection of technology, vehicle dynamics, and safety, laying the groundwork for future developments in these interconnected domains.

Key words: self balancing motorcycle; equations of motion; PID control; Matlab Simulink

ДИЗАЈН И ИМПЛЕМЕНТАЦИЈА НА САМОБАЛАНСИРАЧКИ МОТОЦИКЛ

А п с т р а к т: Во овој истражувачки труд е спроведено истражување за развој на мехатронички системи за возила на две тркала, со примарен фокус на самобалансирачки мотоцикл. Мотоциклот со самобалансирање, кој моментално е во фаза на развој, има примарна цел да ја зајакне безбедноста во сообраќајот преку елиминирање на потребата од надворешна помош. Студијата навлегува во неговиот дизајн, програмирање и потенцијал за понатамошно подобрување и евентуално комерцијално искористување. Изведени се равенки на динамиката на мотоциклот, а PID-контролер е употребен за контрола на управувањето. Трудот опфаќа презентација на усовршувања на системот за повратни информации, обезбедувајќи и прикажувајќи добиени резултати во севкупните перформанси на системот. Истражувањето започнува со почетокот на развојот на технологијата, динамиката на возилата и безбедноста.

Клучни зборови: самобалансирачки мотоцикл; равенки на движење; PID-контрола; Matlab Simulink

1. INTRODUCTION

In the rapidly evolving technological landscape the advancements of self-balancing vehicles marks a significant transformation in the field of transportation. As we observe this progression, it becomes increasingly important to delve into the development of smaller, energy-efficient vehicles, specifically focusing on two-wheeled self-driving motorcycles. The authors of [1, 2, 3] have delved into the study of the stability and dynamics of bicycles and how they affect its balance. In [4], a comprehensive review of dynamic modeling for single-track vehicles is presented. Some straightforward second-order dynamic models are introduced in [5] to examine the stability of balance in a bicycle. Conversely, certain researchers have delved into motorcycle dynamics using a multi-body approach [6, 7, 8], which, due to its complexity, is less suitable for control system design.

These compact vehicles offer distinct advantages in terms of space utilization and energy efficiency for individual transportation. To make these vehicles truly practical, the implementation of an effective balancing system is crucial. This research project primarily revolves around the development of a self balancing motorcycle (SBM) controlled by a microcontroller-based PID controller, aimed at enhancing its stability and navigational capabilities. While two-wheeled commercial human vehicles such as SEGWAY, NBot, and JOE have already entered the market, their high-tech, high-quality components have rendered them scarce, costly, and largely inaccessible. In contrast, this research project seeks to build a prototype using off-the-shelf components, thereby reducing costs and increasing accessibility. The scope of this research encompasses the assembly of the SBM robot, its mathematical kinematic modeling, and the design and implementation of an Arduino-based PID controller on the assembled robot. This scientific paper is part of an undergraduate thesis with the topic "Development of a concept of a mechatronic self-balancing motorcycle".

2. DERIVING EQUATIONS OF MOTION FOR A BALANCING MOTORCYCLE

The motorcycle balancing issue can be assumed as an inverted pendulum with an attached inertia wheel. The two primary assumptions are that:

A pendulum rod that is fixed to the ground via a revolute joint, thereby possessing one degree of freedom. For modeling purposes, it is assumed that the pendulum rod takes the form of a cylinder characterized by a radius denoted as 'r' in further equations.

An inertia wheel that is linked to the pendulum rod through an additional revolute joint. Similar to the pendulum rod, the inertia wheel is also represented as a cylinder, with a radius designated as 'R' in further equations. Notably, the axes of rotation for the two considered revolute joints are parallel to each other.

The model of the SBM which will be used in the following equations is represented in Figure 1, where *A* represents the rotation axis of the revolute joint connecting the pendulum rod to the ground and has a length l_{AD}, which corresponds to the length of the motorcycle frame. *B* signifies the center of mass of the pendulum rod. It's important to note that for our modeling purposes, we assume that the pendulum rod possesses a uniform density, which implies that point *B* is positioned at the midpoint between points *A* and *D*. *C* denotes the rotation axis of the revolute joint connecting the pendulum rod to the inertia wheel.

In this paper the system under consideration has two degrees of freedom and its state can be characterized using two coordinates: the angle θ, corresponding to the pendulum rod's lean angle, and the rotational speed of the inertia wheel ω.

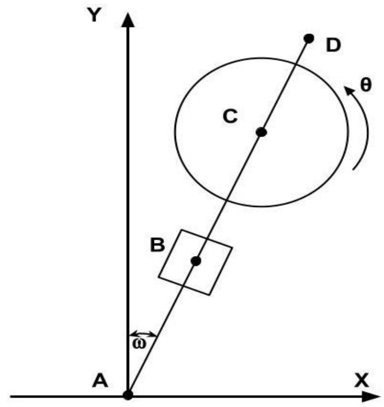

Fig. 1. Scheme of self-balancing motorcycle

The inertia wheel rotates around point *C*. and is in rotational movement about point *A* in conjunction with the pendulum rod. The parallel axis theorem is used in order to calculate the moment of inertia of the inertia wheel concerning point *A*, denoted as I_W^A

$$I_w^A = I_w^C + m_w l_{AC}^2 = 0.5 m_w R^2 + m_w l_{AC}^2 = \\ = m_w(0.5R^2 + l_{AC}^2), \quad (1)$$

where m_w is the mass of the inertia wheel and l_{AC} is the distance between the points *A* and *C*.

The pendulum rod rotates around point *A*, not its center of mass *B*, and its moment of inertia is given by the following equation:

$$I_r^A = I_r^B + m_r l_{AB}^2 = \frac{1}{12} m_r (3r^2 + l_{AD}^2) + m_r l_{AB}^2, \quad (2)$$

where m_r is the mass of the rod and l_{AB} is the distance between points *A* and *B* and l_{AD} is the distance between points *A* and *D*.

The torque τ_m of the inertia wheel is given by the following two equations:

$$\tau_m = I_w^C (\omega^{\cdot} + \theta^{\cdot\cdot}) \quad (3)$$

$$\tau_m = 0.5 m_w R^2 (\omega^{\cdot} + \theta^{\cdot\cdot}) \quad (4)$$

Next step is bringing the above equations of motion to state-space format which is defined as:

$$x^{\cdot}(t) = (\theta^{\cdot}\ \theta^{\cdot\cdot}\ \omega^{\cdot}) = \\ = \left(\theta^{\cdot}\ \frac{(\theta)\,(m_r l_{AB} + m_w l_{AC}) - \tau_m}{m_w(0.5R^2 + l_{AC}^2) + \frac{1}{12} m_r (3r^2 + l_{AD}^2) + m_r l_{AB}^2}\ \frac{\tau_m}{I_w^C} - \theta^{\cdot} \right) \quad (5)$$

Finally this equation is used in the software to model the dynamic behavior of the system and in designing the feedback controller

3. BLOCK-BASED MODELING OF THE MOTORCYCLE MOTION

The programming the motorcycle's motion is done through the use of block-based modeling. The modeling process is organized in design phases with a specific objective, ultimately leading to the attainment of the Final Code. In the initial phase of programming within Matlab Simulink, the emphasis is on parameter configuration to facilitate the creation of a simulation model for the motorcycle's motion. Additionally, an algorithm is devised to maintain the vehicle's balance under varying external conditions. Within this phase, a proportional-derivative (PD) controller is implemented to determine the motorcycle's lean angle and its rate of change over time. These parameters are leveraged to construct a Simulink model aimed at regulating the flywheel's speed, thereby contributing to the motorcycle's balance. To achieve this a Simulation Data Inspector (SID) shown in Figure 2 is implemented.

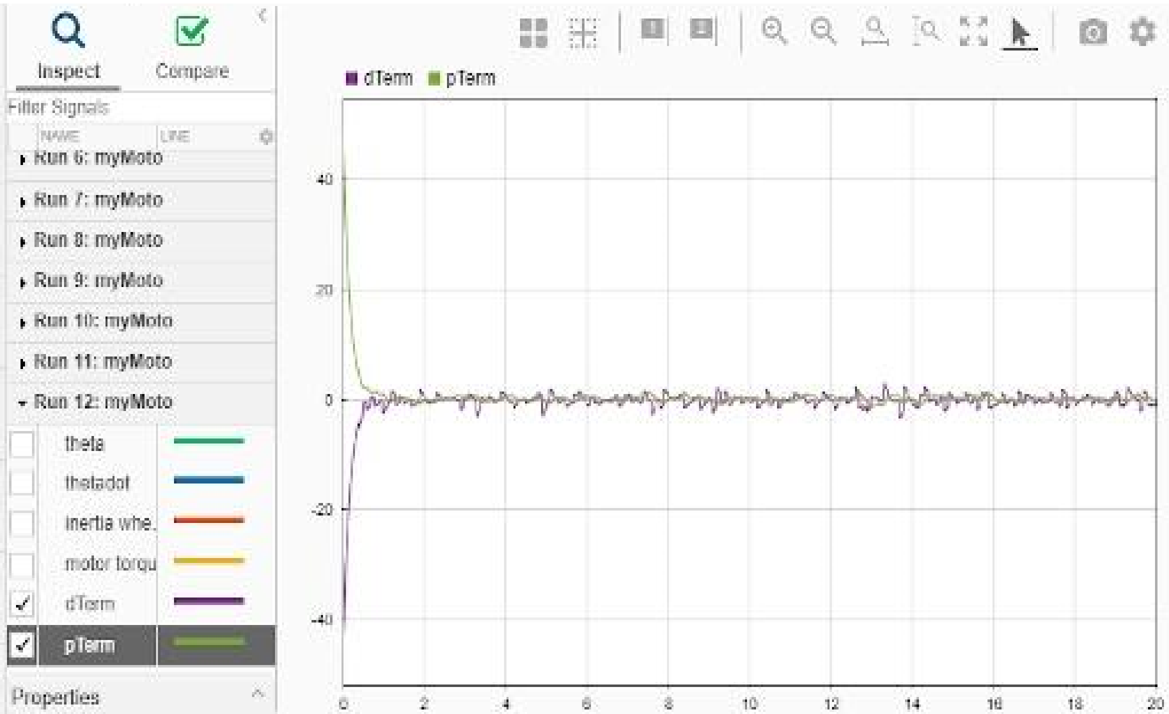

Fig. 2. Control terms in the Simulation Data Inspector (SDI)

The second phase focuses on developing Simulink models to govern the motorcycle's hardware components. Custom algorithms are introduced, enabling direct deployment to the controller from Simulink and the necessary connections with the PD control algorithm are established.

Within the next phase a wireless connection is established and the motorcycle is balanced while moving in a straight path, either forward or backward. To accomplish this, a Wi-Fi connection is established between the controller and the computer, allowing remote monitoring of the motorcycle's status and computer signals without physical linkage. The actuation of the motorcycle is through the rear wheel and the balancing is achieved by the flywheel and gyroscope information from the IMU sensor.

The final phase incorporates the control of the steering servo-motor, enabling left and right maneuvers. This phase tests the ability of the control algorithm to maintain balance while the motorcycle undergoes turns. The act of turning introduces an additional torque component along the wheel-ground axis, necessitating compensation by the flywheel. Altering the steering angle prompts the servo motor to swiftly shift the steering column from its initial angle to the target angle.

4. RESULTS AND DISCUSSION

The final results of the undergraduate thesis are the construction and real time control of a self balancing motorcycle using Matlab Simulink. Having modeled the dynamics of the system and derived the equations of motion the final proportional derivative control could be designed and implemented in order to achieve a stable system. The prototype of the self balancing motorcycle can be seen in Figure 3.

The control of the motorcycle is done through a wireless, Wi-Fi, connection between the MKR1000 controller on the motorcycle and Matlab Simulink. This control allows the motorcycle to move independently without the need of being connected to a computer which will hinder its movements and affect its capabilities. The final code that is used in order to control and balance the motorcycle is given in Figure 4.

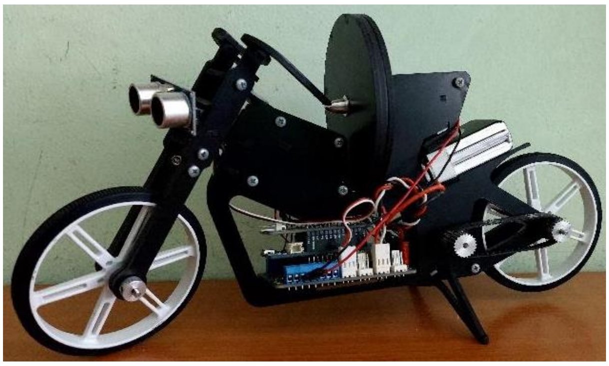

Fig. 3. Prototype of a self-balancing motorcycle

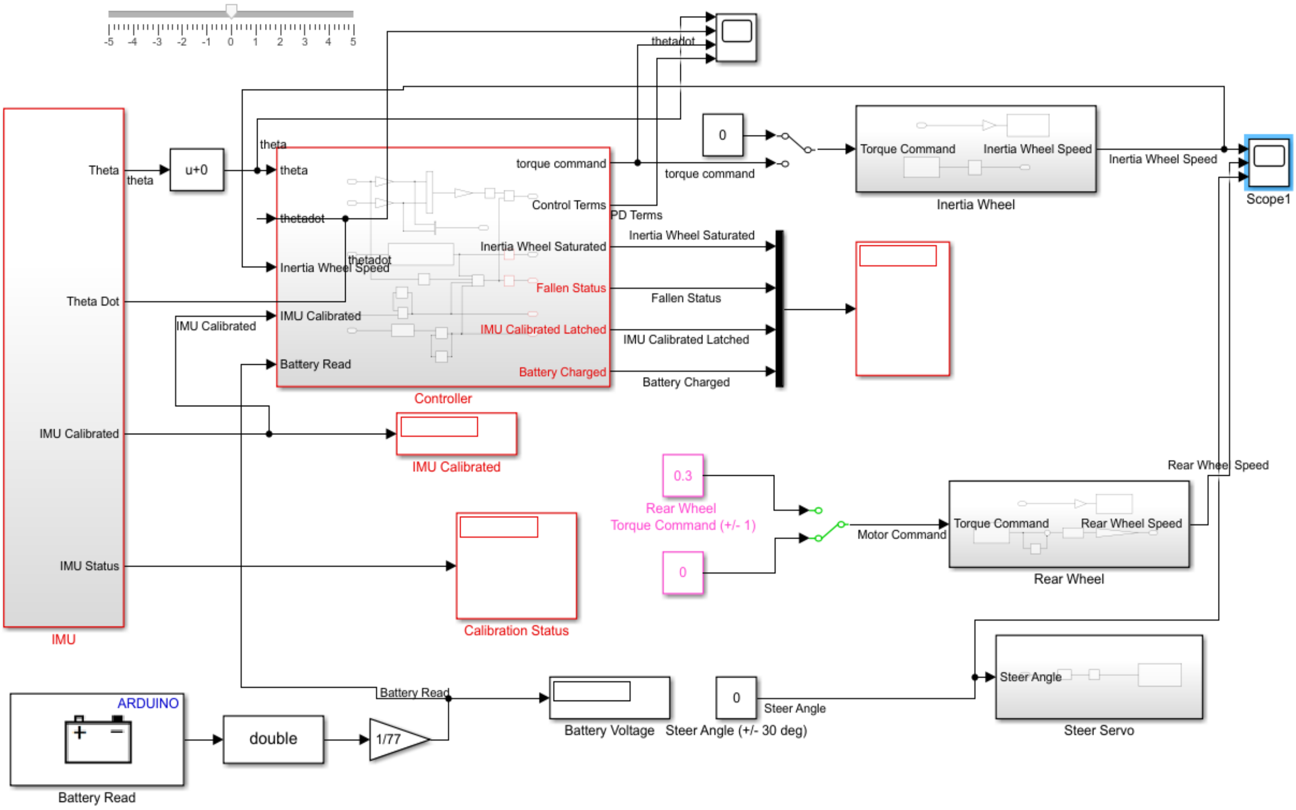

Fig. 4. Schematic of the Final matlab code

The code has multiple aspects which incorporate all of the hardware components on the motorcycle. The IMU sensor gives three-dimensional acceleration, yaw rate and magnetic field strength data in 3 perpendicular axes. This data is used to get the angle and speed at which the motorcycle is leaning in order for the flywheel to stabilize the system. The information from the IMU sensor is fed into the controller which calculates the torque needed for the inertia wheel in order to balance the motorcycle. The PD control is used in order to control the flywheel based on the data from the IMU sensor in order to achieve balance of the motorcycle while the other movements, such as speed of the actuating wheel and the steering are done by user input. The rear wheel speed is commanded as a fractional duty cycle with positive values indicating forward motion and a manual switch is provided to enable or disable the rear wheel motor. While steering of the motorcycle is done by manually inputting the angle at which the motorcycle should turn.

5. CONCLUSION

Within this paper the dynamics of a self balancing motor were presented and its equations of motion have been derived.With the use of Arduino hardware components have been used in the construction of the prototype of the self balancing motorcycle and matlab simulink in its operation. Tuning of the PD controller has been made in order to stabilize the system and ensure it will not fall over while riding. Future work will encompass the addition of extra weight to the motorcycle which will shift position to simulate a rider. Scaling the motorcycle to a bigger version and seeing the hardware needs and costs for such a solution. Finally the work will be done in automating the full system not just the balancing of the motor, this will incorporate automating the steering and the speed of the motorcycle so that they are no longer user input defined but defined based on a task.

Acknowledgement: The authors wish to thank Prof. Viktor Gavriloski Ph.D., from the Faculty of Mechanical Engineering in Skopje for his contributions in this work. This work has been made as part of an undergraduate thesis under the mentorship of Prof. Gavriloski. The construction and practical testing of the self balancing motorcycle have been made in the laboratory of mechatronics in the Faculty of Mechanical Engineering in Skopje.

REFERENCES

[1] Limebeer, D. J., Sharp, R. S. (2006): Bicycles, motorcycles, and models. *IEEE Control Systems Magazine*, vol. **2**6. no. 5. pp. 34–61.

[2] Koenen, C. (1983): *The dynamic behaviour of a motorcycle when running straight ahead and when cornering*, Doctoral dissertation, Delft University.

[3] Schwab, A. L., Meijaard, J. P., Papadopoulos, J. M. (2005): Benchmark results on the linearized equations of motion of an uncontrolled bicycle. *Journal of Mechanical Science and Technology*, Vol. **19**, pp. 292–304.

[4] Kooijman, J. D. G., Schwab, A. L. (2011): A review on handling aspects in bicycle and motorcycle control. In: *Proceeding of the ASME International Design Engineering Technical Conferences and Computers and Information in Engineering Conference*. Vol. **54815**, pp. 597–607. DOI:10.1115/DETC2011-47963

[5] Lowell, J., McKell, H. D. (1982): The stability of bicycles. *American Journal of Physics*, Vol. **50**. no. 12, pp. 1106–1112.

[6] Kessler, P. (2004): *Motorcycle navigation with two sensors*. Master thesis, Department of Mechanical Engineering, University of California, Berkeley, CA.

[7] Sharp, R. S. (2001): Stability, control and steering responses of motorcycles. *Vehicle System Dynamics*, Vol. **35**, no. 4–5, pp. 291–318.

[8] Cossalter, V. (2006): *Motorcycle Dynamics*. Lulu. com. ISBN 9781430308614

Mechanical Engineering – Scientific Journal, Vol. **41,** No. 2, pp. 115–121 (2023)
Number of article: 671
Received: November 3, 2023
Accepted: December 4, 2023
In print: ISSN 1857–5293
On line: ISSN 1857–9191
UDC: 621.791.5.037:004.896
https://doi.org/10.55302/MESJ23412671115k

Original scientific paper

PROCEDURES OF WELDING METAL PRODUCTS WITH MIG/MAG ROBOT WELDING

Aleksandra Krstevska, Filip Zdraveski, Zoran Bogatinoski

Faculty of Mechanical Engineering, "Ss. Cyril and Methodius" University in Skopje, P.O.Box 464, MK-1001 Skopje, Republic of North Macedonia
aleksandra.krstevska@mf.edu.mk

A b s t r a c t: This research paper describes robot welding programming and different approach of three applications in manufacturing processes by welding. It gives an overview of robot manipulator and its main components. For the experimental work a 6-axis robot arm is used and three different welds are made. Detailing of programming for every example with or without synchronization with the positioner and the trajectory is discussed. The paper presents steps of software development for online programming of a robot arm with or without synchronization.

Key words: robot; welding; programming

ПОСТАПКИ НА ЗАВАРУВАЊЕ МЕТАЛНИ ПРОИЗВОДИ СО РОБОТСКОТО ЗАВАРУВАЊЕ МИГ/МАГ

А п с т р а к т: Овој труд го опишува програмирањето на роботското заварување и различниот пристап на три апликации во производните процеси со заварување. Даден е преглед на робот манипулатор и неговите главни компоненти. Во експерименталниот дел се користи роботска рака со 6 оски и се направени три различни завари. Дискутирани се деталите на програмирањето за секој пример со или без синхронизација со позиционерот и траекторијата. Во трудот се претставени чекорите на развој на софтвер за онлајн програмирање на роботска рака со или без синхронизација.

Клучни зборови: робот; заварување; програмирање

1. INTRODUCTION TO ROBOTIC WELDING

Robots are very important equipment in today modern industry. The international standard ISO 8373:2012 defines a robot as "an actuated mechanism programmable in two or more axes with a degree of autonomy, moving within its environment, to perform intended tasks" [1]. Robot refers to any device or mechanism that performs intended tasks and meets three conditions at the same time: sense, think and act. Depending on the application area the classification in ISO 8373:2012 is accepted as industrial robots and service robots.

Welding plays a significant role in manufacturing, particularly in industries that use complex metal components and structures. One of the advantages of welding is the creation of joint with high strength but as disadvantage is the heating of the metal up to temperature of recrystallization and creating changes in thermos-deformation cycle [2].

To perform a quality weld requires experienced personnel who can control the process of welding. With the development of technology, creating a quality weld in short time and low cost for manufacturer become a need. With the development of Industry 3.0 and Industry 4.0 the automation of physical production processes is a key component for improving productivity and robots have played an important role in the automation of various operations, simultaneously enhancing the quality of manufactured products [3].

There are a huge number of products that require welding operations in their assembly processes and that is why industrial robots are most popular applications of robotics worldwide [4]. The car industry is probably the most important example, with the Metal Inert Gas (MIG) / Metal Active Gas (MAG) welding operations in the car body workshops of the assembly lines [5]. Nevertheless, there are an increasing number of smaller businesses, client oriented, manufacturing small series or unique products designed for each client. These users require a good and highly automated welding process in a way to respond to client needs in time and with high quality.

2. MIG/MAG ROBOT WELDING

Welding is the key factor in the development of industry, of every new construction made with metallic materials produced or used in constructions. In assembly processes every product requires welding operations with a good and highly automated welding process and to respond to client needs in time and quality.

MIG/MAG weldings, according to ISO 4063, proceses number 131 and 135 [6], respectively are widely used welding processes in industrial sector [7]. Uses heat created from an electric arc between a consumable metal electrode and a workpiece, creating a weld pool and fusing them together, forming a joint. The weld pool and the arc are protected from the environment and contaminants by a shielding gas, inert or active, depending on the chosen welding process.

Robotic welding is far from being a solved automatic technological process and this is due to the complexity of the process, difficult to parameterize and to effectively monitor and control. When welding with MIG/MAG, the process imposes extremely high temperatures concentrated in small zones, which makes the material experiencing extremely high and localized thermal expansion and contraction cycles, which introduce changes in the materials that may affect its mechanical behaviour along with plastic deformation [8].

3. COMPONENTS OF ROBOT WELDING STATION

A basic robotic arc welding station is composed of two subsystems: the welding equipment delivering the energy from the welding power source to the workpiece and the robot providing relative positioning of the heat source and the workpiece [9]. A typical robotic arc welding station includes moving mechanisms: welding tool manipulator aimed at moving the weld torch with required speed and orientation relative to the weld joint and positioning table for manipulation of the work piece (Figure 1). In this paper six-axis industrial welding robot is analyzed which is composed of a three-axis lower arm and a three-axis wrist, and they enable the welding torch mounted at the wrist to achieve all positions necessary for welding.

One of the integral parts of robotic welding station is the sensor technology. Sensing technologies designed for robotic welding are the essential elements for creating the desired level of control automation and monitoring. The sensors observe and measure process parameters, they are the input to the control system. With this input information the control system adapts output with the defined welding procedure specifications.

Another essential part of the robotic welding system is the robotic positioner whose role in the system is to hold, to rotate and reposition the part for the welding robot so that can reach the entire piece. It is obtained higher productivity and help automate tasks that would be impossible without rotational capabilities.

Fig. 1. Robotic arc welding station

4. EXPERIMENTAL WORK

For the experimental work a robot arm is used that has 6-axis movement. It is used in industry for advanced systems for adding filler material. The maximum range of the robot arm is 1374 mm and maximum payload is 6 kg (Figure 2).

Fig. 2. Robotic manipulator

The mobile unit has the function of managing the robot, including manipulation of all the processes required for welding. All functions such as programming are performed through the mobile unit for management and communication with the robot controller which is shown on Figure 3. The robot welding torch (Figure 4) is the element which stands on the arm of the robot, it has the function of a wire transmitter and conductor of the protective gas. With the help of the torch, a stable arc is created and thus a good weld joint.

Fig. 3. Mobile management unit AUR 010558

Fig. 4. Robot welding torch

5. AN APPROACH TO WELDING ROBOT PROGRAMMING

Programming of the robot remains the most costly and time-consuming task which demands a high degree of precision and reliability and basic knowledge of programming and robotics of the operator [10, 11].

Robot programming methods of industrial robots which play vital roles in welding are divided into online and offline programming [12]. With offline programming the method does not requires the robot and a virtual representation of the robot and its workspace is constructed. With online programming the method requires the presence of the robot and consists of recording the path with a management unit.

5.1. *Synchronized programming of chair*

The programming is done online with the mobile management unit. The trajectory of programming is shown in Table 1 and discussed below.

The next step is testing the program without welding, with good visual trajectory, approaching the future weld. The weld is performed with synchronization, the positioner rotates, moves, and the weld is performed in the best possible welding position. The welding program has 16 positions, the whole chair requires about 457 welding positions. There is a total of 10 complete or 20 individual welds. The welding process of the chair is 5 minutes (Figure 5) and on Figure 6 is shown one completed weld of the chair.

Table 1

Trajectory of the programming

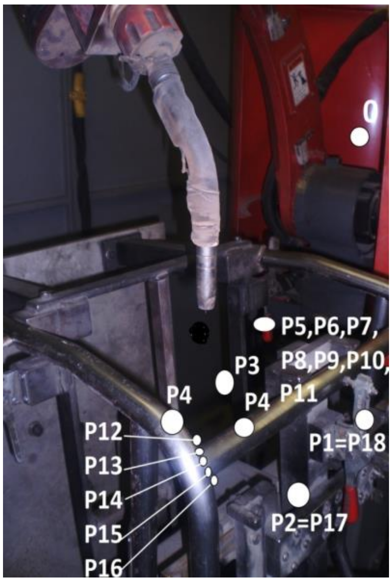

Position name	Task description
P0	Reset the sensor from the previous program (0 position).
P1	Deleting the previously saved points.
P2	Turn on the sensor before start.
P3	Approaching to tube with speed of 0.3 m/min
P4	Tube check with the weld torch, where there is a closed-circuit sensor
P5	Is saved as point GDI
P6	After each saving of the point the sensor is reset for a new point
P7	The sensor turns off
P8	Command to read the points, recall from memory
P9	Referring to sensed position
P10÷11	Moves according to sensing, the starting point is synchronized with the previous points
P12÷16	Setting the weld trajectory with 5 – points and speed S = 0,3 m/min, A = 90, V=14,7.
P17	Position 17 – turn off the sensor
P18	Resetting the sensor and erasing the previous points, returning to position 1
	Return to zero position.

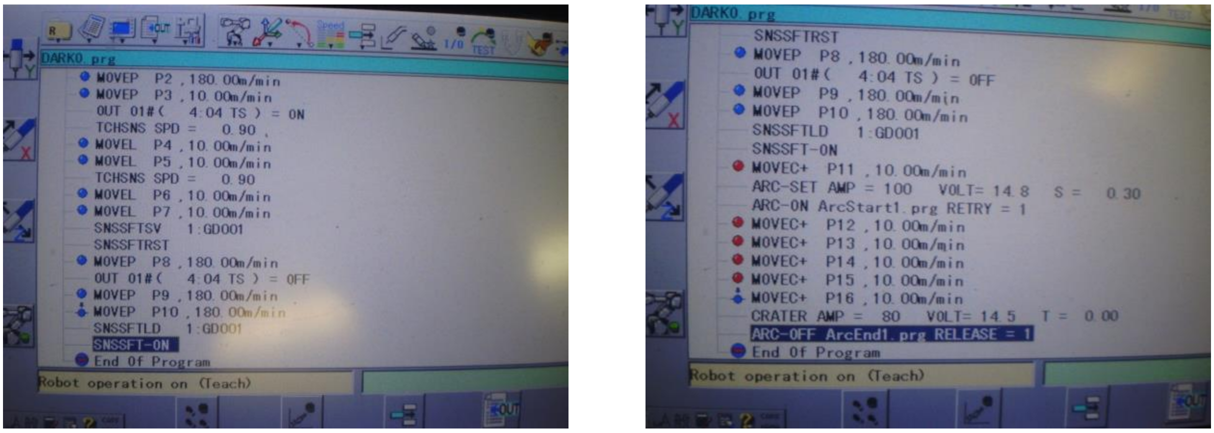

Fig. 5. Online programming of welding chair

Fig. 6. Completed weld with 16 positions

5.2. *Non-synchronized programming welds on "Plate 1"*

Welding programming is performed by online method, indirectly, where the welding program for the "Plate 1" is programmed with the mobile control unit. In non-synchronized welding the positioner does not rotate. The welding movement is performed by the robotic arm that moves along a given programmed trajectory. In such non-synchronized welding, welding in vertical or overhead position is not applied (Table 2).

Welding parameters are following:

- Welding current: 80-85 A
- Welding voltage: 14.5 – 14.8 V
- Welding speed: 10m/min

To perform all three welds, 20 positions were programmed, run the program without welding which is required for visual inspection and then perform the welding itself.

T a b l e 2.

Trajectory of programming of Plate 1

Position name	Task description
P0	Resetting the sensor from previous programs
P1	Deleting previous saved points
P2	Before starting linear movement, the sensor is turned off
P3	Starting point for the weld trajectory
P4	End point of the trajectory for the first weld
P5	Switch off the sensor
P6	After each point saving, the sensor is reset for new points
P7÷11	Moving along the weld trajectory and saving points
P12	Turn off the sensor
P13	After each point saving, the sensor is reset for new points
P14÷18	Turns on circular motion and moves along the trajectory of the circle
P19	Turn off the sensor
P20	Resetting the sensor and erasing the previous points
	Return to zero position

5.3. *Non-synchronized programming of "Plate 2" example with set amplitudes of welding gun movement*

In the third experiment, it is performed non-synchronized programming of example "Plate 2" with set amplitudes of movement of the welding gun. The welding parameters are the same as example no. 2, plate 1. To perform all three welds, 25 positions needs to be programmed. The program runs without welding, which is necessary for a visual inspection and then performing the welding. Non-synchronized welding with set amplitudes produces a wider weld and is used in thicker materials where a larger deposit of filler material is required (Table 3).

Welding parameters are following:

- Welding current: 80 – 85 A
- Welding voltage: 14.5 – 14.8 V
- Welding speed: 10 m/min.

To perform all three welds, 25 positions were programmed. Then run the program without welding, which is necessary for a visual inspection and then to perform the welding itself. Non-synchronized welding with set amplitudes produces a wider weld and is used in thicker materials where a larger deposit of filler material is required.

Table 3

Trajectory of programming of plate 2

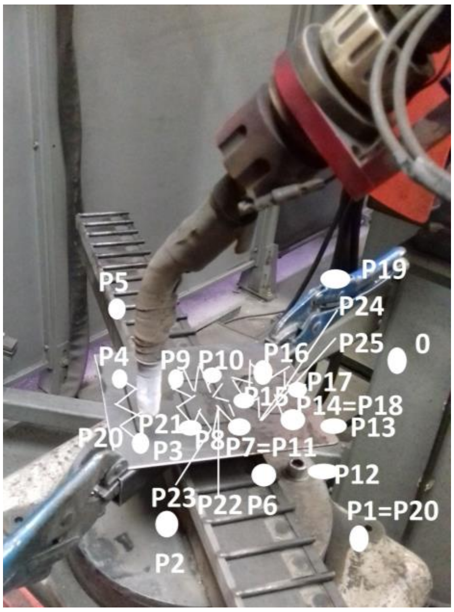

Position name	Task description
P0	Resetting the sensor from previous programs
P1	Deleting previous saved points
P2	Before starting linear movement, the sensor is turned off
P3	Starting point for the weld trajectory
P4	End point of the trajectory for the first weld
P5	Switch off the sensor
P6	After each point saving, the sensor is reset for new points
P7÷11	Moving along the weld trajectory and saving points
P12	Turn off the sensor
P13	After each point saving, the sensor is reset for new points
P14÷18	Turns on circular motion and moves along the trajectory of the circle
P19	Turn off the sensor
P20	Resetting the sensor and erasing the previous points
	Return to zero position

6. CONCLUSIONS

One of the important advantages of automated welding is precision and productivity. Robotic welding has an advantage over manual welding, the program is written only once, and will always produce precise and identical welds on parts with the same dimensions and specifications.

Automated gun movements reduce potential error, which plays a major role in production, waste management and repairs. With robotic welding, the risk of injury is minimized, and the impact of harmful fumes is minimized by distancing the worker from the work area.

The first example is performed with synchronization, the positioner rotates so that the welds are performed with positions that does not requires overhead and vertical welding. The second example is performed without synchronization, the positioner does not rotate and welding is performed in a plane. The second and the third example are performed without synchronization, but the third example is with set amplitudes of welding gun movement. Thus, the third example gives a wider weld than the second. This type of welding is used for thicker materials where it is necessary larger deposit of filler material.

REFERENCES

[1] ISO 8373:2012. *Robots and Robotic Devices*

[2] Runchev, D. (2014): *Tehniki na spojuvanje*. Univerzitet “Sv. Kiril i Metodij”, Skopje.

[3] Farkas, A. (2018): *IOP Conf. Ser.: Mater. Sci. Eng.* **448** 012034.

[4] United Nations and International Federation of Robots. *World Industrial Robots 1996: Statistics and Forecasts.* New York: ONU/IFR, 2000.

[5] https://www.fronius.com/en/welding-technology/world-of-welding/robotic-welding-automotive-industry [Accessed on 16th March 2023]

[6] ISO 4063:2009: Welding and allied processes – Nomenclature of processes and reference numbers.

[7] Pal, K., Pal, S. K. ((2011): *Eng. Perform*., **20**, 918–931.

[8] Loureiro, A., Velindro, M., Neves, F. (1998): *The Influence of Heat Input and the Torch Weaving Movement on Robotized MIG Weld Shape*. 10. 85–91.

[9] https://www.twi-global.com/technical-knowledge/job-knowledge/robotic-arc-welding-135 [Accessed on 23th May 2023]

[10] Calinon, S. (2018): Learning from demonstration (Programming by demonstration), Ang, M. H., Khatib, O. and Siciliano, B. (eds), *Encyclopedia of Robotics,* Springer.

[11] Zhang, F., Lai, C. Y., Simic, M., Ding, S. (2020): Augmented reality in robot programming, *Procedia Computer Science,* vol. **176**, pp. 1221–1230.

[12] Kaczmarek, W., Panasiuk, J. (2017): *Programming Industrial Robots;* PWN Scientific Publishing House: Warsaw, Poland.

Mechanical Engineering – Scientific Journal, Vol. **41,** No. 2, pp. 123–129 (2023)
Number of article: 672
Received: November 6. 2023
Accepted: December 15, 2023
In print: ISSN 1857–5293
On line: ISSN 1857–9191
UDC: 658:[330.341:004
https://doi.org/10.55302/MESJ23412672123a

Original scientific paper

ENHANCING MANUFACTURING EFFICIENCY: A LEAN INDUSTRY 4.0 APPROACH TO RETROFITTING

Aleksandar Argilovski, Ema Vasileska, Bojan Jovanoski

Faculty of Mechanical Engineering, "Ss. Cyril and Methodius" University in Skopje, Skopje, Republic of North Macedonia
aleksandar.argilovski@mf.edu.mk

A b s t r a c t: Industry 4.0 technologies are already affecting global supply chains by revolutionizing how companies manufacture and distribute their products and services. Many companies are affected by this transformation, especially small and medium-sized enterprises (SMEs) that are keen to enhance their market competitiveness as quickly and easily as possible. The transformation from traditional approaches to Industry 4.0 can bring many benefits, however, this transition involves adopting technologically advanced machinery with a high level of digitalization and communication. The cost and time to replace old machines could be unsustainable for many SMEs and that is why these enterprises seek alternative solutions for the digitalization of their legacy machines, such as retrofitting. This paper conducts a review of both retrofitting and Lean Industry 4.0 (Lean 4.0) to identify the challenges and benefits of both concepts and explore how they can interact and merge with each other to help SMEs to increase their market competitiveness.

Key words: Lean industry; Industry 4.0; retrofit; manufacturing; digitalization

ПОДОБРУВАЊЕ НА ПРОИЗВОДСТВЕНАТА ЕФИКАСНОСТ: ПРИСТАП НА ПОСНАТА ИНДУСТРИЈА 4.0 КОН РЕФОРМИРАЊЕТО

А п с т р а к т: Технологиите на Индустријата 4.0 веќе влијаат на глобалните синџири на снабдување, посебно во начинот на кој компаниите ги произведуваат и дистрибуираат своите производи и услуги. Многу компании се погодени од оваа трансформација, особено малите и средни претпријатија (МСП), кои сакаат што побрзо и за што пократко време да ја подобрат својата конкурентност на пазарот. Трансформацијата од традиционалните пристапи кон Индустрија 4.0 може да донесе многу придобивки, но оваа транзиција вклучува усвојување технолошки напредни концепти со високо ниво на дигитализација. Трошоците и времето за замена на старите машини може да не бидат одржливи или достижни за многу МСП, и затоа овие претпријатија бараат алтернативни решенија за дигитализација на нивните постоечки машини. Овој труд спроведува преглед на концептот на реформирање преку призмата на Посната и Индустријата 4.0, за да ги идентификува предизвиците и придобивките од двата концепта и да истражи како тие можат да им помогнат на МСП да ја зголемат својата конкурентност на пазарот.

Клучни зборови: Посна индустрија; Индустрија 4.0; реформирање; производство; дигитализација

1. INTRODUCTION

Industry 4.0 (I4.0) offers many modern technologies that companies could utilize to enhance their manufacturing processes, such as smart sensors, the Internet of Things (IoT), cloud computing, artificial intelligence (AI), robotics, simulations, and 3D printing. These technologies enhance efficiency, cut costs, boost production speed, and improve product quality. They enable real-time data collection and analysis, empowering informed decision-making and operational optimization. However, to prepare the organization for I4.0, it is not necessary to incorporate all the available features and technologies that I4.0 offers. Also, many companies, especially small and medium enterprises (SMEs), are not financially capable of implementing these technologies and/or buying entirely new machines that employ these technologies [9]. Considering this challenge, an alternative to taking off to I4.0 with low cost and agility is known as retrofitting, which is the reuse of old equipment and its integration with new I4.0 technologies [15]. By prioritizing the implementation of I4.0 technologies that align with important company objectives, such as process optimization, continuous improvement, and lean manufacturing, organizations can achieve significant improvements while minimizing costs and realizing a quick return on investment.

If we investigate the reports about the digitalization of enterprises (mainly SMEs), it is easy to observe that many of them struggle to digitally transform, mainly due to the high cost of digitalization [4, 21, 23]. Although many of these SMEs have digital transformation strategies in place, less than half can implement these strategies successfully due to the shift in investment priorities during the pandemic [21]. Whilst the economic uncertainties in recent times have also added unique challenges – the high implementation cost, cash flow challenges, the workforce digital upskilling gap, and low awareness of government initiatives are some common drawbacks faced by SMEs along their digital transformation journey [14].

Retrofitting, which involves modifying existing machinery, is not new and predates Industry 4.0. However, its practical implementation has gained popularity for its cost-effectiveness. In digital transformation (DT), retrofitting is crucial for integrating legacy machinery into a networked production environment. While retrofit projects aren't always low-cost, a strategic approach can help identify and address inefficiencies, bottlenecks, and waste in processes and equipment. This concept also addresses the Sustainability Development Goals (SDG) set by the United Nations as a common objectives for "peace and prosperity for people and the planet, now and into the future" [42]. Considering retrofit's nature of enabling easier digitalization and avoiding replacement of legacy machinery, it can be associated with the following SDG:

– SDG8 Decent work and economic growth,

– SDG9 Industry, innovation, and infrastructure,

– SDG12 Responsible consumption and production.

The following chapter of this paper focuses on the methodology that was utilized to perform this research. In the third chapter, literature review on retrofit in manufacturing is shown. The fourth chapter introduces Lean 4.0 including a brief introduction to both Lean manufacturing, Industry 4.0, and the relationship between them. The fifth chapter focuses on the joint benefits of Lean manufacturing and retrofit towards faster, easier, and low-cost digital transformation of the companies.

2. METHODOLOGY

The research methodology used for this paper is shown in Figure 1. The paper is intended as a preliminary investigation of the topic of retrofitting and its relation to Lean manufacturing and Industry 4.0. The first three steps include more general literature review regarding the main topics: retrofit (in manufacturing), Lean and Industry 4.0 (Lean 4.0), followed by a discussion regarding the mutual impact of Lean 4.0 and retrofit.

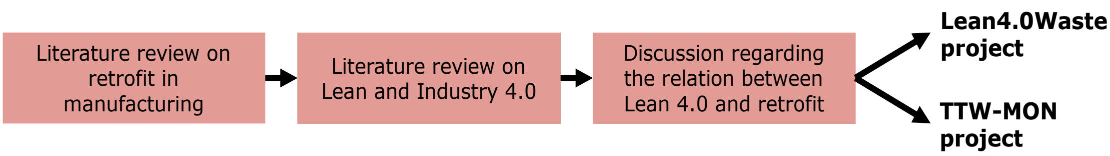

Fig. 1. Research methodology

This paper is also an initial input to two scientific projects that are currently on-going at the Faculty of Mechanical Engineering in Skopje: Lean 4.0 Waste and TTW-MON. This research helped the project teams to establish general understanding of retrofit, Lean 4.0 and their joint benefits towards the digital transformation. The Lean 4.0 Waste project aims to eliminate Lean wastes using digital technologies like sensors and augmented reality. The experiments will take place at the Smart Learning Factory – Skopje (SLFS). TTW-MON, focuses on retrofitting a legacy turning machine with a monitoring system. This system enables predictive maintenance by tracking tool wear during processing. Monitoring cutting forces and vibrations, advanced signal processing, and machine learning algorithms will model tool wear in real-time. The experiments within this project will take place at the laboratory for production engineering and FabLab Skopje.

Findings from Lean4SMEs project [34] as well as DigiTS-ME project [35] will also be incorporated within the paper.

3. RETROFITTING IN MANUFACTURING

Retrofitting can be defined as the process of extending a system, *e.g.*, an industrial production line, with an additional functionality that was not available when it was originally designed and built [11]. Another definition of retrofitting states that it is a process of replacing obsolete operating systems and machine components to extend their working lives. It benefits the organizations as retrofitting incurs lower costs as compared to purchasing the new machine, enhances the precision of the machine and delivers higher quality output [26].

When it comes to manufacturing, considering the new digitalization trends, the need for retrofitting legacy equipment instead of completely new machinery is a preferred option [52], especially for SMEs in less developed countries that have limited resources to invest in bigger digitalization projects. However, although retrofitting seems like a simple solution, there are many factors that could make manufacturers' minds up on whether to retrofit or not [9, 11], including:

– current process readiness/leanness – leaner processes tend to be more flexible and ready for changes,

– cost and duration of the retrofit projects, considering that retrofit projects size can vary therefore the cost and the duration of such projects are not always certain,

– upskilling/reskilling of the personnel – due to the change investment in additional training for the operators is needed.

According to the literature, retrofitting provides many benefits for the manufacturing industry, including extending the lifecycle of legacy machines and enabling the implementation of cost-effective, easily deployable solutions. These retrofits facilitate the integration of modern Industry 4.0 technologies, improving connectivity in existing equipment. Furthermore, retrofitting enhances machine monitoring for predictive maintenance, preventing maintenance-related issues and downtime. A detailed analysis by [11] categorizes the benefits of retrofitting into sustainability, viability, compatibility, and functionality. Even though the benefits of retrofitting in manufacturing are notable, during the literature review, it was observed that there has been a lack of practical examples of retrofitting in manufacturing in recent years. Retrofit concepts are much more present in the research areas such as energy efficiency [6], building efficiency [22], CO_2 capture [19], and sustainability in general [7].

No matter the research field, many authors addressed the need for structured approach to retrofitting. Such is [36], who designed detailed methodology for retrofitting of production systems focusing on low-cost and user-friendly approach to retrofitting in SMEs. There are also many companies that work in the field of digitalization such as FESTO [17] and Siemens [24] who developed their own methodological approaches to retrofitting. Most of these methodologies consist of four general phases as shown in Figure 2.

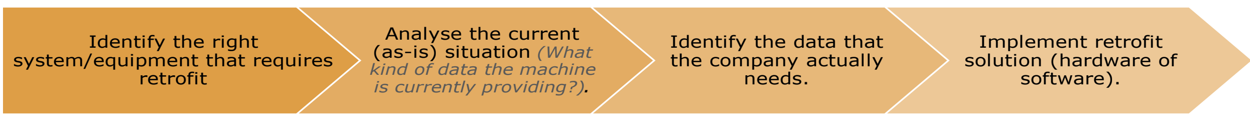

Fig. 2. General retrofit implementation methodology

4. LEAN 4.0

The term "Industry 4.0" originated in 2011 [43]. In the following year, a working group on Industry 4.0 presented implementation recommendations to the German Federal Government where manufacturing and logistics systems, embodied as Cyber Physical Production Systems (CPPS), extensively leverage the globally accessible information and communications network for highly automated information exchange [44, 45]. This system aligns production and business processes seamlessly [37]. On the other hand, Lean Manufacturing is a systematic approach to identifying and eliminating waste (non-value-added activities) through continuous improvement by flowing the product or service at the pull of the customer in pursuit of perfection [38].

The relationship between Lean and Industry 4.0 is often discussed in the scientific community, and in the previous research of the authors of this article [5]. In a comprehensive elaboration regarding the relationship between Lean and Industry 4.0, [46] states that there are several possible scenarios of this relationship:

– Lean and Industry 4.0 have nothing in common,
– Lena is the foundation for implantation of Industry 4.0,
– Industry 4.0 is the foundation for implementation of Lean,
– Lean and Industry 4.0 overlap and create new concept – Lean 4.0,
– Lean and Industry 4.0 oppose each other,
– Lean and Industry 4.0 are the same thing.

According to this, the development of the relationship between Lean and Industry 4 can be described in three phases: ignoring, opposing, and finally – getting together.

Table 1

Development phases of the relationship between Lean and Industry 4.0

Phase	Discussion
Ignoring	This potentially comes from the fact that the definitions regarding Lean and Industry 4.0 are usually different. Lean is a manufacturing philosophy that focuses on waste elimination through following the principles of Lean, while Industry 4.0 focuses on technologies that are not necessarily related to each other. In the other hand, many times, Industry 4.0 is defined as simple as a period of time just like the past three revolutions, while Lean is more related to the organizational culture that have been around no matter what type of technology is used in the manufacturing processes.
Opposing	Some authors do indicate that they oppose each other [47, 48], and this is due to the fact that Lean focuses heavily on the people, while one of the biggest risks when relying on technology is reduction of the teams. Additionally, Lean is considered as an "on-budget" initiative, as opposed to the Industry 4.0 technologies which are a costly investment in the most cases.
Getting together	Lean being the foundation for the implementation of Industry 4.0 technologies is quite an expected perspective considering the complexity of the digital technologies. It is very important that whenever manufacturers upgrade their existing processes with some of the digital technologies, these processes should be previously optimized (waste to be eliminated), so that they could adopt the digitalization easier and faster [49]. According to previous literature review on this topic [5, 50], most of the authors indicate that Lean is the needed foundation that the organization needs to implement before implementing the technologies of Industry 4.0. This provides a perspective of strong synergy between the two terms.

In order to clarify the relationship between these two concepts, a new concept is arising in the literature, known as Lean 4.0 – a concept that unites both Industry 4.0 and Lean [5, 39, 40, 41]. Lean 4.0, also known as Digital Lean or Lean Industry 4.0, is a concept that describes the enhancement of the traditional Lean methods with I4.0 capabilities. While the question whether Lean and Industry 4.0 are compatible concepts still remains attractive to the scientific community [50], many authors have already published successful examples of traditional Lean tools that have been digitalized such as Digital Kanban [12], CPS oriented smart Jidoka systems [12, 15, 17], IoT supported JIT production systems [51], and Lean Six Sigma 4.0 [3].

5. RETROFIT WITH LEAN 4.0 PERSPECTIVE

Lean is constantly evolving, especially in the ever-changing context of I4.0 [9]. However, the transition from traditional production systems and Industry 3.0, especially for SMEs in North Macedonia has been, and still is, very poor. This can be clearly seen during the research project DigiTS-ME, where the digital maturity of the Macedonian SMEs is investigated [35]. Companies are lacking both Lean and digital solutions. Lean is an approach that needs time to be implemented, and the same goes for digital transformation. However, smaller steps should be undertaken as soon as possible if the companies want to stay competitive on the global market. This is where retrofit solutions should play their role, especially in fast, targeted to specific areas or indicators, and cost-friendly delivery of results towards leaner and more digitalized production process [1, 10]. Figure 3 shows the benefits of merging retrofit and lean practices [25, 29, 30, 31, 32].

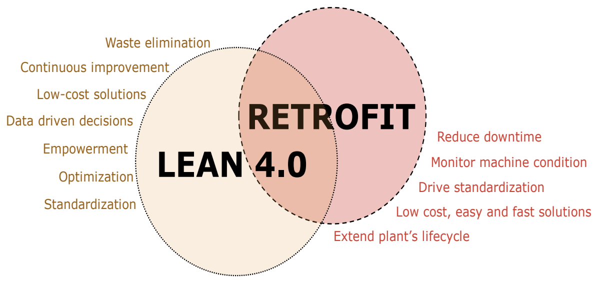

Fig. 3. Joint benefits of retrofit in manufacturing and Lean 4.0

The two main concepts of Lean, continuous improvement, and waste elimination can be clearly addressed by retrofit. It is important to note that the applicative examples of employing retrofitting to foster continuous improvement and waste elimination are very rare, however from a more philosophical aspect this relation is evident.

Continuous Improvement (CI), a concept that revolves around Kaizen which is an activity that continuously improves all functions and involves the entire organization. Kaizen relies heavily on data, and retrofitting can play a vital role in supporting this process by digitalizing machines and processes to provide data to the Kaizen teams, therefore supporting the entire process of CI. It is also important to mention that some retrofit projects can easily be classified as Kaizens since Kaizens are considered as improvements that involve minimal or no financial investments. The same goes for problem-solving methodologies such as Six Sigma which is based on shopfloor data, especially in the Measure and Analyze phases of the DMAIC framework [13]. This methodology, which is strongly connected to the Lean philosophy, would be carried out more efficiently and effectively with more reliable and up-to-date data.

Eliminating waste, as another perspective where retrofitted systems help Lean 4.0 production systems. Traditional Lean philosophy defines seven (or eight, depending on literature source) different wastes. Waste in Lean Manufacturing is defined as activities that do not add any value for the customer. They can come in the form of time, material, and labor. The seven wastes according to Toyota Production Systems include: transport, inventory, motion, waiting, overproduction, over-processing, and defects. In literature, usually one more waste is included in this list which is the non-utilized talent [12]. The relation of this aspect with the retrofit concept will be explained through the example of employing sensors on legacy equipment.

Legacy equipment lacks sensors to indicate their operating status, making sensors one of the most common retrofitting solutions when it comes to enhancing manufacturing efficiency through digital means. Led by this, both aforementioned projects Lean4.0Waste and TTW-MON that are currently running at the Faculty of Mechanical Engineering – Skopje, the possibilities of sensors in an attempt to step into the digitalization era without replacing the legacy equipment are exploring.

As it is planned within both aforementioned projects, Lean4.0Waste and TTW-MON, by employing sensors within selected areas of the manufacturing, we can foster continuous improvement and low-cost digitalization (retrofitting). Some of the examples found in literature for this type of improvements include employment of temperature sensors for avoiding downtime due to machine overheat [20], or accelerometers for detecting abnormal vibrations. Many quality aspects of the products and the processes can be addressed through low-cost digitalization such as detection of the right position of the products during the process, avoiding additional operator motion [27, 2], detecting unwanted parts in the products and therefore avoiding rework and defects [8]. Force sensors can help avoid product variations (therefore avoid defects or reworks) by measuring the weight of the raw material, parts, or assemblies [28].

6. CONCLUSIONS

By retrofitting the legacy equipment, many Lean 4.0 challenges can be addressed. Retrofitting can foster some of the main Lean aspects such as continuous improvement and waste elimination. This paper performed a literature review on three seemingly different concepts: Lean, I4.0, and retrofit, and focuses specifically on the relationship between Lean 4.0 and retrofit, building upon previous research that has established and defined the relationship between Lean and I4.0 [4, 5]. Although there are not many production-related retrofitting examples, there are meaningful aspects where both Lean 4.0 and retrofitting benefit from each other. Starting from the cost of implementation to the easier transition from traditional to digital Lean, retrofit projects could help the manufacturers, especially SMEs, reach their digitalization goal in an easier and faster manner while they contribute to keeping the established Lean standards and/or enhancing leanness.

Considering the lack of literature in the field of practical manufacturing applications, more such solutions should be explored and verified. This will partially be done during the aforementioned projects Lean4.0Waste and TTW-MON. Additionally, there is a lack of standardized approach/methodology to retrofit, specifically in the manufacturing sector where existing concepts such as Lean, should be considered in the base.

Acknowledgement: The authors would like to thank EIT Manufacturing, OeAD-Austria's Agency for Education and Internationalization, Macedonian Ministry of Education and Science, Ss. Cyril and Methodius University in Skopje and the Student Assembly of Ss. Cyril and Methodius University for participating in the financing of the projects mentioned in this paper.

REFERENCES

[1] Müller, J., Voigt, K.-I., Kiel, D. (2018): What drives the implementation of Industry 4.0? The role of opportunities and challenges in the context of sustainability. *Sustainability*. **10**(1) DOI:10.3390/su10010247

[2] Anjoran, R. (n.d.). 14 *Mistake Proofing Examples: Improve Quality at Virtualy no Cost*. Retrieved from CMC: cmc-consultants.com

[3] Antony, J., McDermott, O., Powell, D., Sony, M. (2022): The evolution and future of lean Six Sigma 4.0. *The TQM Journal*. **35**(4), DOI:10.1108/TQM-04-2022-0135

[4] Argilovski, A., Jovanoski, B., Minovski, R., Kochov, A. (2022): Industry 4.0 for more competitive SMEs – Review of existing Industry 4.0 maturity models. *15th EPIEM Conference* 2022, (pp. 41–47). Graz. DOI:10.3217/978-3-85125-889-9

[5] Argilovski, A., Jovanoski, B., Minovski, R., Musliji, A. (2022): Mapping the current research on the different viewpoints regarding relationship between Lean and Industry 4.0. *8th International Conference on Industrial Engineering*. Belgrade.

[6] Boldyryev, S., Gil, T., Ilchenko, M. (2022): Environmental and economic assessment of the efficiency of heat exchanger network retrofit options based on the experience of society and energy price records. *Energy*, Volume **260**, 125–155. https://doi.org/10.1016/j.energy.2022.125155

[7] Chen, G., Cheng, L., Li, F. (2022): Integrating Sustainability and Users' Demands in the Retrofit of a University Campus in China. *Sustainability*. Volume. **14**, Issue 16, DOI: 10.3390/su141610414

[8] Elmedint. (n.d.). A guide to metal detection in the food manufacturing industry. Retrieved from: www.elmedint.com: https://www.elmedint.com/uploads/editor/Guide_to_Metal_Detection.pdf

[9] Etzab, D., Brantnera, H., Kastnera, W. (2020): Retrofitting-based Development of Brownfield Industry 4.0 and Industry 5.0 Solutions. *Procedia Manufacturing*, 327–332. https://doi.org/10.1016/j.promfg.2020.02.085

[10] Ingaldi, M., Ulewicz, R. (2019): Problems with the implementation of Industry 4.0 in enterprises from the SME sector. *Sustainability*. **12**(1) https://doi.org/10.3390/su12010217

[11] Jaspert, D., Ebel, M., Eckhardt, A., Poeppelbuss, J. (2021): Smart retrofitting in manufacturing: A systematic review. *Journal of Cleaner Production*. Vol. **312**,127555, https://doi.org/10.1016/j.jclepro.2021.127555

[12] Kirchbach, K., Koskela, L., Gehbauer, F. (2014): Digital Kanban for earthwork site management. *Proceedings IGLC-22*, pp. 663–673, Oslo.

[13] Kochov, A., Argilovski, A. (2021): Six sigma approach to enhance concurrency of the procurement process for raw materials. *Tehnički glasnik*, Vol. **15**, No. 4, 510–517. https://doi.org/10.31803/tg-20210304095657

[14] Lin, D.-Y., Rayavarapu, S. N., Tajeddine, K., Jeoh, R. (2022): Beyond financials: Helping small and medium-size enterprises thrive. Retrieved from: www.mckinsey.com: https://www.mckinsey.com/industries/public-and-social-sector/our-insights/beyond-financials-helping-small-and-medium-size-enterprises-thrive

[15] Lins, T., Ricardo, R., Correira, L., Silva, J. S. (2018): Industry 4.0 retrofitting. *2018 VIII Brazilian Symposium on Computing Systems Engineering (SBESC)*. DOI:10.1109/SBESC.2018.00011

[16] Ma, J., Wang, Q., Zhao, Z. (2017): SLAE–CPS: Smart Lean Automation Engine Enabled by Cyber-Physical Systems Technologies. *Sensors* **17** (7), 1500. DOI:10.3390/s17071500

[17] Middleton, P. (2017): FESTO – Industry 4.0 and the retrofit opporunity. Retrieved from: https://www.crown.co.za/latest-news/mechchem-africa-latest-news/4286-industry-4-0-and-the-retrofit-opportunity

[18] Mohamad, E., Rahman, M. S., Ito, T., Rahman, A. A. (2019): Framework of Andon Support System in Lean Cyber-Physical System Production Environment. *The Proceedings of Manufacturing Systems Division Conference*. DOI:10.1299/jsmemsd.2019.404

[19] Ordorica-Garcia, G., Wong, S., Faltinson, J., Singh, S. (2009): CO_2 capture retrofit options for a gasification-based integrated bitumen extraction and upgrading facility. *Energy Procedia*, Vol. **1**, Is. 1, 3977–3984. https://doi.org/10.1016/j.egypro.2009.02.202

[20] Paduloh, P., Muhendra, R. (2022): Overheat protection for motor crane hoist using Internet of Things. *International Journal of Computer Applications in Technology*. DOI:10.1504/IJCAT.2022.10050316

[21] PwC. (2020): Digital transformation for small and medium businesses. Retrieved from: www.pwc.com: https://www.pwc.com/sg/en/services/reimagine-digital/digital-transformation-for-small-and-medium-businesses.html

[22] Rucińska, J. (2018): Improving the energy quality and indoor environmental quality in retrofit buildings. In: *Design Solutions for nZEB Retrofit Buildings*. DOI:10.4018/978-1-5225-4105-9.ch008

[23] Sharma, S. S., Khatri, R. (2021): Introduction to Lean Waste and Lean Tools. In: *Lean Manufacturing*. DOI:10.5772/intechopen.97573

[24] Siemens. (2022): Retrofit Services: Protecting investments, safeguarding the future. Retrieved from https://www.siemens.com/global/en/products/services/digital-enterprise-services/service-programs-platforms/motion-control-services.html

[25] Smart retrofitting in manufacturing: A systematic review. (2021): *Journal of Cleaner Production*. DOI: https://doi.org/10.1016/j.jclepro.2021.127555

[26] Technosoft Engineering (2020): What is the role of retrofit engineering in product development? Retrieved from: www.technosofteng.com: https://technosofteng.com/what-is-the-role-of-retrofit-engineering-in-product-development

[27] THOMAS. (n.d.). All about position sensors. Retrieved from: https://www.thomasnet.com/articles/instruments-controls/all-about-position-sensors/

[28] LOMA systems (2020): *A Guide to Metal Detection in the Food Manufacturing Industry*. www.elmedint.com.

[29] Ingaldi, M., Ulewicz, R. (2019): Problems with the implementation of Industry 4.0 in enterprises from the SME Sector. *Sustainability*, **12** (1): 217. DOI:10.3390/su12010217

[30] Tran Tuan-anh, Ruppert Tamas, Eigner Gyorgy, Abonyi Janos (2022): Retrofitting-based development of brownfield Industry 4.0 and Industry 5.0 solutions. *IEEE Access*, Vol. **10** (IEEE), pp. 64348–64374. DOI: 10.1109/ACCESS.2022.3182491

[31] Alqoud, A., Schaefer, D., Milisavljevic-Syed, J. (2021): Industry 4.0: Retrofitting of legacy machines for smart manufacturing.

[32] Zambetti, M., Muztoba A. K., Pinto, R., Wuest T. (2020): Enabling servitization by retrofitting legacy equipment for Industry 4.0 applications: benefits and barriers for OEMs. *Procedia Manufacturing,* **48** (5), pp. 1047–1053.

[33] Rosin, F., Pascal F., Pellerin, R., Lamouri, S. (2019): Impacts of Industry 4.0 technologies on Lean principles.

[34] Lean4SMEs. (2022): *Learning Factory for Improving Digital Competitiveness of SME*s. Retrieved from https://learningfactory.mf.edu.mk/projects/#learn4smes

[35] DigiTS-ME. (2022–2023): *Lean Industry 4.0 for more competitive production and maintenance in the Small and Medium-Sized Enterprises*. Retrieved from https://learningfactory.mf.edu.mk/projects/#digitsme

[36] Pueo, M., Santolaria, J., Acero, R. (2019): Design methodology for production systems retrofit in SME. *International Journal of Production Research*, Vol. **58**, Iss. 14, pp. 4306–4324.

[37] Saurabh, V., Prashant, A., Santosh, B. (2018): Industry 4.0 – A Glimpse. *Procedia Manufacturing*, Vol. **20**, pp. 233–238. DOI: https://doi.org/10.1016/j.promfg.2018.02.034

[38] Womack, J. P., Jones, D. T. (2003): *Lean Thinking: Banish Waste and Create Wealth in Your Corporation,* Revised and Updated.

[39] Elafri, Nedjwa, Tappert, J., Rose B., Maleh Yassine (2022): Lean 4.0: Synergies between Lean Management tools and Industry 4.0 technologies. *IFAC-PapersOnLine* **55** (10), pp. 2060–2066.

[40] Mayr, A., et al. (2018): *Lean 4.0 – A Conceptual Junction of Lean Manufacturing and I4.0*. 2018.

[41] Javid, Mohd, Abid Haleem, Ravi Pratap Singh, Shanay Rab, Rajiv Shuman, Shahbaz Khan (2021): *Exploring relationships between Lean 4.0 and manufacturing industry*.

[42] Secher, A. Q., Collin C., Linnet, A. (2018): Construction product declarations and sustainable development goals for small and medium construction enterprises. *Procedia CIRP*, **69**, pp. 54–58, https://doi.org/10.1016/j.procir.2017.12.011

[43] Zhanybek, S., Sabit, S., Dikhanbayeva, D., Shehab, E., Turkyilmaz, A. (2022): Industry 4.0: Clustering of concepts and characteristics. *Cogent Engineering* **9** (1), https://doi.org/10.1080/23311916.2022.2034264

[44] Madsen, D. Ø. (2019): The Emergence and Rise of Industry 4.0 Viewedt Tthrough the Leans of Management Fashion Theory. *Administrative Sciences*, **9** (3) https://doi.org/10.3390/admsci9030071

[45] Szozda, N. (2017): Industry 4.0 and its impact on the functioning of supply chains. *Scientific Journal of Logistics* **13** (4), pp. 401–414, https://doi.org/10.17270/J.LOG.2017.4.2

[46] Roser, C. (2017): Lean and Industry 4.0, Wroclaw: AllA boutLean, Lean Management Conference

[47] Malavasi, M. (2017): Lean Manufacturing and Industry 4.0: an empirical analysis between Sustaining and disruptive change.

[48] Larsson, J., Wollin, J. (2020): Industry 4.0 and Lean – Possibilities, Challenges and Rise for Continuous improvement.

[49] Pereira, A. C., Dinis-Carvalho, J., Alves, A. C., Arezes, P. (2019): How Industry 4.0 can enhance Lean practices.

[50] Buer, S.-V., Strandhagen, J. O. Chan, F. T. S. (2018): The link between Industry 4.0 and Lean manufacturing: Mapping current research and establishing a research agenda. *International Journal of Production Research* **56** (8): 2924–2940.

[51] Xu, Yuchun, Mu Chen. (2016): Improving Just-in-Time Manufacturing Operations by Using Internet of Things Based Solutions. *Procedia CIRP* **56**, 326–331, 2016. https://doi.org/10.1016/j.procir.2016.10.030

[52] Pietrangeli, I., Mazzuto, G., Ciarapica, F. E., Bevilacqua, M. (2023): Smart Retrofit: An Innovative and Sustainable Solution. *Machines* **11** (5), p. 523, https://doi.org/10.3390/machines11050523

Mechanical Engineering – Scientific Journal, Vol. **41,** No. 2, pp. 131–140 (2023)
Number of article: 673
In print: ISSN 1857–5293
Received: November 10, 2023
On line: ISSN 1857–9191
Accepted: December 15, 2023
UDC: 621.715.2.044.4:658.512.2
https://doi.org/10.55302/MESJ23412673131t

Original scientific paper

EXPERIMENTAL RESEARCH OF THE MECHANICAL PROPERTIES OF THE INJECTION MOLDED PARTS IN MOLDS PRODUCED BY ADDITIVE MANUFACTURING

Ognen Tuteski, Atanas Kočov

Faculty of Mechanical Engineering, "Ss. Cyril and Methodius" University in Skopje, P.O. Box 464, MK-1001 Skopje, Republic of North Macedonia
ognen.tuteski@mf.edu.mk // atanas.kochov@mf.edu.mk

A b s t r a c t: In this study, additive manufacturing emerges as an innovative technology for concurrent engineering in the design and production of molds for injection molding processes. The primary objective is to conduct experimental research on the mechanical properties of injection-molded parts using a non-conventional mold produced through additive manufacturing technologies. The state-of-the-art additive manufacturing technologies provide various methodologies and techniques for designing and printing parts. Utilizing these diverse technologies significantly expands the possibilities for rapidly creating molds, thereby enhancing the scope of rapid tooling in the molding process. The study begins by designing and fabricating SLA mold inserts according to the relevant tensile testing standards. To evaluate the mechanical properties, a series of tensile tests are conducted and a comparison is made between the properties of the molded parts produced with SLA mold inserts. The results demonstrate that SLA mold inserts made with additive manufacturing can effectively produce injection molded parts with comparable tensile strength to those manufactured using traditional steel molds.

Key words: additive manufacturing; injection molding; rapid tooling; stereolithography; tensile testing

ЕКСПЕРИМЕНТАЛНО ИСТРАЖУВАЊЕ НА МЕХАНИЧКИТЕ СВОЈСТВА НА ДЕЛОВИ ДОБИЕНИ СО ИНЈЕКТИРАЊЕ ВО КАЛАПИ ИЗРАБОТЕНИ СО АДИТИВНО ПРОИЗВОДСТВО

А п с т р а к т: Во ова истражуваење адитивното производство се разгледува како иновативна технологија за конкурентно инженерство во дизајнот и производството на калапи за процесот на инјектирање. Примарната цел е да се спроведе експериментално истражување на механичките својства на деловите изработени со помош на неконвенционален алат направен со технологии за адитивното производство. Најсовремените технологии за адитивното производство овозможуваат различни методологии и техники за дизајнирање и печатење на делови. Користењето на овие разновидни технологии значително ги проширува можностите за брза изработка на алати во процесот на инјектирање. Студијата започнува со дизајн и изработка на гравури со технологијата SLA според релевантните стандарди за испитување на истегнување. За да се проценат механичките својства, се спроведуваат повеќе тестови и се прави споредба на својствата на деловите изработени во SLA-гравурите. Резултатите покажуваат дека во гравурите изработени со технологијата SLA на адитивно производство може ефикасно да се произведат делови со инјектирање кои имаат споредлива јакост на истегнување со деловите изработени со употреба на традиционални метални алати.

Клучни зборови: адитивно производство; инјектирање; брза изработка на алати; стереолитографија; испитување со истегнување

1. INTRODUCTION

The implementation of additive manufacturing in injection molding represents a groundbreaking approach in the design and production of molds. By leveraging state-of-the-art technologies, this method enables the creation of non-conventional molds, offering increased flexibility and efficiency in the injection molding process. This innovative application facilitates rapid prototyping, customization, and the exploration of diverse design possibilities, ultimately revolutionizing traditional manufacturing practices.

Stereolithography (SLA) additive manufacturing has emerged as a groundbreaking technology with the potential to revolutionize the field of injection molding. Traditional mold production techniques have long posed challenges in terms of time, cost, and design limitations. However, recent advancements in SLA additive manufacturing have paved the way for accelerated prototyping, enhanced design flexibility, cost efficiency, faster time to market, customization, iterative improvements, and material diversity in the injection molding process. Moreover, the cost-effectiveness and reduced lead times associated with molds made with SLA additive manufacturing provide manufacturers with a competitive edge, enabling them to respond rapidly to market demands and optimize production schedules. The customization and iterative improvement capabilities of molds made with SLA additive manufacturing further enhance the product development cycle, allowing for on-the-fly adjustments based on feedback and design iterations. Additionally, the versatility of material selection in SLA additive manufacturing ensures compatibility with various manufacturing requirements, expanding the range of materials that can be utilized in injection molding processes. Both standard SLA and other SLA based technologies like Stratasys's Polyjet have been used to manufacture various tooling inserts (Figure 1).

Using SLA additive manufactured molds is a valuable tool in the prototyping process for injection molding, particularly due to their ability to produce prototypes with the intended plastic as the final product. This feature allows designers and engineers to test the functionality, fit, and aesthetics of their designs accurately before investing in expensive production molds. By using molds made with SLA additive manufacturing, they can create prototypes using the same material that will be used in the injection molding process, ensuring a high degree of accuracy in terms of mechanical properties and surface finish. This method saves time and resources, as it eliminates the need for multiple iterations and costly material changes during the prototyping stage. Moreover, it enables manufacturers to validate the manufacturability of their designs and make necessary adjustments early in the process, leading to faster product development cycles and improved overall product quality.

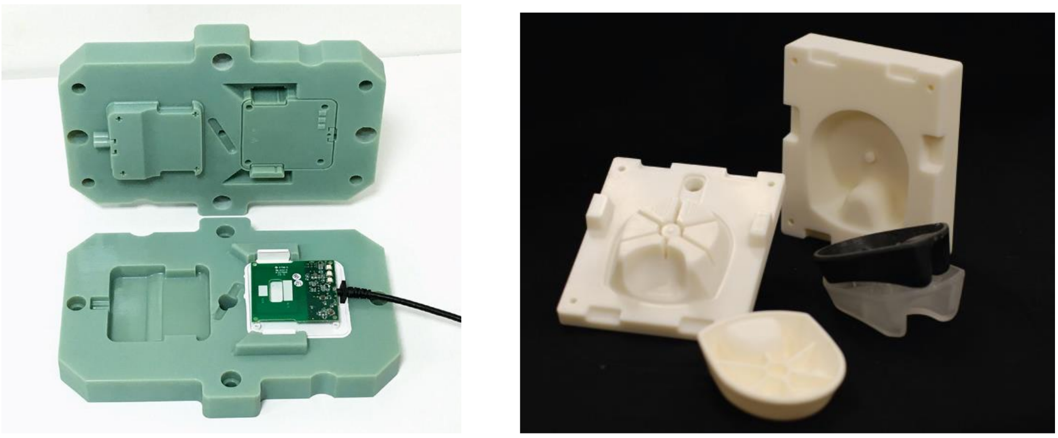

a) *b)*

Fig. 1. Stereolithographic molding inserts: a) Manufactured by the Arad Group using the Stratasys Polyjet technology. b) Manufactured by synthetic engineering using SLA. (Source: [1])

2. THEORETICAL RESEARCH

In addition to the possibility of producing small series of parts using polymer molding inserts, several studies have shown that the physical properties of plastic parts obtained in this way differ from parts obtained from conventional injection molding tools made of steel or aluminum. Segal and Campbell [2] summarize this research very well up to 2001 and their research covers quite a few different types of polymer inserts used in the injection molding process. Stereolithographic molding inserts, inserts obtained by casting polymer resins and other alloys with low melting points were analyzed. Additionally, the polymers that's injected into these molding inserts also range widely and range from conventional polypropylene to glass fiber reinforced polyamide and polycarbonate. Although all the cited papers show differences in the characteristics of parts obtained from molds made with different rapid prototyping technologies, the exact effects that cause these differences have not yet been explained. Furthermore, various research show that there are contradictory results regarding the investigated mechanical properties, specifically the tensile strength of the material. The analysis clearly shows that on the one hand in certain cases, the tensile strength was higher for the parts obtained from conventional steel molds compared to the parts obtained from stereolithographic molds. On the other hand, certain studies obtained the opposite result and concluded that the tensile strength is higher in the parts made in stereolithographic molded inserts.

Michaeli and Lindner [3] conclude that if the injection mold is made of a material with good thermal conductivity, then the produced parts have thick boundary layers and smaller spherulites, while in molds made of materials with a worse thermal conductivity, the boundary layers are thin and the spherulites in the polymer are larger (Figure 2). The presence of larger spherulites is also associated and highly correlated with an increase in the tensile strength of the produced parts.

Harris et al. [4] showed that the semi-crystalline polymer polyamide 66 (PA66) experienced twice as much thermal shrinkage when processed in a stereolithography tool compared to molding in a standard aluminum tool. The difference in temperature shrinkage was due primarily to the different processing conditions associated with the different behavior of the materials during cooling due to the different thermal conductivity of the material from which the molding inserts were made. Furthermore, a similar test was done with amorphous polymer Acrylnitrile-Butadien-Styrol-Copolymere (ABS) and in this case no visible differences in temperature shrinkage were observed between the two types of different molds, which means that when applying stereolithographic inserts, special attention in the design compensation for temperature shrinkage should be addressed when it comes to crystalline and semi-crystalline polymers.

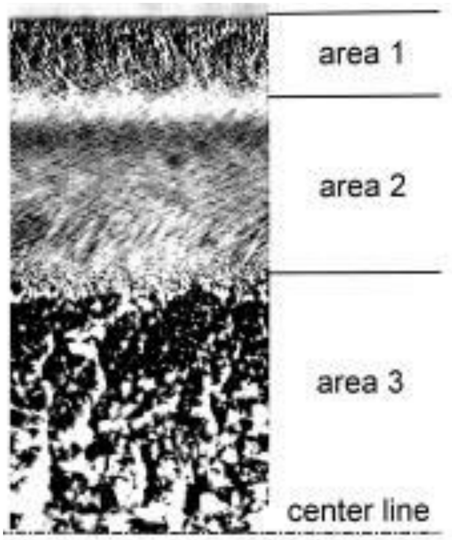

Fig. 2. Boundary layers in a polypropylene sample reflecting the difference in spherulite size of the polymer along its thickness (Source: [3])

Fernandes et al. [5] showed that the mechanical properties of a polypropylene (PP) homopolymer were worse when the part was fabricated in a hybrid tool with an epoxy resin matrix and an aluminum matrix compared to conventional steel tools. The maximum tensile strength, the Young's modulus of elasticity and the maximum elongation until breaking were examined. The degree of crystallization was also investigated and it was concluded that it was higher in the samples obtained by injection molding in the hybrid tool compared to the conventional tool steel. There was also noticeable differences in the transparency of the parts made in the epoxy resin and aluminum composite tooling, as shown in Figure 3.

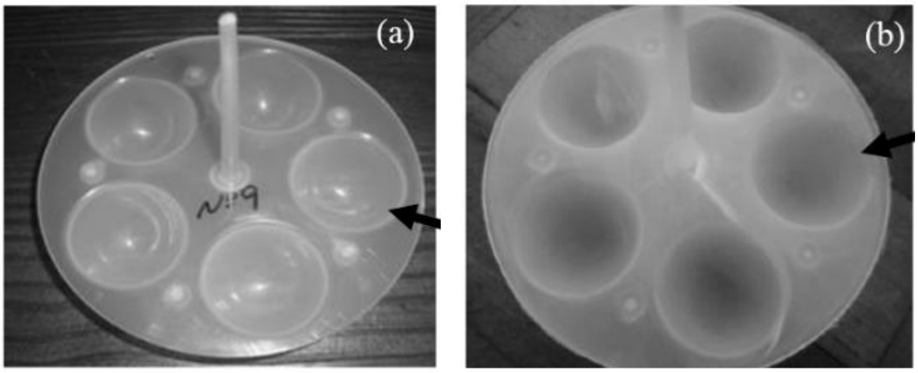

Fig. 3. Difference in transparency of polypropylene parts made in epoxy resin and aluminum molds (a) and AISI P20 steel tooling (b) (Source: [5])

All previous research in this area suggests that the different thermal conditions for processing injection molded parts are the most influential for the varying characteristics of the resulting parts. Harris [6] suggests that control over the degree of crystallization can be performed by regulating the melting temperature and using nucleating agents. Despite all the investigations, there is still no consistent understanding of the influence of tools developed from different materials on the characteristics of manufactured parts, this is mentioned by Segal and Campbell [2] and confirmed by the contradictory results published by Volpato [7].

3. RESEARCH METHODOLOGY

3.1. *Mold design*

Drawing upon both theoretical and experimental investigations, a novel mold design has been formulated. The application of additive manufacturing techniques for rapid tooling and mold production in injection molding processes introduces advanced possibilities for research in the domain of employing cutting-edge designs for injection molding molds. This facilitates a streamlined design process, enabling easier analysis and production. The conventional mold design may be changed by an innovative non-conventional mold design, suported by additive manufacturing principles and rapid tooling methodologies.

Previous experiences involving the use of stereolithographic inserts in injection molding technology have shown that it is optimal to use a universal metal base that houses the core and cavity inserts. This modular approach affords the utilization of a master base for various inserts, minimizing the size of stereolithographic inserts and thereby conserving time and material during their production. In this study, an existing mold equipped with interchangeable inserts was employed. While the use of such molds imposes certain constraints on the design of stereolithographic inserts, it facilitates the application of the aforementioned approach in configuring the experimental setup. The configuration of the used master base and molding inserts is shown in Figure 4.

The experimental research resulted in the development of novel inserts for injection molds, created through the integration of rapid tooling technologies and the SLA additive manufacturing process (Figure 5).

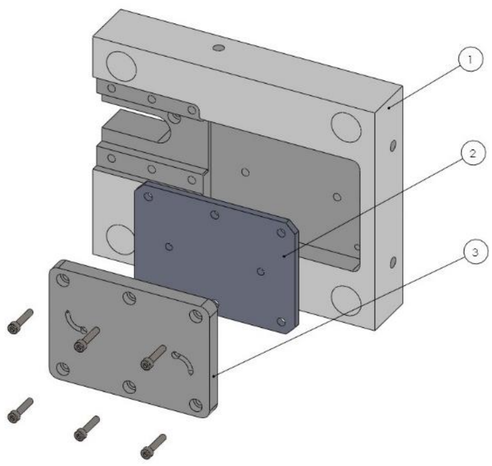

Fig. 4. Exploded view of the mold plate and the molding insert, 1) Mold plate; 2) Support plate; 3) Stereolitography molding insert

Fig. 5. Graphic representation of the basic mechanics of stereolithography (SLA) (Source: https://www.hubs.com)

After printing, the printed models were washed with IPA and post-cured. The post-curing was done by UV radiation from 13 multidirectional LED diodes, each with a power of 39 W and a wavelength of 405 nm [8]. The rotating base of the used device enabled uniform light exposure, with a rotation speed of 1 revolution per minute. The device can provide a post-curing temperature of up to 80 °C [9]. The printed models were cured for 60 min, at a temperature of 70 °C, per the manufacturers' recommendations. The molding insert during 3D printing and the final model are shown in Figure 6.

The Rigid 10k photopolymeric resin that was used for the production of molding inserts has thermal characteristics that make it suitable for use in the injection molding process. To ensure the highest possible Heat Deflection Temperature (HDT) for the material, additional thermal treatment in a laboratory furnace is recommended. This thermal treatment also affects the mechanical characteristics of the material. This procedure was done in a laboratory furnace for 90 min, at a temperature of 125 °C, per the manufacturers' recommendations.

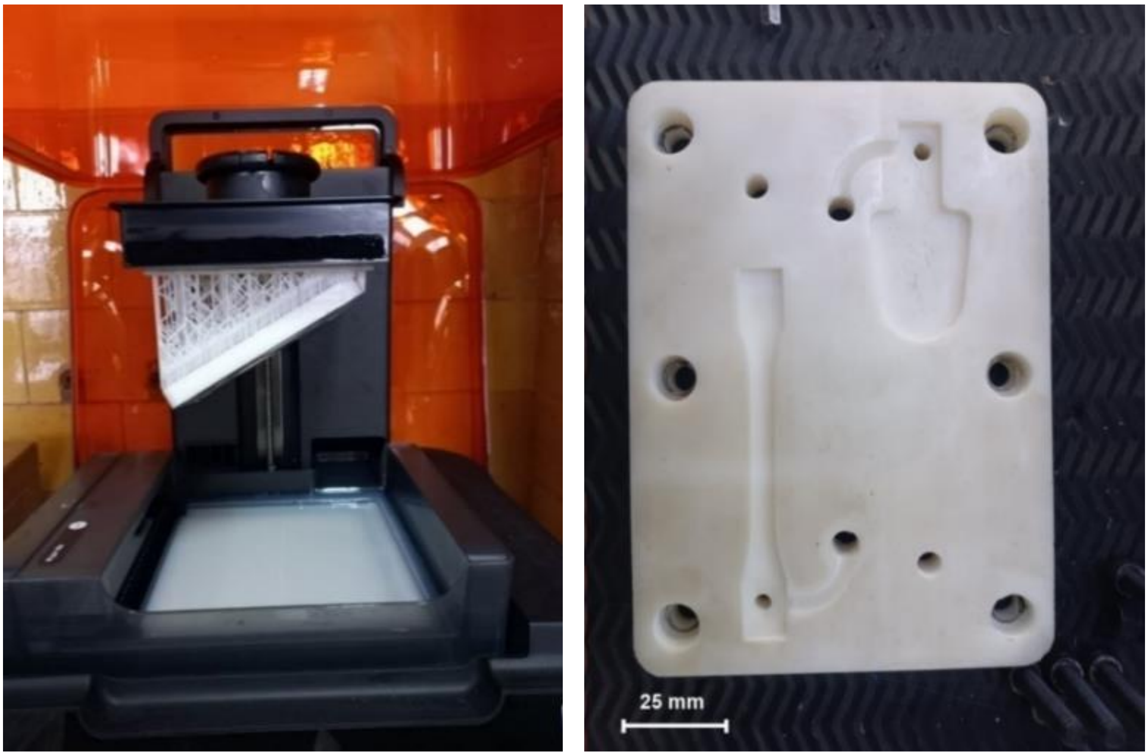

a) b)

Fig. 6. SLA molding insert made from Rigid 10k: a) during printing; b) after removing the support structure

Processing parameters were held constant during injection molding and are given in Table 1. The melt temperature of the used ABS plastic (Table 2) was chosen at the lower limit of the recommended values, which for this polymer range from 200 to 280 °C. The reason for this was that the used mold was not preheated and its temperature was controlled and measured after each cycle so as not to exceed the recommended mold temperature for processing of ABS that is between 50 and 80 °C. The measuring was done using a thermographic camera as shown in Figure 7.

T a b l e 1

Injection molding parameters used during the experiment

Injection pressure (MPa)	48
Injection temperature (°C)	200
Injection speed (mm/s)	120
Clamping force (t)	15
Fill time (s)	1.63
Pack time (s)	3.5
Pack pressure (MPa)	25
Cooling time (s)	48 – 60

T a b l e 2

ABS polymer material – referenced mechanical properties (Source: [12])

ABS-50 Ghaed Basir Petrochemical	Value	Unit	Testing conditions	Test method
Tensile elongation	20	%	@ 23 °C, 50 mm/min	ASTM D638
Tensile strength	44.6	MPa	@ 23 °C, 50 mm/min	ASTM D638

The temperature distribution in the mold insert shown in Figure 7 was constant throughout every molding cycle. The highest measured values were at the injection location of the cavity, near the sprue bushing. After the part ejection, temperature measurements were done on the mold until its temperature was in the recommended value interval. After several cycles, roughly 60 second was shown to provide sufficient cooling time to allow the mold to get into the desired temperature range. The average temperature of the molding inserts throughout the cycles was 62 °C, as per the thermographic camera measurements. The lowest insert temperature was the one for the first molding cycle where the mold was at room temperature of 20 °C (Table 3)

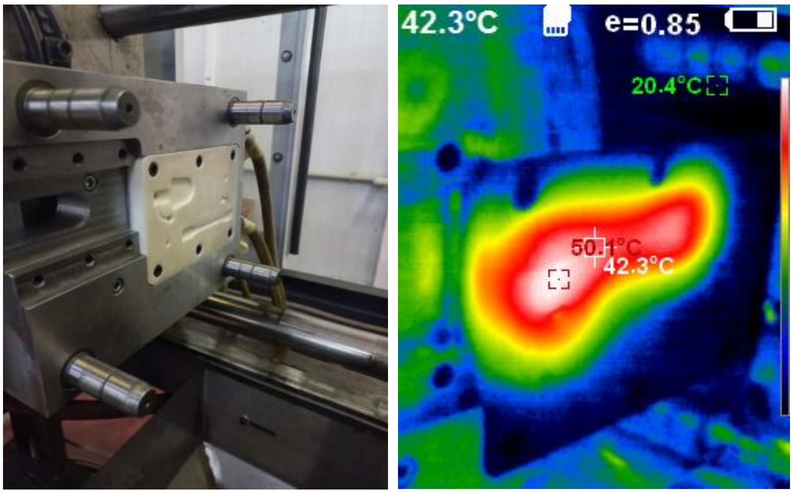

a) b)

Fig. 7. Temperature control of the stereolithographic inserts; measurement done after the 3rd cycle; (a) the molding insert placed in the master housing; (b) thermographic camera image of the insert with temperature distribution after injection

T a b l e 3

Mold insert temperatures before the start of each cycle

Cycle no.	Insert temp. (ºC)	Cycle no.	Insert temp. (ºC)
1	20	26	60.8
2	48.1	27	57.7
3	50.1	28	105.1
4	43	29	59.1
5	36	30	98.1
6	49	31	63.7
7	54.5	32	95.7
8	48.1	33	
9	98.7	34	
10	43.5	35	
11	Incomplete cavity filling-specimens excluded from the analysis	36	
12		37	
13		38	
14		39	
15		40	
16		41	
17	80.7	42	
18	71	43	
19	68.1	44	
20	62.9	45	
21	56.2	46	
22	53.3	47	
23	56.2	48	
24	68.6	49	
25	62.9	50	
Average insert temperature (°C)			**62**
Min insert temperature (°C)			**20.0**
Max insert temperature (°C)			**105.1**

The molding inserts were designed to fulfill dual objectives within the testing framework. Primarily, one model was needed to facilitate investigations into the impact of stereolithographic molds on the mechanical properties of components produced by injection molding. Consequently, one of the cavities needed to have the shape of a standardized specimen for tensile testing. Given the spatial constraints in the stereolithographic mold (refer to Figure 6), the selection was made in favor of the Type 1BA specimen per ISO 527 standards ([10], [11]). The second cavity in the shape of a trapezoidal plate was designed to monitor deviations in both angle and radii curvature for further analysis. This study focuses only on the mechanical properties of the components and the models produced from the second cavity are not used in this experimental study.

The mold made from Rigid 10k, withstood all of the intended 50 cycles without critical failure. Flash formation was the only conventional defect observed in the specimens. The first small traces of flash appeared after the 25th injection cycle (Figure 8). The intense progressive deterioration occurred after the 40th cycle.

Figure 9 shows the dimensions of the 1BA sample used. According to the standard, this sample is allowed to be used when the standard samples of type 1A or 1B cannot be used due to any restrictions. The dimensions of these standard test tubes are proportionally reduced compared to Type 1B specimens by a factor of 1:2.

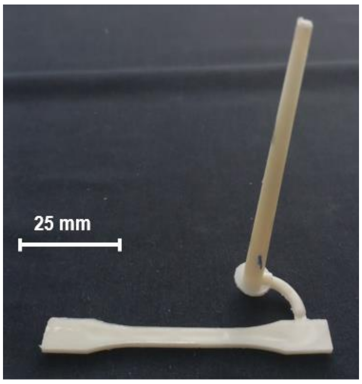

a) b)

Fig. 8. (a) Injection molded specimen, (b) the progressive increase of the flash formation (cycles 1, 33, 50)

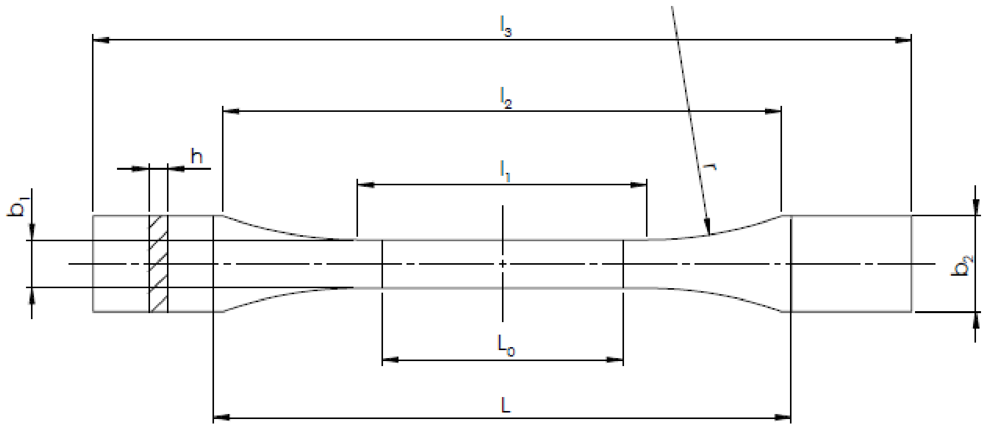

	Type of specimen 1BA	mm
l_3	Overall length	≥75
l_1	Length of narrow parallel-sided portion	30 ± 0,5
r	Radius	≥30
l_2	Distance between broad parallel-sided portions	58 ± 2
b_2	Head width	10 ± 0,5
b_1	Width of narrow portion	5 ± 0,5
h	Thickness	≥2
L_0	Gauge length	25 ± 0,5
L	Initial distance between grips	l_2^{+2}

Fig. 9. Dimensions of the standard specimen 1BA for tensile testing for polymers according to ISO 527 (Source: [10])

3.2. *Tensile testing*

The tensile test of each specimen was done according to the guidelines in the standard EN ISO 527-2:1996 ([10], [11]), without removing the excess flashing from the specimens. The reasoning behind this is that the thickness of the flash in the gauge length area was negligibly thin. Figure 9 and Figure 10 show that the width of the flash was most prominent in the head area of the specimens. In the gauge length area, the thickness of the flash is 0.12 mm which is only 6% of the nominal thickness of the specimens.

The tensile test was done in the Forming processes laboratory of the Faculty of Mechanical Engineering in Skopje on the Shimatzu Autograph AGS-X machine (Figure 11) with a load cell capacity of 10 kN with a crosshead speed of 1 mm/min. The low test, speed was chosen to ensure quasi-static test conditions.

From each of the test pieces the ultimate tensile stress was calculated as:

$$\sigma_m = \frac{F_M}{A_0}.$$

F_m is the highest measured force and A_0 is the starting cross-section area ($b \times h$) of 10 mm^2.

From each of the test pieces the relative strain was calculated as:

$$\varepsilon = \frac{L - L_0}{L_0}.$$

L_0 is the initial gauge length of 25 mm and L is the length that corresponds with σ_m.

Fig. 10. Flash formation width near the gauge lenght of the specimen

Fig. 11. Shimatzu Autograph AGS-X uniaxial testing machine

4. RESULTS AND DISCUSSION

In this chapter, a summary of the data acquired during the experiment is presented. The standard test pieces produced using the stereolithography inserts underwent a tensile test following the ISO 527 standard. The measured values for the tensile strength and maximum relative deformation were then compared with the reference values provided by the manufacturer of the ABS used during the injection molding process. The summarized findings from all conducted tests are displayed in Table 4.

Table 4

Statistical results of the tensile tests

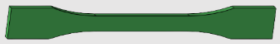	Max. tensile strength σ_m (MPa)	Max. relative deformation ε (%)
Number of measurements	44	43
Measured values ≥ then the reference values provided by the manufacturer	17	17
Measured values < then the reference values provided by the manufacturer	27	26
Nominal values	44.6	20
Min	36.961	6.820
Max	51.534	28.932
Range	14.572	22.112
Average	43.702	16.763
Median	43.113	16.768
Standard deviation	3.395	6.334
Average error	–0.898	–3.237
% acceptable	39%	40%

The testing involved a total of 44 fully injected specimens derived from the SLA inserts. The maximum tensile strength (σ_m) was measured across all samples, while the examination of the maximum relative deformation (ε_m) was performed only on 43 samples. One sample, the 10th in the series, encountered a technical issue during the testing wherein the Shimatzu Autograph AGS-X machine lost connection with the testing software, rendering the deformation measurement incomplete. However, since the point of maximum tensile strength had been surpassed, that particular value was known and accounted for in the statistical computations pertaining to the strength evaluation of the injection molded specimens.

Figure 12 and Figure 13 show the charts for the measured maximum tensile strength and maximum relative deformation. The shown nominal value for each chart is taken from the manufacturer's data sheet for the polymer used in the study (Table 2).

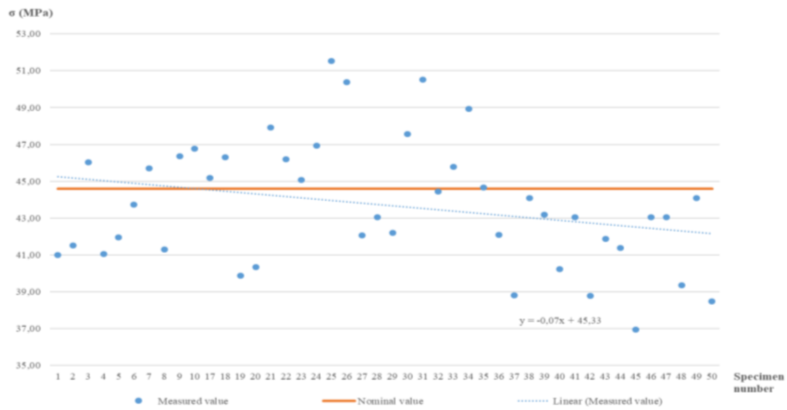

Fig. 12. Chart for the measured values for the ultimate tensile strength of the specimens

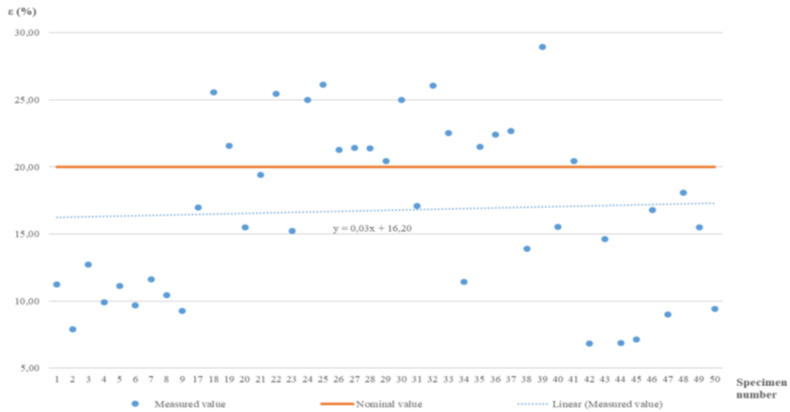

Fig. 13. Chart for the measured values for the relative deformation of the specimens

The results of the tests showed that only 39% of the tested samples have a strength greater than or equal to the nominal one, which according to the official Datasheet of the ABS plastic is 44.6 MPa. However if we take a closer look at the measurements, most of the specimens, 86.36% to be exact, showed a tensile strength that is only 10% lower than the nominal. The distribution of the ultimate strength (Figure 14) in all samples also conforms to a good normal probability distribution.

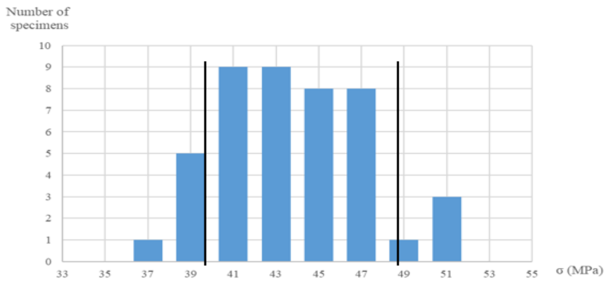

Fig. 14. Chart that shows the distribution of the measured ultimate tensile strength of the specimens

Regarding the maximum elongation, 40% of the samples have a relative deformation greater than or equal to the nominal one, which according to the official Datasheet of the ABS plastic is 20%. In the case of relative deformation, the maximum deviation from the nominal value in some samples is quite large. In 10 of the pieces, a relative deformation of 10% or less was measured, which is more than 2 times less than the nominal value. Moreover, the distribution of the elongation in all samples is quite bad, as can be seen from the chart in Figure 15.

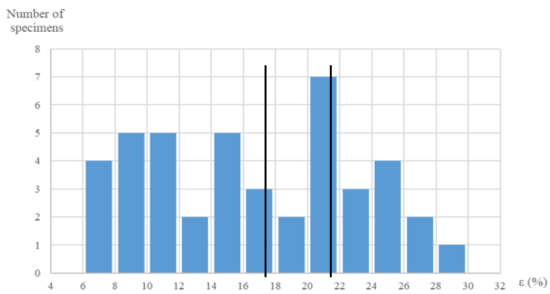

Fig. 15. Chart that shows the distribution of the measured relative deformation of the specimens

5. CONCLUSIONS

The integration of additive manufacturing into injection molding processes brings forth a multitude of benefits that revolutionize traditional manufacturing practices. From accelerated prototyping and enhanced design flexibility to cost efficiency, faster time to market, and easy customization, molds made with SLA additive manufacturing offer a host of advantages that enable manufacturers to drive innovation and efficiency. As the technology continues to evolve, we can expect further advancements in additive manufacturing for injection molding, opening up new possibilities and transforming the landscape of manufacturing.

The findings of this research contribute to the growing field of additive manufacturing by highlighting the potential of SLA mold inserts for producing injection molded parts with satisfactory mechanical properties. The ability to rapidly fabricate mold inserts using SLA technology offers advantages in terms of cost, lead time, and design flexibility. However, further investigations are required to optimize the parameters of the mold inserts made with SLA additive manufacturing and explore their long-term durability and repeatability.

The implication of using molding inserts made with SLA additive manufacturing in the injection molding process causes some unwanted consequences, among which is the appearance of differences in the mechanical characteristics of the manufactured plastic parts. Within this paper, the objective was to investigate the strength of the injection molded parts using the declared strength of the injection molded material from the manufacturer as a reference value for evaluating the obtained material properties.

In conclusion, this study demonstrates that molding inserts made with SLA additive manufacturing can be successfully used for injection molding, producing parts with comparable mechanical properties to those manufactured using traditional steel molds. This research provides valuable insights into the design and optimization of SLA mold inserts, paving the way for cost-effective and time-efficient manufacturing processes in various industries that heavily rely on injection molding.

Based on this research, it can be concluded that the stereolithographic photopolymer from which the mold is made has a generally negative impact on the mechanical characteristics of the manufactured parts, especially on the toughness of the material. Given that the rest of the process parameters were maintained at constant values during injection, this assumption holds validity. However, due to the limited quantity of test specimens, further investigation into this phenomenon is warranted. This is particularly crucial, with a specific emphasis on the method and duration of mold cooling. Previous research in this field has established that the thermal characteristics of photopolymers, notably their low thermal conductivity, emerge as potential factors contributing to the diminished mechanical characteristics observed in parts produced within molds of this nature..

REFERENCES

[1] DSM Somos, "DSM Somos® Material Selection Guide." DSM Somos, 2016.

[2] Segal, J. I., Campbell, R. I. (2001): A review of research into the effects of rapid tooling on part properties," *Rapid Prototyp J*, Vol. **7**, no. 2, pp. 90–98. DOI: 10.1108/13552540110386718

[3] Michaeli, W., Lindner, F. (2001): *Influence of Mould Materials on the Morphological and Mechanical Properties of Injection-Moulded Prototypes*, Macromolecular Materials and Engineering, Wiley. https://doi.org/10.1002/1439-2054(20010401)286:4%3C232:AID-MAME232%3E3.0.CO;2-0

[4] Harris, R. A., Newlyn, H. A., Hague, R. J. M., Dickens. P. M. (Jul. 2003): Part shrinkage anomilies from stereolithography injection mould tooling, *Int J Mach Tools Manuf*, vol. **43**, no. 9, pp. 879–887, DOI: 10.1016/S0890-6955(03)00080-4

[5] Fernandes, A. D. C., De Souza, A. F., Howarth, J. L. L. (2016): Mechanical and dimensional characterisation of polypropylene injection moulded parts in epoxy resin/aluminium inserts for rapid tooling," *International Journal of Materials and Product Technology*, vol. **52**, no. 1/2, pp. 37. DOI: 10.1504/IJMPT.2016.073618

[6] Harris, R. A., Hague, R. J. M., Dickens, P. M. (Oct. 2003): Crystallinity control in parts produced from stereolithography injection mould tooling, *Proceedings of the Institution of Mechanical Engineers, Part L: Journal of Materials: Design and Applications*, vol. **217**, no. 4, pp. 269–276. DOI: 10.1177/146442070321700402

[7] Volpato, N., Solis, D. M., Costa, C. A. (2016): An analysis of Digital ABS as a rapid tooling material for polymer injection moulding, *International Journal of Materials and Product Technology*, Vol. **52**, no. 1/2, pp. 3. DOI: 10.1504/IJMPT.2016.073616.

[8] FormLabs (2019): Form 3 Tech Specs.

[9] Formlabs (2023): *Post-Processing Tech Specs*. https://formlabs.com/post-processing/wash-cure/tech-spe cs/.

[10] The International Organization for Standardization (2012): *Test conditions for moulding and extrusion plastics.* EN ISO 527-2 Plastics.

[11] The International Organization for Standardization (2019): *General principles for determination of tensile properties*. EN ISO 527-1 Plastics.

[12] Tecves Materials Selection Guide (2023): *Ghaed Basir Petrochemical ABS-50 ABS Datasheet*. http://materials.tecves.com/en/262/abs-50

Mechanical Engineering – Scientific Journal, Vol. **41,** No. 2, pp. 141–144 (2023)
CODEN: MINSC5
In print: ISSN 1857–5293
On line: ISSN 1857–9191

INSTRUCTIONS FOR AUTHORS

The *Mechanical Engineering – Scientific Journal* is published twice yearly. The journal publishes **original scientific papers, short communications, reviews** and **professional papers** from all fields of mechanical engineering.

The journal also publishes (continuously or occasionally) the bibliographies of the members of the Faculty, book reviews, reports on meetings, informations of future meetings, important events and data, and various rubrics which contribute to the development of the corresponding scientific field.

Original scientific papers should contain hitherto unpublished results of completed original scientific research. The number of pages (including tables and figures) should not exceed 15 (28 000 characters).

Short communications should also contain completed but briefly presented results of original scientific research. The number of pages should not exceed 5 (10 000 characters) including tables and figures.

Reviews are submitted at the invitation of the Editorial Board. They should be surveys of the investigations and knowledge of several authors in a given research area. The competency of the authors should be assured by their own published results.

Professional papers report on useful practical results that are not original but help the results of the original scientific research to be adopted into scientific and production use. The number of pages (including tables and figures) should not exceed 10 (18 000 characters).

Acceptance for publication in the Journal obliges the authors not to publish the same results elsewhere.

SUBMISSION

The article and annexes should be written on A4 paper with margins of 2.5 cm on each side with a standard font Times New Roman 11 points and should be named with the surname of the first author and then if more and numbered. It is strongly recommended that on MS Word 2003 or MS Word 2007 and on PDF files of the manuscript be sent by e-mail:

mesj@mf.edu.mk.

A letter must accompany all submissions, clearly indicating the following: title, author(s), corresponding author's name, addres and e-mail addres(es), suggested category of the manuscript and a suggestion of five referees (their names, e-mail and affiliation).

Articles received by the Editorial Board are sent to two referees (one in the case of professional papers). The suggestions of the referees and Editorial Board are sent to the author(s) for further action. The corrected text should be returned to the Editorial Board as soon as possible but in not more than 30 days.

PREPARATION OF MANUSCRIPT

The papers should be written in the shortest possible way and without unnecessary repetition.

The original scientific papers, short communications and reviews should be written in English, while the professional papers may also be submitted in Macedonian.

Only SI (Système Internationale d'Unites) quantities and units are to be used.

Double subscripts and superscripts should be avoided whenever possible. Thus it is better to write $\nu_3(PO_4)$ than $\nu_{3_{PO_4}}$ or exp(–E/RT) than $e^{-E/RT}$. Strokes (/) should not be used instead of parentheses.

When a large number of compounds have been analyzed, the results should be given in tabular form.

Manuscript should containt: title, author(s) full-name(s), surname(s), address(es) and e-mail of the corresponding author, short abstract, key words, introduction, experimental or theoretical background, results and discussion, acknowledgment (if desired) and references.

The **title** should correspond to the contents of the manuscript. It should be brief and informative and include the majority of the key words.

Each paper should contain an **abstract** that should not exceed 150 words, and **3–5 key words**. The abstract should include the purpose of the research, the most important results and conclusions.

The **title**, **abstract** and **key words** should be translated in Macedonian language. The ones written by foreign authors will be translated by the Editorial Board.

In the **introduction** only the most important previous results related to the problem in hand should be briefly reviewed and the aim and importance of the research should be stated.

The **experimental** section should be written as a separate section and should contain a description of the **materials used and methods** employed – in form which makes the results reproducible, but without detailed description of already known methods.

Manuscripts that are related to **theoretical studies**, instead of experimental material, should contain a sub-heading and the **theoretical background** where the necessary details for verifying the results obtained should be stated.

The **results and discussion** should be given in the same section. The discussion should contain an analysis of the results and the conclusions that can be drawn.

Figures (photographs, diagrams and sketches) and **mathematical formulae** should be inserted in the correct place in the manuscript, being horizontally reduced to 8 or 16 cm. The size of the symbols for the physical quantities and units as well as the size of the numbers and letters used in the reduced figures should be comparable with the size of the letters in the main text of the paper. Diagrams and structural formulae should be drawn in such a way (e.g. black Indian ink on white or tracing paper) as to permit high quality reproduction. The use of photographs should be avoided. The tables and the figures should be numbered in Arabic numerals (e.g., Table 1, Figure 1). Tables and figures should be self-contained, i.e. should have captions making them legible without resort to the main text. The presentation of the same results in the form of tables and figures (diagrams) is not permitted. The use of equation editor (MS Word, Microsoft Equation, Math Type 6.0 Equation) for typesetting the equations is recommended. Strokes (/) should not be used instead of parentheses.

Figures and tables must be centred in the column. Large figures and tables may span across both columns (Figure 1).

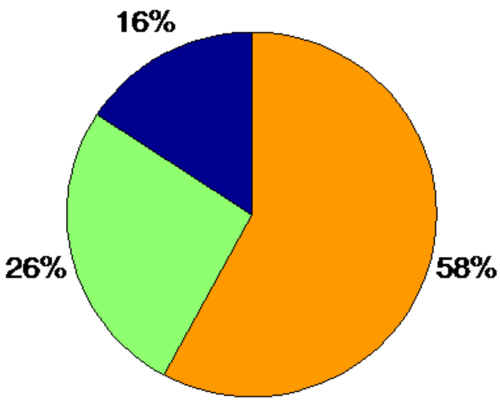

Fig. 1. Example of a graph and a single-line caption (colour)

Graphics may be full colour. Please use only colours which contrast well both on screen and on a black-and-white hardcopy because the Journal is published in black-and-white, as shown in Figure 2. The colour version is only for the electronic version of the Journal.

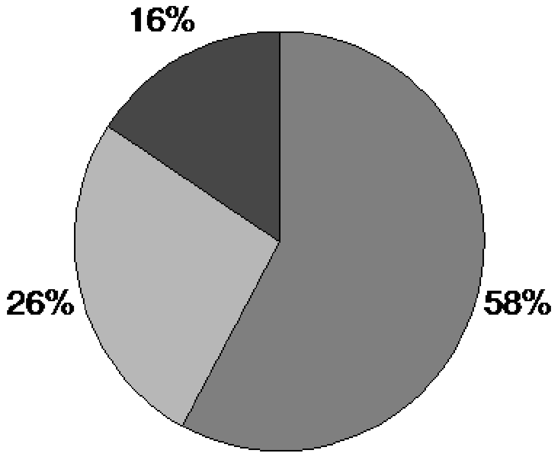

Fig. 2. Example of a graph and a single-line caption (bleck and vhite)

Please check all figures in your paper both on screen and on a black-and-white hardcopy. When you check your paper on a black-and-white hardcopy, please ensure that:

– the colours used in each figure contrast well (Figure 3),

– the image used in each figure is clear,

– all text labels in each figure are legible.

Please check all figures in your paper both on screen and on a black-and-white hardcopy. When you check your paper on a black-and-white hardcopy, please ensure that the image used in each figure is clear and all text labels in each figure are legible.

Fig. 3. Example of an image as it will appear at the electronic version of the Journal and a multi-line caption

Footnotes are also not permitted.

The **reference** should be given in a separate section in the order in which they appear in the text. The surname of one or two authors may be given in the text, whereas in the case of more than two authors they should be quoted as, for example:

Examples of reference items of different categories shown in the References section include:

- example of a book in [1]
- example of a book in a series in [2]
- example of a journal article in [3]
- example of a conference paper in [4]
- example of a patent in [5]
- example of a website in [6]
- example of a web page in [7]
- example of a databook as a manual in [8]
- example of a datasheet in [9]
- example of a master/Ph.D. thesis in [10]
- example of a technical report in [11]
- example of a standard in [12]

All reference items must be in 9 pt font. Please use Regular and Italic styles to distinguish different fields as shown in the References section. Number the reference items consecutively in square brackets (e.g. [1]).

When referring to a reference item, please simply use the reference number, as in [2]. Do not use “Ref. [3]” or “Reference [3]” except at the beginning of a sentence, e.g. “Reference [3] shows …”. Multiple references are each numbered with separate brackets (e.g. [2], [3], [4–6]).

The **category** of the paper is proposed by the author(s), but the Editorial Board reserves for itself the right, on the basis of the referees' opinion, to make the final choice.

Proofs are sent to the author(s) to correct printers' errors. Except for this, alterations to the text are not permitted. The proofs should be returned to the Editorial Board in 2 days.

The author(s) will receive, free of charge, 1 reprints of every paper published in the Journal.

REFERENCES

[1] Surname, N(ame).; Surname, N(ame). (Year): *Name of the Book*, Publisher.

[2] Surname, N(ame).; Surname, N(ame). (Year): *Name of the Book*, Name of the Series. Publisher, **vol.** XXX.

[3] Surname, N(ame).; Surname N(ame). (Year): Title of the article, *Name of the Journal*, **vol. XX,** No. XX, pp. XXX–XXX.

[4] Surname, N(ame).; Surname N(ame). (Year): Title of the article, *Proceedings of the Name of the Conference*, vol. **XX,** pp. XXX–XXX.

[5] Surname, N(ame).; Surname, N(ame).: *Name of the Patent*, Institution that issued the patent and Number of the patent (Date dd. mm. yyyy).

[6] N.N. (Year): *The XXX web site*, web address.

[7] Surname, N. (Year): *XXX homepage on XXX*, web address.

[8] N.N. (Year): *Title of the Manual*, Name of the Organization.

[9] N.N.: *XXX data sheet*, Name of the Organization.

[10] Surname, N. (Year): *Title of the Thesis*, Master/Ph.D. thesis (in Language), Institution.

[11] Surname, N(ame).: Surname, N(ame). (Year): *Title of the Report*, Organization that issued the report, number of the report.

[12] Institution that issued the standard (Year): *Name of the Standard* & Number of the standard.